SRR-CWDA-2013-00073
Revision 2

Updates to the Saltstone Disposal Facility Stochastic Fate and Transport Model

August 2014

Prepared by: Savannah River Remediation LLC
Waste Disposal Authority
Aiken, SC 29808

Prepared for U.S. Department of Energy Under Contract No. DE-AC09-09SR22505

APPROVALS

Author:

Barry Lester
Savannah River Remediation LLC
Waste Disposal Authority

8/26/14
Date

Technical Review (per ENG.51):

Steven Hommel
Savannah River Remediation LLC
Waste Disposal Authority

8/26/14
Date

Management Review:

Kent Rosenberger
Savannah River Remediation LLC
Waste Disposal Authority

8/26/2014
Date

TABLE OF CONTENTS

APPROVALS 2
TABLE OF CONTENTS 3
LIST OF FIGURES 5
LIST OF TABLES 10
ACRONYMS 11
1.0 EXECUTIVE SUMMARY 12
2.0 PURPOSE 14
2.1 Advective-Dispersive Transport Simulation 15
2.1.1 GoldSim SDF All-Species Model 15
2.1.2 GoldSim SDF Tc-99 Release Model 17
2.2 Dose Calculator Model 18
3.0 SDF GOLDSIM MODEL UPDATES 19
3.1 Special Analysis Specific Updates 19
3.1.1 375-Foot Diameter SDUs 19
3.1.2 Omission of the Grout Clean-Cap in the 150-Foot Diameter SDUs 21
3.1.3 FY2014 SDF SA Inventory Values 21
3.1.4 Updates to the PORFLOW Generated Flow Field Files 24
3.2 Improvements to Computational Efficiency 27
3.2.1 The GoldSim SDF Tc-99 Release Model 27
3.2.2 Transition Time Dynamic Link Library 29
4.0 STRUCTURE OF THE SDF GOLDSIM MODEL 31
4.1 GoldSim SDF All-Species Model Organization 31
4.1.1 Radionuclide Transport Modeling 36
4.2 GoldSim SDF Tc-99 Release Model Organization 57
4.2.1 Structure of the GoldSim SDF Tc-99 Release Model 57
4.2.2 Transition Time Dynamic Link Library 69
5.0 MODEL BENCHMARKING and alternative conceptual model results 73
5.1 Benchmarking Results 73
5.1.1 Mass Releases to the Saturated Zone 74
5.1.2 Radionuclide Concentrations at the 100-Meter Boundary 108
5.1.3 MOP Dose Time Histories 112
5.1.4 IHI Well Dose Time Histories 120
5.1.5 Mass Releases to the Saturated Zone 125

5.2 Benchmarking Conclusion 126
6.0 REFERENCES 128

LIST OF FIGURES

Figure 2.0-1: Conceptual Layout of SDUs as Modeled in the FY2014 SDF SA 15
Figure 3.1-1: Conceptual Model for 375-foot Diameter SDUs (Typical) 20
Figure 4.1-1: SDF GoldSim Model Organization 34
Figure 4.1-2: Sectors Along the 100-Meter Boundary for the FY2014 SDF SA 35
Figure 4.1-3: Contents of Container *DisposalUnits* 37
Figure 4.1-4: Contents of Container *FDCs* 38
Figure 4.1-5: Contents of Container *OuterLoop* 39
Figure 4.1-6: Contents of Container *InnerLoop* 39
Figure 4.1-7: External Element Controlling *TSProc1.dll* 40
Figure 4.1-8: Contents of *FDC_TransportSubmodel* 41
Figure 4.1-9: Typical GoldSim Time Series Element Used in *FDC_Transport_Results* 42
Figure 4.1-10: *FDC_TransportSubmodel* Submodel-Interface 43
Figure 4.1-11: Contents of the *Vault_4* Container 44
Figure 4.1-12: Contents of the *FDCs* Container 44
Figure 4.1-13: Contents of the *VaultCells* Container for FDCs 48
Figure 4.1-14: Contents of the *CellRow_01* Container for FDCs 49
Figure 4.1-15: Contents of the *Grout* Container for FDCs 49
Figure 4.1-16: Contents of the *InnerZone* Container for FDCs 50
Figure 4.1-17: Contents of the *OuterZone* Container for FDCs 50
Figure 4.1-18: Contents of the *FastZone* Container for FDCs 51
Figure 4.1-19: Contents of the *SheetDrain* Container for FDCs 51
Figure 4.1-20: Contents of the *Wall* Container for FDCs 52
Figure 4.1-21: Contents of the *HDPE* Container for FDCs 52
Figure 4.1-22: Contents of the *Fill* Container for FDCs 53
Figure 4.1-23: Contents of the *VaultFloor1* Container for FDCs 53
Figure 4.1-24: Contents of the *FastZone* Container for FDCs 54
Figure 4.1-25: Contents of the *Joint1 and Joint 2* Containers for FDCs 54
Figure 4.1-26: Contents of the *Joint3* Container for FDCs 55
Figure 4.1-27: Contents of the *UnsatZone* Container for FDCs 55
Figure 4.1-28: Contents of the *WasteFootprint* Container for FDCs 56
Figure 4.1-29: Contents of the *NearWell* Container for FDCs 56

Figure 4.2-1: Upper Tier of the GoldSim SDF Tc-99 Release Model Hierarchy 57
Figure 4.2-2: Contents of *DisposalUnits* 60
Figure 4.2-3: Contents of *SDU_ReleaseCalculations* 61
Figure 4.2-4: Contents of *OuterLoop* 61
Figure 4.2-5: Contents of *InnerLoop* 63
Figure 4.2-6: Contents of the GoldSim Submodel Container SDU_TransportSubmodel 64
Figure 4.2-7: Contents of *SDU_Abstraction* 65
Figure 4.2-8: Contents of *SaltStoneRelease* 65
Figure 4.2-9: Contents of *Disposal Unit* 66
Figure 4.2-10: Contents of *SDUCells* 66
Figure 4.2-11: Contents of Each Container in *SDUCells* 67
Figure 4.2-12: Contents of *UZ* 68
Figure 4.2-13: Contents of *UZSet2* 68
Figure 4.2-14: GoldSim External Element Used for Reading in Flow Transition Time Data 70
Figure 4.2-15: Contents of the GoldSim Container *TTADLLData* 71
Figure 4.2-16: Contents of the GoldSim Container *TTADLLData_a* 71
Figure 4.2-17: *TransitionTime.dll* Control File *TTAdata.in* 72
Figure 5.1-1: SDU 1 I-129 Release to the Saturated Zone 76
Figure 5.1-2: SDU 1 I-129 PORFLOW Model Release to the Saturated Zone at 1,000 Years 77
Figure 5.1-3: SDU 1 Flow Field at 1,000 Years 77
Figure 5.1-4: UZ and Vault Component I-129 Releases for SDU 1 (GoldSim) 78
Figure 5.1-5: SDU 1 Cs-135 Release to the Saturated Zone 79
Figure 5.1-6: SDU 1 Cs-135 PORFLOW Model Release to the Saturated Zone at 7,250 Years 80
Figure 5.1-7: SDU 1 Flow Field at 18,900 years 80
Figure 5.1-8: SDU 1 Ra-226 Release to the Saturated Zone 81
Figure 5.1-9: SDU 1 Tc-99 Release to the Saturated Zone 82
Figure 5.1-10: Semi-Log Plot of SDU 1 Tc-99 Release to the Saturated Zone 82
Figure 5.1-11: SDU 1 Tc-99 Release to the Saturated Zone (FY2013 SDF SA) 83
Figure 5.1-12: Semi-Log Plot of SDU 1 Tc-99 Release to the Saturated Zone (FY2013 SDF SA) 83
Figure 5.1-13: SDU 1 Slag Concentrations at Saltstone/Wall Contact (28,500 Years) 84
Figure 5.1-14: SDU 1 Tc-99 Concentrations at Saltstone/Wall Contact (28,500 Years) 85

Figure 5.1-15: SDU 4 I-129 Release to the Saturated Zone 86
Figure 5.1-16: SDU 4 Cs-135 Release to the Saturated Zone 86
Figure 5.1-17: SDU 4 Cs-135 PORFLOW Model Release to the Saturated Zone at 4,250 Years 87
Figure 5.1-18: UZ and Vault Component Releases for SDU 4 (GoldSim) 87
Figure 5.1-19: SDU 4 Ra-226 Release to the Saturated Zone 88
Figure 5.1-20: Semi-Log Plot of SDU 4 Ra-226 Release to the Saturated Zone 89
Figure 5.1-21: SDU 4 Ra-226 (from Th-230) PORFLOW Model Release to the Saturated Zone at 4,250 Years 89
Figure 5.1-22: SDU 4 Ra-226 (from U-234) PORFLOW Model Release to the Saturated Zone at 4,250 Years 90
Figure 5.1-23: SDU 4 Tc-99 Release to the Saturated Zone to 20,000 Years 91
Figure 5.1-24: Semi-Log Plot of SDU 4 Tc-99 Release to the Saturated Zone to 50,000 Years 91
Figure 5.1-25: SDU 4 Tc-99 Concentrations at Saltstone/Wall Contact (20,000 Years) 92
Figure 5.1-26: SDU 4 Slag Concentrations at Saltstone/Wall Contact (20,000 Years) 92
Figure 5.1-27: SDU 3A I-129 Release to the Saturated Zone 94
Figure 5.1-28: UZ and SDU Component I-129 Releases for SDU 3A (GoldSim)..... 94
Figure 5.1-29: SDU 3a Cs-135 Release to the Saturated Zone..... 95
Figure 5.1-30: SDU 3A Cs-135 Release to the Saturated Zone at 11,000 Years 96
Figure 5.1-31: SDU 3A Flow Field from 10,000 to 11,000 Years 96
Figure 5.1-32: UZ and Vault Component Cs-135 Releases for SDU 3A (GoldSim)..... 97
Figure 5.1-33: SDU 3A Ra-226 Release to the Saturated Zone 98
Figure 5.1-34: SDU 3A Tc-99 Release to the Saturated Zone to 20,000 Years 99
Figure 5.1-35: SDU 3A Tc-99 Release to the Saturated Zone (Log Scale) to 50,000 Years 99
Figure 5.1-36: SDU 3A Tc-99 Concentrations at Saltstone/Wall Contact (40,000 Years) 100
Figure 5.1-37: SDU 3A Slag Concentrations at Saltstone/Wall Contact (40,000 Years) 100
Figure 5.1-38: SDU 6 I-129 Release to the Saturated Zone 102
Figure 5.1-39: UZ and Vault Component I-129 Releases for SDU 6 (GoldSim)..... 102
Figure 5.1-40: SDU 6 Cs-135 Release to the Saturated Zone 103
Figure 5.1-41: UZ and Vault Component Cs-135 Releases for SDU 6 (GoldSim)..... 104
Figure 5.1-42: SDU 6 Ra-226 Release to the Saturated Zone 105
Figure 5.1-43: SDU 6 Ra-226 Release to the Saturated Zone (Log Scale) 105
Figure 5.1-44: Contours of SDU 6 Ra-226 Concentrations at 6,750 years 106

Figure 5.1-45: SDU 6 Tc-99 Release to the Saturated Zone 106
Figure 5.1-46: SDU 6 Tc-99 Release to the Saturated Zone 107
Figure 5.1-47: SDU 6 Tc-99 Concentrations at Saltstone/Wall Contact (40,000 Years) 107
Figure 5.1-48: SDU 6 Slag Concentrations at Saltstone/Wall Contact (40,000 Years) 108
Figure 5.1-49: Maximum Radionuclide Concentrations at 100-Meter Boundary, Sector B 109
Figure 5.1-50: Maximum Radionuclide Concentrations at 100-Meter Boundary, Sector I 110
Figure 5.1-51: Maximum Radionuclide Concentrations at 100-Meter Boundary, Sector J 111
Figure 5.1-52: Maximum Radionuclide Concentrations at 100-Meter Boundary, Sector K 112
Figure 5.1-53: PORFLOW Evaluation Case, Sector MOP Dose Results over 20,000 Years ... 113
Figure 5.1-54: GoldSim Evaluation Case, Sector MOP Dose Results over 20,000 Years 113
Figure 5.1-55: Comparison of Maximum MOP Dose Evaluation Case Results over 20,000 Years 114
Figure 5.1-56: Individual Radionuclide Contributions to the PORFLOW Sector B 100-meter Peak Groundwater Pathway Dose Results within 20,000 Years 115
Figure 5.1-57 Individual Radionuclide Contributions to the GoldSim Sector B 100-meter Peak Groundwater Pathway Dose Results within 20,000 Years 116
Figure 5.1-58: Individual Radionuclide Contributions to the PORFLOW Sector I 100-Meter Peak Groundwater Pathway Dose Results within 20,000 Years 117
Figure 5.1-59 Individual Radionuclide Contributions to the GoldSim Sector I 100-meter Peak Groundwater Pathway Dose Results within 20,000 Years 117
Figure 5.1-60: Individual Radionuclide Contributions to the PORFLOW Sector J 100-meter Peak Groundwater Pathway Dose Results within 20,000 Years 118
Figure 5.1-61 Individual Radionuclide Contributions to the GoldSim Sector J 100-meter Peak Groundwater Pathway Dose Results within 20,000 Years 118
Figure 5.1-62: Individual Radionuclide Contributions to the PORFLOW Sector K 100-meter Peak Groundwater Pathway Dose Results within 20,000 Years 119
Figure 5.1-63 Individual Radionuclide Contributions to the GoldSim Sector K 100-meter Peak Groundwater Pathway Dose Results within 20,000 Years 120
Figure 5.1-64: PORFLOW Model IHI Well Dose Time Histories 121
Figure 5.1-65: GoldSim Model IHI Well Dose Time Histories 122
Figure 5.1-66: PORFLOW Model IHI Well Dose Time Histories for the Northern Wells 123
Figure 5.1-67: GoldSim Model IHI Well Dose Time Histories for the Northern Wells 123
Figure 5.1-68: PORFLOW Model IHI Well Dose Time Histories for the Southern Wells 124
Figure 5.1-69: GoldSim Model IHI Well Dose Time Histories for the Southern Wells 124

Figure 5.1-70: GoldSim and PORFLOW Model Maximum IHI Well Dose Time Histories.... 125

Figure 5.1-71: Comparison of PORFLOW and GoldSim MOP Dose Profiles for Selected Flow Cases for 20,000 Years 126

LIST OF TABLES

Table 3.1-1: Material Parameters for 375-foot Diameter SDU Conceptual Model 20

Table 3.1-2: SDF Inventory Estimates in Curies for Use in Transport Modeling 22

Table 3.1-3: Summary of Flow Cases 26

Table 3.1-4: Summary of Evaluation Flow Cases for the FY2014 SDF SA 27

Table 4.1-1: SDU Numbering In GoldSim Models 33

Table 4.2-1: Instruction Data Passed to *TransitionTime.dll* 69

Table 5.1-1: GoldSim and PORFLOW Model Peak Unsaturated Zone Release Comparisons for SDU 1 within 20,000 years 75

Table 5.1-2: GoldSim and PORFLOW Model Peak Unsaturated Zone Release Comparisons for SDU 4 within 20,000 years 85

Table 5.1-3: GoldSim and PORFLOW Model Peak Unsaturated Zone Release Comparisons for 150-Foot Diameter SDUs within 20,000 years 93

Table 5.1-4: GoldSim and PORFLOW Model Peak Unsaturated Zone Release Comparisons for 375-Foot Diameter SDUs within 20,000 years 101

ACRONYMS

CZ	Contamination Zone
DLL	Dynamic Link Library
FDC	Future Disposal Cell
FTR	Fractional Transfer Rate
FY	Fiscal Year
GTG	GoldSim Technology Group LLC
HDPE	High-Density Polyethylene
IHI	Inadvertent Human Intruder
LHS	Latin Hypercube Sampling
MCC	Moisture Characteristic Curve
MCL	Maximum Contaminant Level
MOP	Member of Public
NRC	U.S. Nuclear Regulatory Commission
PA	Performance Assessment
SA	Special Analysis
SDF	Saltstone Disposal Facility
SDU	Saltstone Disposal Unit
SRS	Savannah River Site
SZ	Saturated Zone
UMM	Upper Mud Mat
UZ	Unsaturated Zone

1.0 EXECUTIVE SUMMARY

This report documents the revision (Version 5.006) of the Saltstone Disposal Facility (SDF) Stochastic Fate and Transport Model (referred to herein as the GoldSim SDF All-Species Model). In addition this report documents the development of the GoldSim SDF Tc-99 Release Model (Version 1.006), a self-contained module of the Saltstone Disposal Facility (SDF) Stochastic Fate and Transport Model designed to evaluate the migration of Tc-99 through saltstone disposal units (SDUs) when the transport process is dominated by a "shrinking-core" mechanism. Both SDF GoldSim Models are object-oriented, probabilistic models designed to evaluate parameter sensitivity and the influence of parameter uncertainty on the potential for migration, of radionuclides stored at the SDF, to the accessible environment. Together, both models may collectively be referred to as the SDF GoldSim Model, as the GoldSim SDF All-Species Model reads in data from the GoldSim SDF Tc-99 Release Model.

For each realization of a Monte Carlo or Latin Hypercube Sampling (LHS) of data, the SDF GoldSim Model calculates radionuclide concentrations along a 100-meter boundary surrounding the Saltstone Disposal Units (SDUs) and at seven Inadvertent Human Intruder (IHI) wells. Based on these concentrations the model then calculates doses along the boundary for use in the Member of Public (MOP) dose analysis. In addition, the model calculates associated doses at possible well locations at the down gradient edge of seven SDUs for use in the IHI analysis and doses from drill cuttings for the Acute Intruder analysis.

The dose-calculation module within the GoldSim SDF All-Species Model can calculate doses from radionuclide concentrations generated by the SDF GoldSim Model or from concentrations generated by the SDF PORFLOW Model. Note that IHI doses, generated from the SDF PORFLOW Model results are based on both the IHI Well concentrations and maximum concentrations derived along a 1-meter boundary surrounding the SDUs. The radionuclide transport modules of the two SDF GoldSim Models are simplified abstractions of the three-dimensional (3-D) SDF PORFLOW Model, allowing for a computationally efficient solution to the contaminant transport process, which is necessary for multi-realization runs.

This report (SRR-CWDA-2013-00073 Rev. 1) describes the updates implemented within the SDF GoldSim Model Version 5.006, relative to Version 4.101 (SRR-CWDA-2013-00073 Rev. 0), to support the FY2014 SDF Special Analysis (SA) and future SAs. The differences between the models used in the previous two special analyses (SDF GoldSim Models Version 4.101 and Version 3.02) are documented in SRR-CWDA-2013-00073 Rev. 0. The differences between Version 3.02 of the SDF GoldSim Model and the Performance Assessment (PA) SDF GoldSim Model are documented in SRR-CWDA-2011-00178. The SDF PA SDF GoldSim Model is documented in SRR-CWDA-2009-00017.

Note that updates to the GoldSim SDF All-Species Model are also implemented in the new GoldSim SDF Tc-99 Release Model. The updates to the GoldSim SDF All-Species Model allow the model to consider additional information regarding the degradation of cementitious material, the conceptual model for release of technetium from reducing cementitious materials, and inventory values. In addition, the updates take into consideration the future replacement of the clean cap with contaminated saltstone and the replacement of 150-foot diameter SDUs with 375-foot diameter SDUs, in future construction. The major differences between SDF GoldSim Model, Version 5.006 and SDF GoldSim Model, Version 4.101 include:

- The replacement of PORFLOW generated flow field files with updated files reflecting changes in the degradation rates of cementitious materials
- The development of a self-contained GoldSim SDF Tc-99 Release Model
- The replacement of inventory by the latest Savannah River Site (SRS) inventory data and SDF SDU actuals
- Restructuring the model to allow for waste to replace the grout clean cap
- Addition of the logic and data needed to consider a fourth SDU-type, the 375-foot diameter cylindrical SDU, in the transport calculations
- Updating of data needed to consider the new locations of future SDUs

Section 2 of this report defines the purposes of Version 5.006 of the GoldSim SDF All-Species Model and of Version 1.006 of the GoldSim SDF Tc-99 Release Model. Section 3 of this report discusses the changes implemented in the radionuclide transport modules of the GoldSim SDF All-Species Model and the conceptual model abstraction upon which Version 1.006 of the GoldSim SDF Tc-99 Release Model, is based. Section 4 of this report discusses the general structure of the GoldSim SDF All-Species Model and of the GoldSim SDF Tc-99 Release Model.

The final section (Section 5.0) of this report documents the benchmark testing performed to show that this abstraction of the SDF GoldSim Model is a valid surrogate for the 3-D SDF PORFLOW Model. During the testing, results from the SDF GoldSim Models and the SDF PORFLOW Model were compared, showing that the abstraction can adequately approximate the trends and results produced by the SDF PORFLOW Model.

2.0 PURPOSE

The SDF GoldSim Model is an object-oriented, probabilistic model designed to evaluate parameter sensitivity and the influence of parameter uncertainty on the potential for migration of radionuclides in the SDF to the accessible environment. For the purpose of compliance, the accessible environment is defined by a 100-meter perimeter surrounding the Saltstone disposal units.

The SDF GoldSim Model is comprised of two components; 1) an abstraction of the SDF PORFLOW model, and 2) a dose calculator. The abstraction is designed specifically to approximate the process of radionuclide transport from disposal units in a manner that would allow for uncertainty and sensitivity analyses to be performed in a time-efficient manner, while still allowing the influence of parameters on the transport processes to be examined.

The abstraction of the SDF PORFLOW model described herein, is comprised of two separate modules, an All-Species module (Version 5.006 of the GoldSim SDF All-Species Model), and a self-contained Tc-99 module (Version 1.006 of the GoldSim SDF Tc-99 Release Model). The All-Species module is used to evaluate advective-dispersive transport through individual SDUs, into and through the unsaturated zone (UZ) to the water table, and through the saturated zone (SZ) to the 100-meter boundary. Radionuclide migration from the SDUs to the seven IHI wells is also calculated. The GoldSim SDF Tc-99 Release Model is used to evaluate Tc-99 release from the SDUs, when the "shrinking-core" release model is emulated (which is the case for the FY2014 SDF SA). When the GoldSim SDF Tc-99 Release Model is utilized, the All-Species module automatically reads in a set of Tc-99 release-rate files (one for each SDU) generated by the GoldSim SDF Tc-99 Release Model. After importing the set of time series, the All-Species model uses the imported data as input to the its saturated zone analysis. The All-Species module also includes a dose calculator, which can be used to evaluate dose at points of compliance (the 100-meter boundary and IHI wells) based on the concentrations generated by the transport abstraction module or generated by the PORFLOW SDF model.

This volume serves mainly as a documentation to:

1) the changes to the abstraction of the PORFLOW radionuclide transport model implemented in Version 5.006 of the GoldSim SDF All-Species Model, as provided in the model file: *SRS Saltstone v5.006.gsm,* and
2) the abstraction of the PORFLOW radionuclide transport "shrinking-core" model found in Version 1.006 of the GoldSim SDF Tc-99 Release Model, as provided in the model file: *Tc99_SDU_V1.006.gsm*.

The dose module is documented elsewhere as noted in Section 2.2. The present versions of the SDF GoldSim Model were specifically developed to be used in conjunction with the SDF PORFLOW Model in a FY2014 SDF SA to update the model for consistency with the replacement of future 150-foot diameter SDUs with 375-foot diameter SDUs. The updates allow the model to consider additional information regarding:

- the degradation of cementitious material,
- radionuclide inventory and its effect on flow and associated radionuclide transport,

- the conceptual model for the release of technetium from reducing cementitious materials, and the replacement of the 150-foot diameter SDUs with 375-foot diameter SDUs.

A conceptual drawing of the planned SDF layout is presented in Figure 2.0-1. This version of the SDF GoldSim Model was developed using the GoldSim software (B-SQP-C-00002).

Figure 2.0-1: Conceptual Layout of SDUs as Modeled in the FY2014 SDF SA

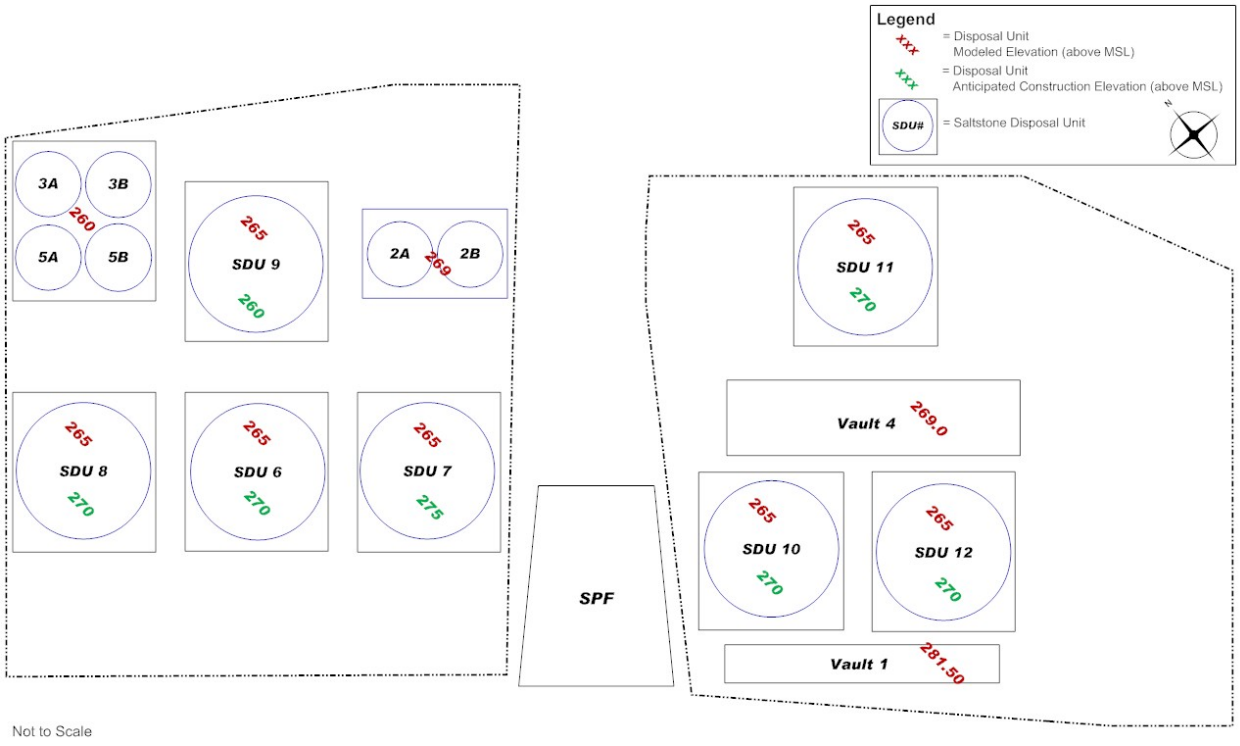

2.1 Advective-Dispersive Transport Simulation

2.1.1 GoldSim SDF All-Species Model

The GoldSim SDF All-Species Model solves the general equations for transport of dissolved radionuclides within the engineered barriers (the disposal units) and the natural barriers (the unsaturated zone and saturated zone). The GoldSim SDF All-Species Model takes advantage of the GoldSim mixing cell-network elements and the 1-D analytical solution-based pipe elements to evaluate the advective-dispersive transport of contaminants through the engineered and natural barriers (GTG-2010e).

The abstraction of the SDF PORFLOW Model included in the GoldSim SDF All-Species Model to simulate radionuclide transport in the SDUs and unsaturated zone beneath, is based on the simplifying assumption that vertical flow controls the radionuclide release from the SDUs and unsaturated zone (UZ) except relatively early in simulations when matrix diffusion as a release mechanism may be important. Molecular diffusion in the horizontal direction, is also modeled explicitly in the SDF GoldSim Model because diffusion into and through the walls to the backfill can be relatively important at early times when flow rates are low. The transport module of the SDF GoldSim Model simulates the transport of non-conservative

species subject to sorption and either simple decay or ingrowth along decay chains. Other processes controlling the mass release from the disposal units include time-dependent physical and chemical degradation of saltstone and concrete zones (floors, columns, and walls and for the cylindrical SDUs (referred to as Future Disposal Cells (FDCs) in the model) the high-density polyethylene (HDPE) liners and mud mats). The influence of mechanical dispersion is not explicitly considered in the disposal unit structure, backfill, or unsaturated zone although a certain degree of numerical dispersion is inherent in the use of mixing cells.

In the saturated zone, the abstraction of the SDF PORFLOW Model assumes that 1-D transport along streamlines emanating from center of each SDU dominates the transport of radionuclides released by the SDUs. As noted earlier, the 1-D transport along streamlines is modeled using the GoldSim pipe elements. The governing equation for 1-D advective-dispersive transport of a dissolved species in a unidirectional flow field, as solved for in the pipe elements, can be written as follows:

$$\frac{\partial(\varphi RC)}{\partial t} = D\frac{\partial^2 C}{\partial l^2} - v\frac{\partial C}{\partial l} - \varphi R\lambda C + \sum_{i=1}^{Np} \varphi R\lambda_{pi} C_{pi} \qquad (2\text{-}1)$$

where:

C	=	solute concentration (M/L^3)
R	=	retardation coefficient
φ	=	effective porosity
t	=	time (T)
D	=	dispersion coefficient = $v\alpha + \varphi D_{eff}$ (L^2/T)
v	=	Darcy velocity (L/T)
α	=	dispersivity (L)
D_{eff}	=	effective diffusion coefficient (L^2/T)
λ	=	decay coefficient (T^{-1})
λ_{pi}	=	decay coefficient of the i^{th} parent (T^{-1})
Np	=	number of parent species
l	=	transport pathway coordinate (L)

Horizontal and vertical transverse dispersion may also be important contributors to plume attenuation and therefore also are explicitly modeled in the GoldSim SDF All-Species Model. The influence of transverse horizontal and vertical dispersion are included through the use of the GoldSim plume function (GTG-2010e), a built-in function based on Green's function solutions, that can be used to superimpose the influence of transverse (horizontal and vertical) dispersion on the results generated by the 1-D transport analysis. Equation 2-1 can be rewritten to include the effects of horizontal and vertical transverse dispersion as follows:

$$\frac{\partial(\varphi RC)}{\partial t} = D_l \frac{\partial^2 C}{\partial s_l^{\,2}} + D_{t_h} \frac{\partial^2 C}{\partial s_{t_h}^{\,2}} + D_{t_v} \frac{\partial^2 C}{\partial s_{t_v}^{\,2}} - v_l \frac{\partial C}{\partial s_l} - \varphi R \lambda C + \sum_{i=1}^{Np} \varphi R \lambda_{pi} C_{pi} \qquad (2\text{-}2)$$

where:

D_l = longitudinal dispersion coefficient = $v_l \alpha_l + \varphi\, D_{eff}$ (L^2/T)

D_{th} = horizontal transverse dispersion coefficient = $v_l \alpha_{th} + \varphi\, D_{eff}$ (L^2/T)

D_{tv} = vertical transverse dispersion coefficient = $_{vl}\alpha_{tv} + \varphi\, D_{eff}$ (L^2/T)

s_l = direction of the flow line

s_{th} = direction normal to the flow line (horizontal)

s_{tv} = direction normal to the flow line (vertical)

As in the SDU release model, the saturated zone transport module of the GoldSim SDF All-Species Model simulates the transport of non-conservative species subject to sorption and either simple decay or ingrowth along decay chains.

2.1.2 GoldSim SDF Tc-99 Release Model

The GoldSim SDF Tc-99 Release Model is comprised of two components, (1) a GoldSim module, which evaluates the migration of Tc-99 transport through the individual SDUs, and (2) a FORTRAN dynamic link library (DLL) which evaluates the oxygen front movement through the SDUs and the associated oxidation of slag to develop cell-by-cell solubility-control mechanism transition times. The transport analysis performed in the GoldSim module is based on advective-diffusive transport through two sets of GoldSim mixing cells linked in series. The first set of cells is used to evaluate transport via vertical flow and matrix diffusion through the saltstone and the floor beneath (or the floor and upper mud mat for the 150-foot diameter and 375-foot diameter SDUs). The mass exiting the first set of mixing cells is linked to a second set of cells linked in series, which is used to simulate dissolved species transport through the UZ via vertical flow and matrix diffusion. In the first series of cells, the number of active cells is automatically set to the number of saltstone and floor (or floor and upper mud mat) layers used in the PORFLOW model for the SDU-type being simulated. Because of their initial oxidation state and relative thinness, the HDPE liner and the lower mud mat do not provide much of a barrier to Tc-99 release (except for the possible influence of the HDPE on flow) so they are not explicitly modeled. Note that any influence of the HDPE liner on flow rates through the SDU, is implicitly considered by the use of PORFLOW generated flow rates in the model.

Transport through each SDU is evaluated one column of cells at a time. This column-by-column analysis circumvents GoldSim limitations on cell network size and helps decrease analysis time to a practical level. Note that the assumption implicit to a single column analysis is that vertical flow through the SDUs dominates the release of Tc-99 from the SDUs.

In general, the influence and relative importance of horizontal diffusion on the Tc-99 release is minimized by the solubility control on the Tc-99. The exception is for cells, when dissolution of a large quantity of precipitated Tc-99 occurs at cell-specific oxidation

transition times. This is mainly important for cells near the outer perimeter of the saltstone. For interior cells, in a two-dimensional or quasi-two-dimensional model, the diffusion of mass at transition time moves the mass to adjacent cells where can be resorbed in a reducing environment or transported downward through previously oxidized cells. To account for releases by diffusion along the outside perimeter of the saltstone mass, the model allows the user to specify a percentage of a cells mass in place to be released to the UZ at cell-specific transition times.

The data requirements of the GoldSim SDF Tc-99 Release model include the cell-specific transition times associated with oxidation of reducing slag. For each cell, the transition time represents the time at which all of the slag in the cell has been oxidized. These times can be generated by PORFLOW, but the length of time needed for PORFLOW to calculate each simulated realization, limits the number of realizations that can be considered. For instance, the PORFLOW Tc-99 release simulations (for all SDUs) took approximately 24 days to complete. To allow for a reasonable number of parameter samplings for parameters that influence transition times such as flow fields, a FORTRAN DLL, *TransitionTime.dll* (Version 1.0), which evaluates cell-by-cell solubility-control transition times, was developed.

The DLL, *TransitionTime.dll*, is based upon the assumption that advection controls the oxygen front propagation. The transition time calculations proceed by following the oxygen front vertically through each column and horizontally through each row and choosing the minimum time needed to go through a cell, by either of the two processes, as the transition time. In the vertical column analysis, the oxygen front positions are determined by assuming purely advective retarded transport from cell to cell from the top of the saltstone to the bottom of the floor (or floor and upper mud mat (UMM) layers). In the horizontal row analysis, the oxygen front positions are determined by assuming purely advective retarded transport from cell to cell proceeding from the outside of the wall into the saltstone and from the column zone edges towards the inside and outside of the zone. The saltstone grout and concrete retardation values are based upon the ratios of the O_2 saturation to the saltstone grout and concrete reducing capacities.

The implications of the above assumptions on radionuclide transport results generated by the GoldSim SDF Tc-99 Release Model, are discussed in the benchmarking analysis presented in Section 5.1. As can be seen in Section 5.1, the use of the simplified process model produces Tc-99 release results with trends similar to the more rigorous fully coupled PORFLOW results.

2.2 Dose Calculator Model

In addition to simulating radionuclide transport, the GoldSim SDF All-Species Model contains a dose calculator designed to calculate MOP or IHI exposure levels, at specified points of assessment based on 1) the results from the transport abstraction module, or 2) output from the SDF PORFLOW Model. The dose calculations are abstracted from conceptualizations of possible exposure pathways. The SDF GoldSim Model implements dose calculations according to the dose methodology described within SRR-CWDA-2013-00058, Rev1.

3.0 SDF GOLDSIM MODEL UPDATES

In response to planned design-changes for future SDUs, the SDF PORFLOW Model has been updated to account for the construction of 375-foot diameter SDUs (see Figures 2.0-1). In addition to consideration of 375-foot diameter SDUs, the PORFLOW model was also updated to account for additional information gathered since the prior SA. These changes include changes to: (1) the degradation model for cementitious material, (2) the technetium release model, (3) radionuclide inventories, and (4) the use of grout clean-caps above the waste. In a parallel effort, Version 4.101 of the GoldSim SDF probabilistic model was updated to Version 5.006 allowing for consideration of the influence of the additional information on parameter sensitivity and parameter uncertainty analyses. Additional updates to the GoldSim model were also made to improve the computational efficiency of the model.

This section describes the updates implemented within the SDF GoldSim Model Version 5.006, relative to Version 4.101, to support the FY2014 SDF SA as well as other future special analyses. The major differences between SDF GoldSim Model Version 5.006 and the prior version, Version 4.101, include:

- The implementation of 375-foot diameter SDUs
- The removal of the clean-cap grout from 150-foot diameter SDUs
- Updating of inventories
- The replacement of PORFLOW generated flow field input files to reflect changes in the cementitious material degradation model
- The development of a standalone Tc-99 release model to allow for more flexible sampling of parameters that may influence O_2 transport and to greatly decrease the computational effort associated with evaluating Tc-99 release when it is considered to be controlled by a "shrinking-core" release mechanism
- Updating of data needed to consider the new locations of future SDUs

3.1 Special Analysis Specific Updates

This section describes the updates to the GoldSim model that were made to evaluate the implementation of 375-foot diameter SDUs, as well as the influence of additional information gathered regarding the radionuclide inventories and the degradation of cementitious material. To differentiate between the main and secondary GoldSim models, the main model is referred to as the GoldSim SDF All-Species Model

3.1.1 375-Foot Diameter SDUs

The major reason for the development of the FY2014 SDF SA is to evaluate the changes in maximum dose rates at the 100-meter compliance boundary and at the seven IHI wells that may occur when the new SDU construction plan, which includes 375-foot diameter SDUs, is implemented. A conceptual diagram of the newly designed 375-foot diameter SDUs, is presented in Figure 3.1-1. Parameters defining the approximate geometry of the conceptual model of a 375-foot diameter SDU, as implemented in the PORFLOW model are presented in Table 3.1-1. Note that the saltstone grout fills the space above the floor slab all the way up to the roof. This is part of the updated design for future SDUs. The spatial distribution of the future and previously constructed SDUs is presented in Figure 2.0-1.

To implement the calculations of radionuclide releases 375-foot diameter SDU, in the GoldSim SDF All-Species model, the submodel used to evaluate radionuclide release from the 150-foot diameter SDU was updated to allow for changes of SDU-specific input parameters based on SDU-type.

Figure 3.1-1: Conceptual Model for 375-foot Diameter SDUs (Typical)

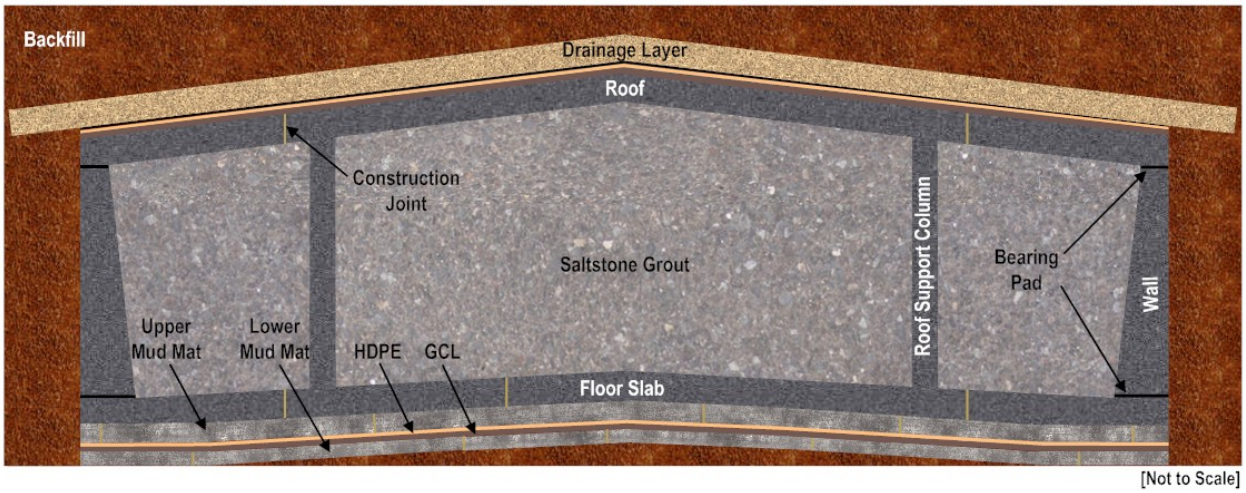

Table 3.1-1: Material Parameters for 375-foot Diameter SDU Conceptual Model

Component	Dimension	Units
Diameter (inner)	375	ft
Height (inner)	43	ft
Roof thickness	12	in
Roof and Floor slope	1.5	%
Floor thickness	12	in
Upper Mud Mat thickness	6	in
Lower Mud Mat thickness	4	in
Wall thickness, bottom	24	in
Wall thickness, top	10	in
HDPE and GCL thickness [a]	1	in
Bearing-pad thickness at roof	2	in
Bearing-pad thickness at floor	2	in
Base (top-of-floor) elevation [b] (relative to mean sea level)	265	ft
Water table depth [c]	42	ft
Sand drain thickness [d]	2	ft
Minimum backfill [d]	7	ft

Notes: These values are from Table 1 of HLW-SSF-TTR-2013-0021, Rev. 2 except as noted below:

(a) Value is assumed as a modeling simplification. Actual thickness is 300 mil.

(b) Nominal value (actual values will vary between units). Value is at the wall. Due to the 1.5% floor slope, the base elevation at the center of each SDU is approximately three feet higher.

(c) From SRNL-STI-2009-00115, Rev. 1, Table 45 and SRR-CWDA-2009-00017, Rev. 0, Table 4.2-11.

(d) From SRNL-STI-2009-00115, Rev. 1, Figure 60.

The number of mixing-cell columns located inside the column zone was also increased. This increase helps to account for the different positions of the column zone in the two models. The column zone (see Figure 3.1-1) is proportionately much farther from the center of the 375-foot diameter SDU than in the 150-foot diameter SDU. For consistency, seven columns of mixing cells are now also used to represent the inner cylinder of the 150-foot diameter SDU. In the simplified abstraction models of the 375-foot diameter and the 150-foot diameter SDUs, 38 columns of mixing cells represent the structure above the floor. In the updated model, seven mixing cell columns represent the inner grout zone, three the support column, 12 the outer grout zone, three the sheet drain, six the wall, three the vertical component of the HDPE, and four the backfill. Each column is comprised of a string of 21 mixing cells. The bottom mixing cells in the inner grout cylinder feed a single string of twenty mixing cells linked in series, ten representing the floor, five the upper mud mat (UMM) and five the lower mud mat (LMM). Similarly, the bottom mixing cells in the support column zone, the outer grout cylinder, and wall, each feed single strings of twenty mixing cells, of similar construct. The wall-to-floor joints are represented by a horizontal string of cells, which is fed by the bottom sheet drain and wall cells and which in turn feed the wall floor and adjacent HDPE cells. The bottom LMM cells and fill cells feed a single string of unsaturated zone (UZ) cells.

3.1.2 Omission of the Grout Clean-Cap in the 150-Foot Diameter SDUs

As can be seen in Figure 3.1-1, the saltstone grout completely fills the newly designed 375-foot diameter SDUs up to the roof. The elimination of the clean-cap and filling of the saltstone grout up to the roof is now the accepted modeling assumption for the 150-foot diameter SDUs. This change is a conservative representation of greater waste-grout fill heights [SRNL-STI-2014-00083]. This updated feature is implemented in the GoldSim SDF All-Species Model and the GoldSim SDF Tc-99 Release Model, as well as the FY2014 SDF SA PORFLOW model [SRNL-STI-2014-00083]. The implementation in the GoldSim SDF All-Species Model, includes the addition of an extra row of mixing cells to represent the waste being allowed to reach the roof. Note that the omission of the clean cap fill is only considered for the 150-foot diameter and 375-foot diameter SDUs, not SDUs 1 and 4.

3.1.3 FY2014 SDF SA Inventory Values

Developed for the FY2014 SDF SA, the radionuclide inventory values, presented in Table 3.1-2, have replaced the previous nominal inventory found in data elements used in the GoldSim SDF All-Species Model. The Tc-99 inventory values, presented in Table 3.1-2, are also used in the inventory data element in the GoldSim SDF Tc-99 Release Model. The SDU-specific radionuclide inventories for the FY2014 SDF SA, are based on the inventory estimates presented in *SDF Inventory Estimates for Transport Modeling,* Table 3.0-1. [SRR-CWDA-2013-00147] As discussed in the inventory estimates report, for radionuclides other than Tc-99, I-129, and Cs-135, conservative inventory assignments were used rather than the best estimate values used in previous analyses. A full description of the approach used to estimate this inventory is provided in the above referenced report.

Table 3.1-2: SDF Inventory Estimates in Curies for Use in Transport Modeling

Radionuclide	SDU 1	SDU 4	SDU 2A	SDU 2B	SDU 3A	SDU 3B	SDU 5A	SDU 5B
H-3	5.8E+00	1.0E+01	3.4E-01	2.7E-01	8.2E+02	8.2E+02	8.2E+02	8.2E+02
C-14	1.3E+00	6.6E+00	2.4E+00	2.3E+00	5.8E+02	5.8E+02	5.8E+02	5.8E+02
Al-26	2.6E-01	9.1E-01	9.1E-04	8.7E-04	2.4E+01	2.4E+01	2.4E+01	2.4E+01
Cl-36	1.9E-07	2.9E-02	1.7E-04	2.1E-04	9.5E-01	9.5E-01	9.5E-01	9.5E-01
K-40	1.9E-07	2.9E-02	1.7E-04	2.0E-04	9.5E-01	9.5E-01	9.5E-01	9.5E-01
Co-60	6.0E-05	8.3E-03	1.1E-05	1.2E-05	7.1E+00	7.1E+00	7.1E+00	7.1E+00
Ni-59	2.3E-03	8.0E-02	1.0E-03	7.0E-04	2.6E+00	2.6E+00	2.6E+00	2.6E+00
Ni-63	1.1E-01	2.7E+00	3.9E-02	2.7E-02	1.8E+02	1.8E+02	1.8E+02	1.8E+02
Se-79	3.4E-01	9.7E+00	1.3E-01	1.3E-01	8.9E+01	8.9E+01	8.9E+01	8.9E+01
Sr-90	7.8E-03	1.6E+03	7.0E+00	8.2E+00	3.6E+06	3.6E+06	3.6E+06	3.6E+06
Zr-93	6.9E-01	6.7E+00	2.8E-01	3.7E-01	9.5E+01	9.5E+01	9.5E+01	9.5E+01
Nb-94	2.0E-03	8.9E-02	1.8E-03	1.4E-03	5.4E-04	5.4E-04	5.4E-04	5.4E-04
Tc-99	5.5E+01	6.4E+02	1.2E+02	1.4E+02	5.4E+02	5.4E+02	5.4E+02	5.4E+02
Pd-107	8.4E-03	3.5E-02	6.1E-03	6.0E-03	9.5E-01	9.5E-01	9.5E-01	9.5E-01
Sn-126	1.2E+00	2.1E+00	7.5E-01	6.6E-01	3.9E+02	3.9E+02	3.9E+02	3.9E+02
I-129	2.0E-01	2.8E-01	8.5E-02	7.9E-02	9.6E-02	9.6E-02	9.6E-02	9.6E-02
Cs-135	9.8E-02	1.7E+00	5.6E-01	4.7E-01	9.0E-03	9.0E-03	9.0E-03	9.0E-03
Cs-137	4.5E+00	1.2E+05	2.6E+03	3.2E+03	2.3E+05	2.3E+05	2.3E+05	2.3E+05
Sm-151	4.2E-03	1.8E+01	1.3E-01	1.1E-01	3.7E+03	3.7E+03	3.7E+03	3.7E+03
Eu-152	7.1E-04	3.4E-02	4.6E-05	4.9E-05	7.8E+00	7.8E+00	7.8E+00	7.8E+00
Eu-154	1.5E-04	9.2E-01	4.7E-04	8.6E-04	9.6E+01	9.6E+01	9.6E+01	9.6E+01
Pt-193	1.3E+00	6.9E+00	9.3E-01	9.9E-01	7.3E+01	7.3E+01	7.3E+01	7.3E+01
Ra-226	4.6E-07	3.0E-05	1.3E-04	4.9E-04	1.3E+01	1.3E+01	1.3E+01	1.3E+01
Ra-228	7.8E-07	2.1E-05	1.4E-07	1.9E-07	2.3E-02	2.3E-02	2.3E-02	2.3E-02
Ac-227	8.1E-07	1.1E-05	1.4E-04	2.3E-07	8.4E-02	8.4E-02	8.4E-02	8.4E-02
Th-229	2.1E-04	3.8E-02	2.3E-03	3.9E-03	1.7E+01	1.7E+01	1.7E+01	1.7E+01
Th-230	4.9E-05	2.7E-03	3.0E-01	1.1E+00	1.3E+01	1.3E+01	1.3E+01	1.3E+01
Th-232	7.7E-06	2.1E-04	1.3E-05	1.8E-05	2.3E-01	2.3E-01	2.3E-01	2.3E-01
Pa-231	2.9E-06	3.8E-05	3.3E-02	1.5E-06	1.5E-01	1.5E-01	1.5E-01	1.5E-01
U-232	5.7E-04	1.0E-01	9.6E-03	9.1E-03	6.8E-02	6.8E-02	6.8E-02	6.8E-02
U-233	7.8E-02	8.7E+00	9.6E-01	1.3E+00	1.6E+01	1.6E+01	1.6E+01	1.6E+01
U-234	1.0E-01	5.7E+00	6.2E-01	8.2E-01	9.3E+00	9.3E+00	9.3E+00	9.3E+00
U-235	2.5E-03	3.4E-02	1.3E-03	1.3E-03	3.8E-01	3.8E-01	3.8E-01	3.8E-01
U-236	6.5E-03	8.1E-02	6.4E-03	8.5E-03	4.3E-01	4.3E-01	4.3E-01	4.3E-01
U-238	1.1E-02	7.9E-02	2.2E-02	2.7E-02	1.6E+01	1.6E+01	1.6E+01	1.6E+01
Np-237	3.9E-03	5.6E-01	1.8E-01	9.2E-02	2.7E+01	2.7E+01	2.7E+01	2.7E+01
Pu-238	8.7E-03	2.7E+02	4.3E+00	4.0E+00	1.5E+03	1.5E+03	1.5E+03	1.5E+03
Pu-239	1.7E-02	5.8E+01	5.7E-01	6.1E-01	1.5E+03	1.5E+03	1.5E+03	1.5E+03
Pu-240	1.7E-02	7.2E+01	5.7E-01	6.1E-01	1.5E+03	1.5E+03	1.5E+03	1.5E+03
Pu-241	9.8E-03	4.3E+01	3.1E-01	2.9E-01	1.6E+04	1.6E+04	1.6E+04	1.6E+04
Pu-242	1.6E-03	4.1E+00	3.8E-01	5.0E-01	4.5E+00	4.5E+00	4.5E+00	4.5E+00
Pu-244	1.0E-05	1.6E-02	1.8E-03	2.3E-03	2.1E-02	2.1E-02	2.1E-02	2.1E-02
Am-241	1.8E-03	1.9E+01	3.2E-02	4.5E-02	1.4E+04	1.4E+04	1.4E+04	1.4E+04
Am-242m	6.3E-05	1.7E-02	6.9E-03	6.2E-03	9.1E+00	9.1E+00	9.1E+00	9.1E+00
Am-243	1.4E-03	5.0E-01	4.9E-03	4.6E-03	6.9E-02	6.9E-02	6.9E-02	6.9E-02
Cm-243	3.2E-04	2.0E-03	2.4E-04	2.4E-04	2.6E-02	2.6E-02	2.6E-02	2.6E-02
Cm-244	1.7E-03	1.8E+01	2.0E-02	3.7E-02	9.4E+01	9.4E+01	9.4E+01	9.4E+01
Cm-245	2.8E-04	1.1E-03	1.9E-04	2.0E-04	5.6E-01	5.6E-01	5.6E-01	5.6E-01

Table 3.1-2 - Inventory Estimates in Curies for Use in Transport Modeling (continued)

Radionuclide	SDU 6	SDU 7	SDU 8	SDU 9	SDU 10	SDU 11	SDU 12
H-3	8.2E+02	8.2E+02	8.2E+02	8.2E+02	8.2E+02	8.2E+02	8.2E+02
C-14	5.8E+02	5.8E+02	5.8E+02	5.8E+02	5.8E+02	5.8E+02	5.8E+02
Al-26	2.4E+01	2.4E+01	2.4E+01	2.4E+01	2.4E+01	2.4E+01	2.4E+01
Cl-36	9.5E-01	9.5E-01	9.5E-01	9.5E-01	9.5E-01	9.5E-01	9.5E-01
K-40	9.5E-01	9.5E-01	9.5E-01	9.5E-01	9.5E-01	9.5E-01	9.5E-01
Co-60	7.1E+00	7.1E+00	7.1E+00	7.1E+00	7.1E+00	7.1E+00	7.1E+00
Ni-59	2.6E+00	2.6E+00	2.6E+00	2.6E+00	2.6E+00	2.6E+00	2.6E+00
Ni-63	1.8E+02	1.8E+02	1.8E+02	1.8E+02	1.8E+02	1.8E+02	1.8E+02
Se-79	8.9E+01	8.9E+01	8.9E+01	8.9E+01	8.9E+01	8.9E+01	8.9E+01
Sr-90	3.6E+06	3.6E+06	3.6E+06	3.6E+06	3.6E+06	3.6E+06	3.6E+06
Zr-93	9.5E+01	9.5E+01	9.5E+01	9.5E+01	9.5E+01	9.5E+01	9.5E+01
Nb-94	5.4E-04	5.4E-04	5.4E-04	5.4E-04	5.4E-04	5.4E-04	5.4E-04
Tc-99	3.7E+03	3.7E+03	3.7E+03	3.7E+03	3.7E+03	3.7E+03	3.7E+03
Pd-107	9.5E-01	9.5E-01	9.5E-01	9.5E-01	9.5E-01	9.5E-01	9.5E-01
Sn-126	3.9E+02	3.9E+02	3.9E+02	3.9E+02	3.9E+02	3.9E+02	3.9E+02
I-129	1.6E+00	1.6E+00	1.6E+00	1.6E+00	1.6E+00	1.6E+00	1.6E+00
Cs-135	1.4E-01	1.4E-01	1.4E-01	1.4E-01	1.4E-01	1.4E-01	1.4E-01
Cs-137	2.3E+05	2.3E+05	2.3E+05	2.3E+05	2.3E+05	2.3E+05	2.3E+05
Sm-151	3.7E+03	3.7E+03	3.7E+03	3.7E+03	3.7E+03	3.7E+03	3.7E+03
Eu-152	7.8E+00	7.8E+00	7.8E+00	7.8E+00	7.8E+00	7.8E+00	7.8E+00
Eu-154	9.6E+01	9.6E+01	9.6E+01	9.6E+01	9.6E+01	9.6E+01	9.6E+01
Pt-193	7.3E+01	7.3E+01	7.3E+01	7.3E+01	7.3E+01	7.3E+01	7.3E+01
Ra-226	1.3E+01	1.3E+01	1.3E+01	1.3E+01	1.3E+01	1.3E+01	1.3E+01
Ra-228	2.3E-02	2.3E-02	2.3E-02	2.3E-02	2.3E-02	2.3E-02	2.3E-02
Ac-227	8.4E-02	8.4E-02	8.4E-02	8.4E-02	8.4E-02	8.4E-02	8.4E-02
Th-229	1.7E+01	1.7E+01	1.7E+01	1.7E+01	1.7E+01	1.7E+01	1.7E+01
Th-230	1.3E+01	1.3E+01	1.3E+01	1.3E+01	1.3E+01	1.3E+01	1.3E+01
Th-232	2.3E-01	2.3E-01	2.3E-01	2.3E-01	2.3E-01	2.3E-01	2.3E-01
Pa-231	1.5E-01	1.5E-01	1.5E-01	1.5E-01	1.5E-01	1.5E-01	1.5E-01
U-232	6.8E-02	6.8E-02	6.8E-02	6.8E-02	6.8E-02	6.8E-02	6.8E-02
U-233	1.6E+01	1.6E+01	1.6E+01	1.6E+01	1.6E+01	1.6E+01	1.6E+01
U-234	9.3E+00	9.3E+00	9.3E+00	9.3E+00	9.3E+00	9.3E+00	9.3E+00
U-235	3.8E-01	3.8E-01	3.8E-01	3.8E-01	3.8E-01	3.8E-01	3.8E-01
U-236	4.3E-01	4.3E-01	4.3E-01	4.3E-01	4.3E-01	4.3E-01	4.3E-01
U-238	1.6E+01	1.6E+01	1.6E+01	1.6E+01	1.6E+01	1.6E+01	1.6E+01
Np-237	2.7E+01	2.7E+01	2.7E+01	2.7E+01	2.7E+01	2.7E+01	2.7E+01
Pu-238	1.9E+04	1.9E+04	1.9E+04	1.9E+04	1.9E+04	1.9E+04	1.9E+04
Pu-239	9.6E+03	9.6E+03	9.6E+03	9.6E+03	9.6E+03	9.6E+03	9.6E+03
Pu-240	1.9E+03	1.9E+03	1.9E+03	1.9E+03	1.9E+03	1.9E+03	1.9E+03
Pu-241	1.6E+04	1.6E+04	1.6E+04	1.6E+04	1.6E+04	1.6E+04	1.6E+04
Pu-242	4.5E+00	4.5E+00	4.5E+00	4.5E+00	4.5E+00	4.5E+00	4.5E+00
Pu-244	2.1E-02	2.1E-02	2.1E-02	2.1E-02	2.1E-02	2.1E-02	2.1E-02
Am-241	1.4E+04	1.4E+04	1.4E+04	1.4E+04	1.4E+04	1.4E+04	1.4E+04
Am-242m	9.1E+00	9.1E+00	9.1E+00	9.1E+00	9.1E+00	9.1E+00	9.1E+00
Am-243	6.9E-02	6.9E-02	6.9E-02	6.9E-02	6.9E-02	6.9E-02	6.9E-02
Cm-243	2.6E-02	2.6E-02	2.6E-02	2.6E-02	2.6E-02	2.6E-02	2.6E-02
Cm-244	9.4E+01	9.4E+01	9.4E+01	9.4E+01	9.4E+01	9.4E+01	9.4E+01
Cm-245	5.6E-01	5.6E-01	5.6E-01	5.6E-01	5.6E-01	5.6E-01	5.6E-01

[SRR-CWDA-2013-00147]

3.1.4 Updates to the PORFLOW Generated Flow Field Files

For the FY2013 SDF SA, a set of 36 flow cases were developed (see Table 3.1-3). The sampling set of 36 flow cases was developed for the FY2013 SDF SA to evaluate the effects on flow from varying the input values for selected parameters. These flow parameters were:

1. Infiltration rate and associated sand drainage layer degradation (minimum, average, or maximum values) as provided in Section 3.3.4 of the FY2013 SDF SA. [SRR-CWDA-2013-00062]
2. Cementitious material degradation (nominal or best estimate) provided in Section 4.2.2 of the FY2013 SDF SA. [SRR-CWDA-2013-00062] In addition some degradation rates were revised to simulate the omission of the clean cap.
3. Initial saturated hydraulic conductivity of saltstone and clean cap (maximum, nominal, or best estimate) provided in Section 4.2.1 of the FY2013 SDF SA. [SRR-CWDA-2013-00062].
4. Moisture Characteristic Curves (MCCs) for joints assuming a gravel medium, as discussed in Section 4.2.3, or assuming a relative permeability of 1 for all suction levels as defined in the FY2013 SDF SA. [SRR-CWDA-2013-00062]

For the FY2013 SDF SA, a subset of 12 of the flow cases (as denoted by the superscript [1] in Table 3.1-3) for each SDU type was simulated using the SDF PORFLOW Model to generate Tc-99 releases to the saturated zone. The Tc-99 release time-histories for the 12 flow cases were generated by PORFLOW. These time-histories were then used as model inputs, which could be sampled from by the saturated zone transport component of the SDF GoldSim Model (Version 4.104). Specifically, flow cases F1, F4, F5, F14, F15, F16, F17, F25, F26, F28, F29, and F30, were selected as cases to be sampled from.

The limited number of flow fields was utilized because of the computational effort needed to generate the Tc-99 releases from each SDU especially when multiple solubilities were considered. The 12 flow fields were chosen, as representative of the 36 flow cases, because they reflect major differences in the volumetric flow rates found in the 36 cases. [SRR-CWDA-2013-00062] Of the 36 flow cases, 18 were screened out from further analysis based on the MCCs of the joints. The preliminary SDF PORFLOW Model simulation results indicated that varying the MCCs of the joints provided a negligible impact with respect Tc-99 release.

For the FY2014 SDF SA, the PORFLOW flow model was revised to reflect minor updates to the cementitious materials degradation rates [SRNL-STI-2013-00118]. As noted in [SRNL-STI-2014-00083], the revised cementitious material degradation analysis produced minor differences in degradation times, except for the 150-foot diameter and 375-foot diameter SDU roof concrete. The differences in the roof degradation times were caused by the omission of the clean-cap fill between waste grout and the roof. In previous degradation time analyses the external sulfate attack, on the underside of the roof, was delayed by the sulfate-free clean cap. Without the clean cap, the roof becomes exposed immediately to sulfate attack resulting in earlier degradation times.

Therefore, the PORFLOW-generated flow field files used by the GoldSim model were regenerated. In addition, since the GoldSim SDF Tc-99 Release Model now generates the Tc-99 release time-histories, the need to limit the number of cases is precluded. For the

FY2014 SDF SA GoldSim uncertainty modeling, it was decided to generate flow fields for a subset of the flow cases listed in Table 3.1-3. Since the choice of the joint material MCC, had negligible effect on the flow fields, the gravel MCC, was assumed and only 18 cases were evaluated. In addition to reduce the computational burden for regenerating the flow fields, only a subset of the flow fields were regenerated for SDUs 1 and 4 (specifically, Flow Cases F1, F4, F5, F14, and F30 were updated). The FY2013 SDF SA flow fields were used for the remainder of the SDUs 1 and 4 flow fields. The final list of flow cases used in the FY2014 SDF SA are listed in Table 3.1.4.

Table 3.1-3: Summary of Flow Cases

Case	Infiltration Rate	Cementitious Material Degradation Rate	Initial Saltstone Saturated Hydraulic Conductivity (cm/sec)	Joint Material for MCC
F1 [1]	Average	Nominal	6.4E-09	Gravel
F2	Average	Nominal	4.5E-07	Gravel
F3	Average	Nominal	3.9E-10	Gravel
F4 [1]	Average	Expected	6.4E-09	Gravel
F5 [1]	Average	Expected	4.5E-07	Gravel
F6	Average	Expected	3.9E-10	Gravel
F7	Average	Nominal	6.4E-09	K_{rel}=1
F8	Average	Nominal	4.5E-07	K_{rel}=1
F9	Average	Nominal	3.9E-10	K_{rel}=1
F10	Average	Expected	6.4E-09	K_{rel}=1
F11	Average	Expected	4.5E-07	K_{rel}=1
F12	Average	Expected	3.9E-10	K_{rel}=1
F13	Maximum	Nominal	6.4E-09	Gravel
F14 [1]	Maximum	Nominal	4.5E-07	Gravel
F15 [1]	Maximum	Nominal	3.9E-10	Gravel
F16 [1]	Maximum	Expected	6.4E-09	Gravel
F17 [1]	Maximum	Expected	4.5E-07	Gravel
F18	Maximum	Expected	3.9E-10	Gravel
F19	Maximum	Nominal	6.4E-09	K_{rel}=1
F20	Maximum	Nominal	4.5E-07	K_{rel}=1
F21	Maximum	Nominal	3.9E-10	K_{rel}=1
F22	Maximum	Expected	6.4E-09	K_{rel}=1
F23	Maximum	Expected	4.5E-07	K_{rel}=1
F24	Maximum	Expected	3.9E-10	K_{rel}=1
F25 [1]	Minimum	Nominal	6.4E-09	Gravel
F26 [1]	Minimum	Nominal	4.5E-07	Gravel
F27	Minimum	Nominal	3.9E-10	Gravel
F28 [1]	Minimum	Expected	6.4E-09	Gravel
F29 [1]	Minimum	Expected	4.5E-07	Gravel
F30 [1]	Minimum	Expected	3.9E-10	Gravel
F31	Minimum	Nominal	6.4E-09	K_{rel}=1
F32	Minimum	Nominal	4.5E-07	K_{rel}=1
F33	Minimum	Nominal	3.9E-10	K_{rel}=1
F34	Minimum	Expected	6.4E-09	K_{rel}=1
F35	Minimum	Expected	4.5E-07	K_{rel}=1
F36	Minimum	Expected	3.9E-10	K_{rel}=1

[1] Used for solubility limit sampling in the FY2013 SDF SA.
Adapted from SRNL-STI-2013-00280 Rev. 0, Table 4-1.

Table 3.1-4: Summary of Evaluation Flow Cases for the FY2014 SDF SA

Case	Infiltration Rate	Cementitious Material Degradation Rate	Initial Saltstone Saturated Hydraulic Conductivity (cm/s)	Joint Material for MCC
F-1	Average	Nominal	6.4E-09	Gravel
F-2	Average	Nominal	4.5E-07	Gravel
F-3	Average	Nominal	3.9E-10	Gravel
F-4	Average	BE	6.4E-09	Gravel
F-5	Average	BE	4.5E-07	Gravel
F-6	Average	BE	3.9E-10	Gravel
F-13	Maximum	Nominal	6.4E-09	Gravel
F-14	Maximum	Nominal	4.5E-07	Gravel
F-15	Maximum	Nominal	3.9E-10	Gravel
F-16	Maximum	BE	6.4E-09	Gravel
F-17	Maximum	BE	4.5E-07	Gravel
F-18	Maximum	BE	3.9E-10	Gravel
F-25	Minimum	Nominal	6.4E-09	Gravel
F-26	Minimum	Nominal	4.5E-07	Gravel
F-27	Minimum	Nominal	3.9E-10	Gravel
F-28	Minimum	BE	6.4E-09	Gravel
F-29	Minimum	BE	4.5E-07	Gravel
F-30	Minimum	BE	3.9E-10	Gravel

"BE" refers to best estimate values for cementitious material degradation rates.

[SRR-CWDA-2013-00064]

3.2 Improvements to Computational Efficiency

To allow for stochastic sampling of SDU inventories and solubility limits, the generation of Tc-99 release time-histories for the 15 SDUs (see Figure 2.0-1), using PORFLOW in conjunction with the "shrinking-core" model, takes approximately 24 days of machine-time. By using multiple machines/processors, the total time needed to generate the files is reduced, but developing multi-realization stochastic input for the SDF GoldSim Model is a formidable task. In order to circumvent the computational effort needed to develop the PORFLOW SDF model Tc-99 release time-histories, a standalone GoldSim-based model (the GoldSim SDF Tc-99 Release Model) was developed to generate the Tc-99 release time-histories.

The GoldSim SDF Tc-99 Release Model is comprised of two components, (1) a GoldSim module, which evaluates the migration of Tc-99 transport through the individual SDUs, and (2) a FORTRAN dynamic link library (DLL) which evaluates cell-by-cell solubility-control mechanism transition times.

3.2.1 The GoldSim SDF Tc-99 Release Model

The transport analysis performed in the GoldSim module, is based on advective-diffusive transport through two sets of GoldSim mixing cells, with all cells in the network linked in series. This one-dimensional network (string) of mixing-cells is used to approximate the vertical migration of Tc-99 through a single PORFLOW SDF model column of cells via advection and matrix diffusion through the saltstone, the floor beneath (or the floor and upper mud mat for the 150-foot diameter and 375-foot diameter SDUs), and finally through the

unsaturated zone beneath the SDU. The mass exiting the first string of mixing cells (representing the saltstone and floor components) migrates via flow and diffusion into a second series of cells (representing the UZ). The mass is then transported through the UZ via vertical flow and matrix diffusion and the mass flux rates out of the last UZ cell are recorded and the sum of releases from all modeling-cell columns (for each SDU) is output as a time-history to be read by the GoldSim SDF All-Species Model. In the first series of cells, the number of active cells is automatically set to the number of saltstone and floor (or floor and upper mud mat) layers used in the PORFLOW model for the SDU-type being simulated.

This one-to-one relationship of cells between the GoldSim and PORFLOW models is needed to effectively approximate the influence of cell-specific solubility control mechanism transition times used in the PORFLOW "shrinking-core" model. The PORFLOW "shrinking-core" model fully couples oxygen transport and slag oxidation to determine the time-dependent solubility control state of each cell in the model. Note that, because of their initial oxidation state and relative thinness, the HDPE liner and lower mud mat do not provide much of a barrier to Tc-99 release (except for the possible influence of the HDPE on flow) and are therefore not explicitly modeled. Any influence of the HDPE liner on flow rates through the SDU, is implicitly considered by the use of PORFLOW generated flow rates in the model. Note that as a simplification, the "shrinking-core" model implemented in the GoldSim model simulates the FY2013 SDF SA PORFLOW version of the "shrinking-core" model. The FY2013 SDF SA PORFLOW "shrinking-core" model assumes that all precipitate in a cell dissolve during a single time step at the time that the last remaining slag in the cell is oxidized. [SRR-CWDA-2013-00062] The more rigorous FY2014 SDF SA version described herein, assumes that precipitated Tc-99 in a cell continuously dissolves as the reducing capacity of the slag is used up.

As noted above, transport through each SDU is evaluated one column of modeling cells at a time. This column-by-column analysis circumvents GoldSim limitations on mixing-cell network size and helps decrease analysis time to a practical level. Note that an assumption implicit to a single modeling-column analysis is that vertical flow through the SDUs dominates the release of Tc-99 from the SDUs. In general, vertical flow controls the releases, and the influence and relative importance of horizontal diffusion on the Tc-99 release is minimized by the solubility control on the Tc-99. The exception is at the time when dissolution of a large quantity of precipitated Tc-99 occurs in a cell at its cell-specific solubility-mechanism transition time. This is process is mainly important for modeling cells near the outer perimeter of the saltstone or near the roof-support column zone where a buildup of mass may occur. For more interior modeling cells, in a two-dimensional or quasi-three-dimensional (radial) model, the diffusion of mass at transition time moves the mass to adjacent cells where can be resorbed in a reducing environment or transported downward through previously oxidized cells.

To account for releases by diffusion along the outside perimeter of the saltstone mass, and near roof-support column zones, the model allows the user to specify an approximate percentage of a cell's Tc-99 mass in place, to be released directly to the UZ at the solubility-control transition time. The release, to the UZ, is controlled by a GoldSim *Direct Transfer Mass Flux Link*, found in each cell. Activation of the link is a function of proximity to the

cell perimeter or roof-support column zone. The release rate is controlled by setting the links fractional transfer rate (FTR) as follows:

$$FTR = \frac{\ln \frac{1}{(100\% - \%_{Transferred})/100}}{T_{step}} \quad (3.2\text{-}1)$$

Where $\%_{Transferred}$ is a user chosen percent of the in-place mass to be transferred and T_{step} is the time step length. Note that because the GoldSim *Direct Transfer Mass Flux Link*, is based on a first order decay term, the use of a single time step, reduces the accuracy.

3.2.2 Transition Time Dynamic Link Library

The data requirements of the GoldSim SDF Tc-99 Release Model include the cell-specific oxidation transition times. These transition times represent the time for each cell, at which all of the slag in the cell has been oxidized. These transition times can be generated by PORFLOW, but because of the length of time needed for each PORFLOW simulation, the number of realizations that can be considered is limited (see Section 3.2). To allow for a greater diversity in sampling of parameters that influence transition times such as flow fields, a FORTRAN DLL, which evaluates cell-by-cell solubility-control transition times, was developed. The DLL, *TransitionTime.dll*, Version 1.0, assumes that the oxygen transport, which controls the slag oxidation rate and timing within each cell, is dominated by advection. The transition time calculations evaluated as two separate processes, one vertical and one horizontal.

To approximate the transition times with minimal computational effort, oxygen front movement is tracked separately in the vertical and horizontal directions. First, the program tracks the oxygen front vertically downward through each column of mixing cells. Note that the mixing –cell column and row discretization used in the calculations is consistent with the PORFLOW model discretization. The front velocity is a function of the PORFLOW-generated vertical flow rate controlling the amount of oxygen moving through the SDU. In addition to the flow rate, the front movement is controlled by the rate at which the slag in the saltstone or concrete is oxidized (the reduction capacity is consumed), which is a function, the oxygen saturation and the solid materials reduction capacity. In the present model, the O_2 saturation value is set to 1.06E-03 milliequivalents per milliliter (meq e-/mL), and the initial reduction capacity for a saltstone cell is 0.607 meq e-/g and the initial reduction capacity for a concrete cell is 0.178 meq e-/g. When the slag's reduction capacity within a cell is entirely consumed, a cell-specific transition time is set.

The calculations proceed downwards from mixing-cell to mixing-cell. When calculating the front movement rate through a cell, the front movement is initiated at the time when the slag in the cell above is completely oxidized. During the calculation an additional component of oxygen from the adjacent cell of the same layer is assumed to flow into the cell. The horizontal component of oxygen entering the mixing-cell is based upon the horizontal flow rate into the cell.

After tracking front movement down the mixing-cell columns, the oxygen front positions are tracked along rows, proceeding from the outside of the wall into the SDU and proceeding from the roof-support column zone edges towards the center of the SDU and outwards from the zone. In the horizontal front tracking procedure, the starting time for slag oxidation in a

cell is set to either the transition time determined for the upgradient cell (during horizontal tracking) or the transition time determined for the upgradient cell in the vertical tracking calculations. The final transition time for mixing-each cell is the minimal value derived from each method.

The simplified methodology described above represents a computationally efficient approximation to the more rigorous fully coupled analysis performed in PORFLOW simulations. The implications of the simplifying assumptions with respect to the GoldSim SDF Tc-99 Release Model, are discussed in the benchmarking analysis presented in Section 5.1. In Section 5.1, the resultant Tc-99 release rates based upon the simplified process model show similar trends to the more rigorous fully coupled PORFLOW runs, capturing the localized effects of the cell-by-cell solubility controls.

4.0 STRUCTURE OF THE SDF GOLDSIM MODEL

Section 4.1 presents a brief overview of updates, to the basic structure of the GoldSim SDF All-Species Model, implemented in Version 5.006. Section 4.2 describes the basic structure of the GoldSim SDF Tc-99 Release Model (Version 1.006) and its relationship with the DLL, *TransitionTime.dll*, which generates the solubility-control mechanism transition times needed by the GoldSim model.

4.1 GoldSim SDF All-Species Model Organization

Like all GoldSim models, the GoldSim SDF All-Species Model, is organized in a hierarchy, with the top level of the model shown in Figure 4.1-1. Model containers, represented as yellow boxes unless assigned special attributes (i.e., looping containers, submodels, etc.), are used to organize model components. The upper tier of the GoldSim SDF All-Species Model hierarchy can be viewed as two components, 1) an abstraction of the SDF PORFLOW model, and 2) a dose calculator. The solute transport abstraction section includes seven GoldSim containers comprised of the input data (*GlobalModel_Input*, *User_Input*, *Materials*, and *Transport*), the model calculation logic (*DisposalUnits*), and transport model output (*Model_Concentrations* and *Benchmark*). Brief descriptions of the upper-level containers and their contents are presented below:

- *UserInput* contains global modeling parameters that control the setup and execution of the model. These parameters include switches that enable specific transport phenomena to be included or excluded, control the specific sources of contamination, and indicate whether or not a transport simulation is to be performed and used as the basis for dose or whether SDF PORFLOW Model results are used as the basis for dose.
- *GlobalModel_Input* container holds various modeling constants that are used throughout the model. In addition, the *GlobalModel_Input* container contains file elements that automatically pass GoldSim SDF Tc-99 Release Model generated Tc-99 release files to the Slave Containers.
- *Transport* contains the data elements necessary to define the geometry of the system being analyzed. In addition to specific data, the container is also comprised of stochastic elements that are used to describe the uncertainty in the geometrical aspects of the system where applicable.
- *Materials* contains the list of radionuclides simulated in the model and their basic properties (atomic weight, half-lives, etc.) and all parameters defining the porous media that are used in the model (such as porosities and bulk densities). Other parameters defining the transport process in a porous media includes the linear soil/water partition coefficients (K_ds) for the various media. The basic definition of the fluid (water) element (including diffusion coefficients) is found in this container, but cloned fluid elements are found in various other containers where the diffusion coefficients are redefined for specific zones such as saltstone, walls, and floor materials. In addition, it should be noted that the FDC submodel contains its own basic fluid element and zone specific clones.
- The *Inventory* container is comprised of inventory data, including nominal values and stochastic elements that define uncertainty in the estimated values. In addition *Inventory*

contains an alternative inventory option, in which tank-based inventories are used and the tank inventories are transferred to the FDCs. The transfer distribution pattern is based on random sampling of the FDC filling order.

- The *Transport* container is comprised of parameters that define the saturated-zone flow fields and geometry for both MOP and IHI calculations.
- The *DisposalUnit* Container includes three transport calculation containers, one for the "Vaults" (SDUs 1 and 4), and one for the 150-foot diameter and 375-foot diameter SDUs (Figure 4.1-2). The container for the 150-foot diameter and 375-foot diameter SDUs, contains a looping environment that cycles through the 13 cylindrical SDUs or a subset of the 13 SDUs (see Table 4.1-1 and Figure 4.1-2) using a single GoldSim submodel (GTG-2010e). The submodel activates a calculation container, *FDCs*, for the set of thirteen 150-foot diameter and 375-foot diameter SDUs or a selected one of the thirteen SDUs. Radionuclide releases from each source and subsequent migration to the 100-meter boundary or IHI well are simulated to derive the concentrations used in dose calculations. *FDC_output* contains the time series elements used to capture results generated in the transport submodel and copied into the time series elements one source FDC at a time. The *PlumeCalc_Sectors* container contains the GoldSim Plume Function calculations (GTG-2010e), which generate dilution/attenuation factors accounting for transverse dispersive processes. The dilution/attenuation factors help determine the contribution from each SDU to the concentration at each MOP sector or IHI observation well (see Figure 4.1-2). The dilution/attenuation factors reflect the influence of transverse horizontal and vertical dispersion on the concentrations generated by the 1-D saturated zone transport pipe-element calculations performed in *DisposalUnits*. *Tc99Input* contains the external elements used to read in Tc-99 mass flux breakthrough curves for SDU 1 and SDU 4 (similar elements for the FDCs are found in the FDC submodel). The *VaultData* container contains the SDU geometry data for each of the four SDU types. The *PoreFlushes* container is comprised of data elements containing pore flush calculation data. Note that the pore-flush data is not presently used in the model since the transition times are read from the SDF PORFLOW Model generated files.
- The *Model_Concentrations* container is comprised of the set of elements used to assemble the final concentrations used in the dose calculations.
- *Benchmark* is comprised of a set of time-series elements containing the PORFLOW concentration outputs used for PORFLOW/GoldSim concentrations comparisons. Time history results comparing result elements for comparing GoldSim and PORFLOW Sector Concentrations are included. These time-series elements have not been updated for Version 5.006 and should not be used for benchmarking.
- *Dose_Parameter_Calculations* is comprised of elements used to calculate doses based on concentrations assembled in *Model_Concentrations*.
- *Dose_Results* contains the results from the dose calculations.
- *SensitivityAnalysis_New* contains the elements necessary to collect information for the sensitivity analysis, including final values of model endpoints (e.g., water concentrations

or dose to a human receptor) and the values of each input stochastic used for each realization in a probabilistic analysis.

Table 4.1-1: SDU Numbering In GoldSim Models

SDU Number	SDU Name
1	SDU 2A
2	SDU 2B
3	SDU 3A
4	SDU 3B
5	SDU 5A
6	SDU 5B
7	SDU 6
8	SDU 7
9	SDU 8
10	SDU 9
11	SDU 10
12	SDU 11
13	SDU 12
14	Vault 1 (also known as SDU 1)
15	Vault 4 (also known as SDU 4)

Figure 4.1-1: SDF GoldSim Model Organization

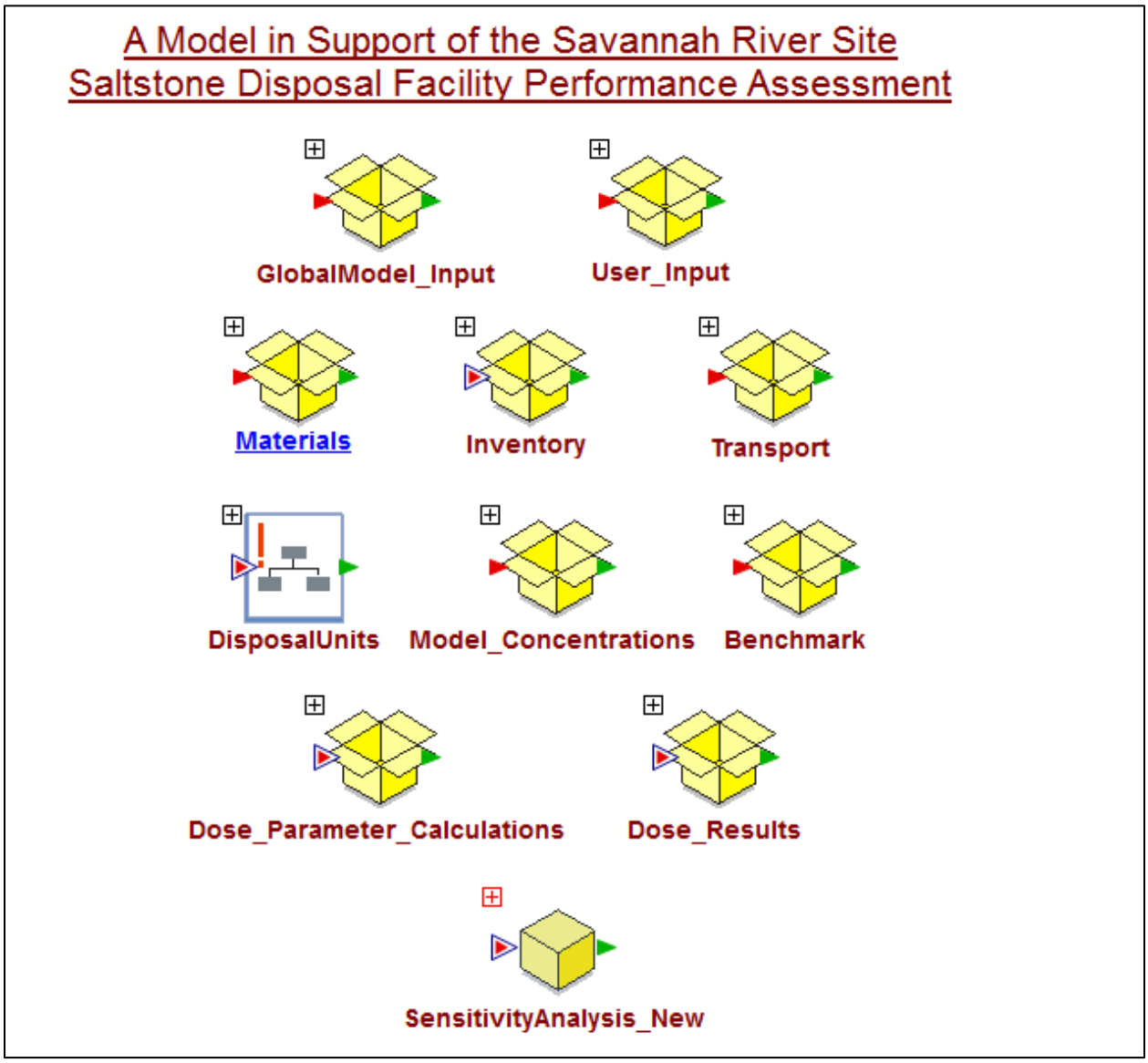

Figure 4.1-2: Sectors Along the 100-Meter Boundary for the FY2014 SDF SA

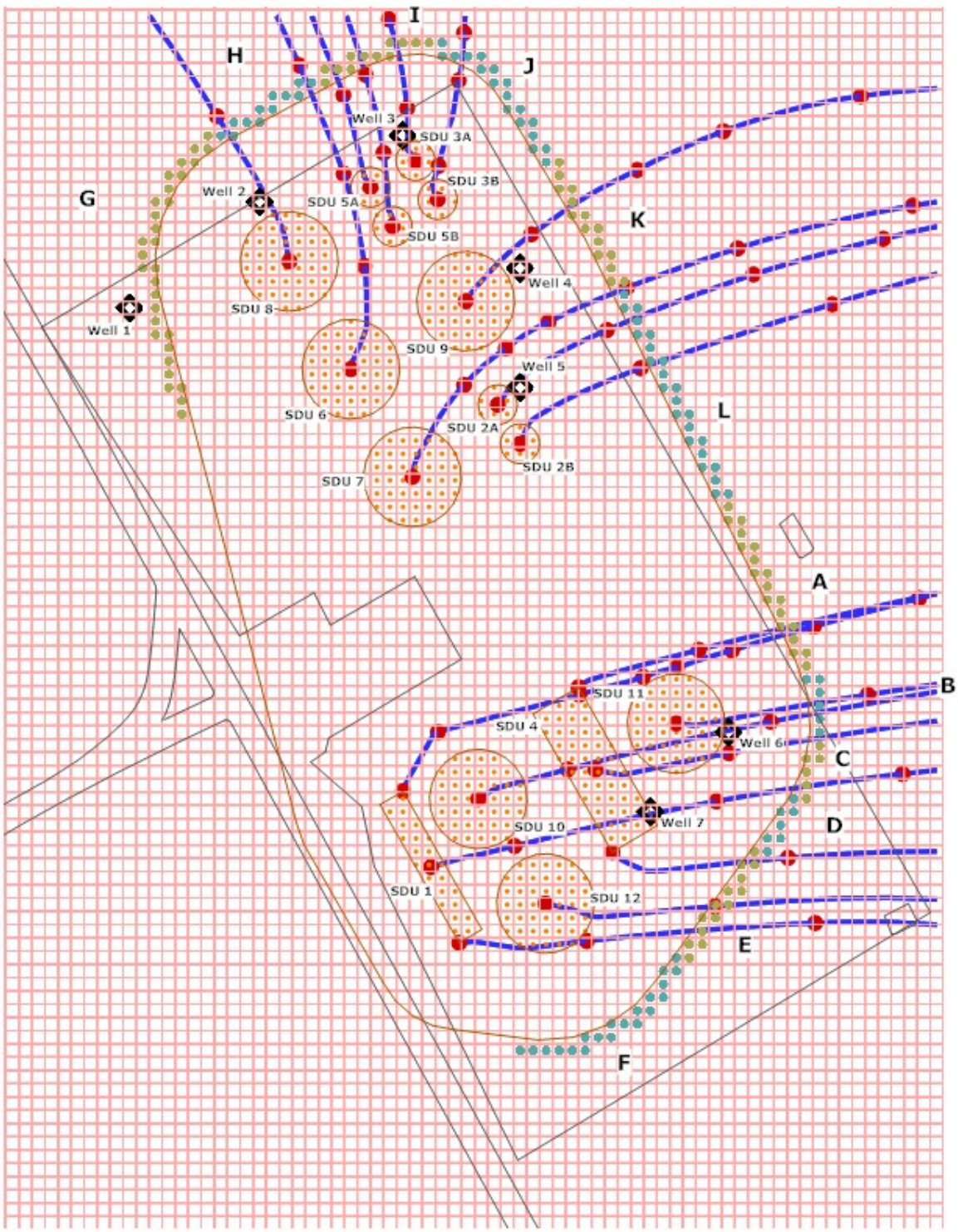

4.1.1 Radionuclide Transport Modeling

The container in which the radionuclide transport calculations take place (*DisposalUnits*), is comprised of four main containers controlling the release of radionuclides from SDUs and the subsequent migration of the radionuclides to the 100-meter boundary and IHI wells (see Figure 4.1-3). Two of the containers (*Vault_1* and *Vault_4*) contain the GoldSim elements used to calculate radionuclide release from the SDUs and subsequent migration through the UZ and SZ to the 100-meter boundary and IHI wells. The container *FDCs* contains the equivalent elements controlling radionuclide release from the 150-foot diameter and the 375-foot diameter SDUs and subsequent migration to the 100-meter boundary and IHI wells.

The contents of a fourth container (*PlumeCalc_Sectors*) are used to calculate the transverse dispersion factors for expanding the saturated zone transport module results to three dimensions. These dilution factors are superimposed on the one-dimensional transport model results generated in the *Vault_1, Vault_4,* and *FDC* containers to approximate three-dimensional results. The *Tc99Input* container contains the logic that controls the importing of data generated from the GoldSim SDF Tc-99 release Model for Vaults 1 and 4 (also known as SDUs 1 and 4, respectively). The *FDC_Output* container, captures time series outputted by the submodel that evaluates radionuclide migration within and from the thirteen 150-foot diameter and 375-foot diameter SDUs. Dose calculations are performed inside *Dose_Parameter_Calculations* and the results are presented inside *Dose_Results.*

The *FDCs* container is comprised of two nested looping containers (see Figures 4.1-4 and 4.1-5). The nested containers (*OuterLoop* and *InnerLoop*) serve the same purpose as nested do-loops in a FORTRAN or C^{++} program looping through the radionuclide transport calculations for each of the 13 FDCs depicted in Figure 4.1-2 (FDCs include the 150-foot diameter and 375-foot diameter SDUs and not the Vault 1 and Vault 4) or a selected one of the thirteen. Within the innermost of the looping containers is a GoldSim submodel element, which serves as a complete "inner model" that is imbedded within the "main model." The submodel element (*FDC_TransportSubmodel*) uses its own time stepping scheme (which under most conditions should be set the same way as the main model time stepping scheme). After the looping containers have evaluated all of the FDCs (or a single FDC), Vault1 and Vault 4, 100-meter boundary and IHI well concentrations are calculated at each time step. After the Vault 1 and Vault 4 concentrations are calculated for a time step, these concentrations are passed to the dose calculator along with previously saved FDC concentrations for processing. The *DisposalUnits* container is comprised of eight active containers (Figure 4.1-3). Containers *Vault_1, Vault_4,* and *FDCs* contain the GoldSim elements used to calculate vadose zone releases of radionuclides and the 1-D advective-dispersive transport of radionuclides through the saturated zone.

Vault_1 and *Vault_*4 contain the radionuclide-transport calculation logic for Vault 1 (SDU 1) and Vault 4 (SDU 4), respectively. The *FDCs* container is comprised of the equivalent logic for the 13 FDCs (six 150-foot diameter and seven 375-foot diameter SDUs as depicted in Figure 4.1-2). *FDCs* contains two nested looping containers that are analogous to do-loops, allowing the model to evaluate the 13 FDCs. The outermost of the nested containers *FDCs,* contains the looping container *OuterLoop* (Figure 4.1-4) which is designed to loop through the 13 FDCs (or a subset of them), calling the transport submodel each time. The two data

elements in the container define the number of FDCs (*NFDCa*) and when desired a specified FDC to simulate (*RunThisFDC).* *RunThisFDC* is controlled by setting *FDC_Choice* (which controls *RunThisFDC*) in *User_Input* to the desired FDC Number (see Table 4.1-1). If *FDC_Choice* is set to zero, the submodel will loop 13 times. If a specific source is defined (e.g., "3" for SDU 3A, as listed in Table 4.1-1), only the requested source will be evaluated and results in the submodel can be saved. The *FDCs* container deactivates when the time stepping begins in the main model.

Figure 4.1-3: Contents of Container *DisposalUnits*

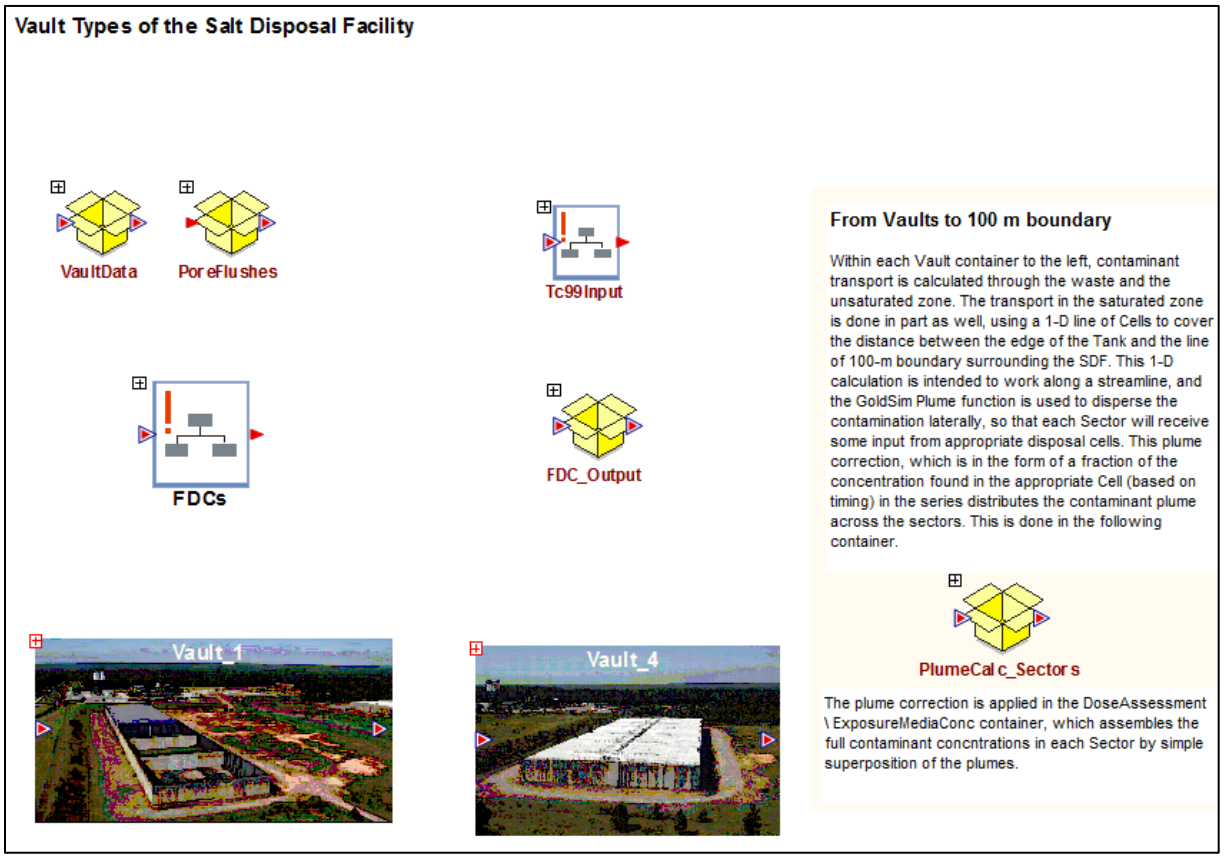

Figure 4.1-4: Contents of Container *FDCs*

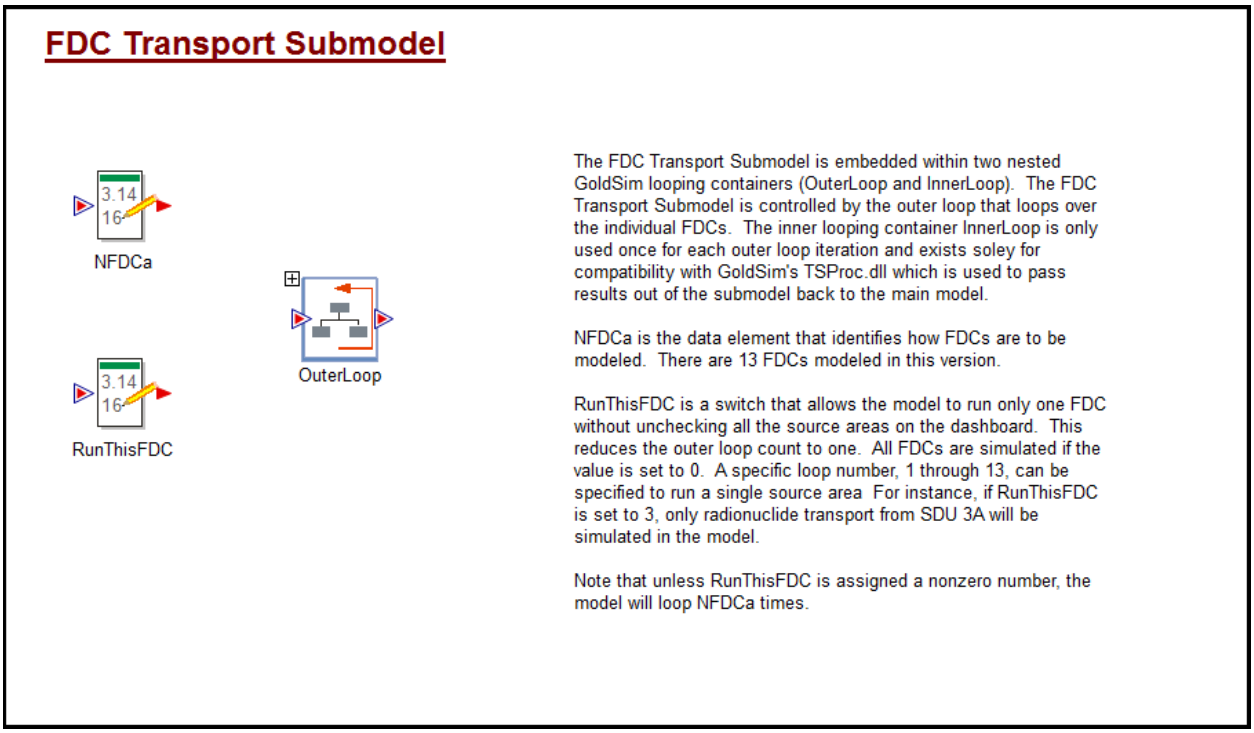

Nested inside the looping container *OuterLoop*, is an inner looping container, *InnerLoop* (Figure 4.1-5). *InnerLoop* is used only once for each outer loop iteration (as indicated by the data element *NInnerLoop*) and exists solely for compatibility with GoldSim's C^{++} software *TSProc.dll*, which is used to pass results out of the transport submodel back to the main model. *OuterLoop* also contains two selector elements which are used to control which source is being run and when the analysis is completed (Figure 4.1-5).

The transport submodel for evaluating the FDCs, *FDC_TransportSubmodel* is located within the innermost of the nested looping containers (Figure 4.1-6), and it is within this GoldSim submodel element that the mass transport calculations are performed. In addition to *FDC_TransportSubmodel*, *InnerLoop* contains a selector switch to indicate when the inner loop is finished.

TS_ProcFDCs (Figure 4.1-7), contains an external element (GTG-2010d), that controls the use of *TSProc1.dll*, which is a DLL used to copy time series, from the submodel into the main model. Note that *TSProc1.dll* is a renamed copy of *TSProc.dll*.

Figure 4.1-5: Contents of Container *OuterLoop*

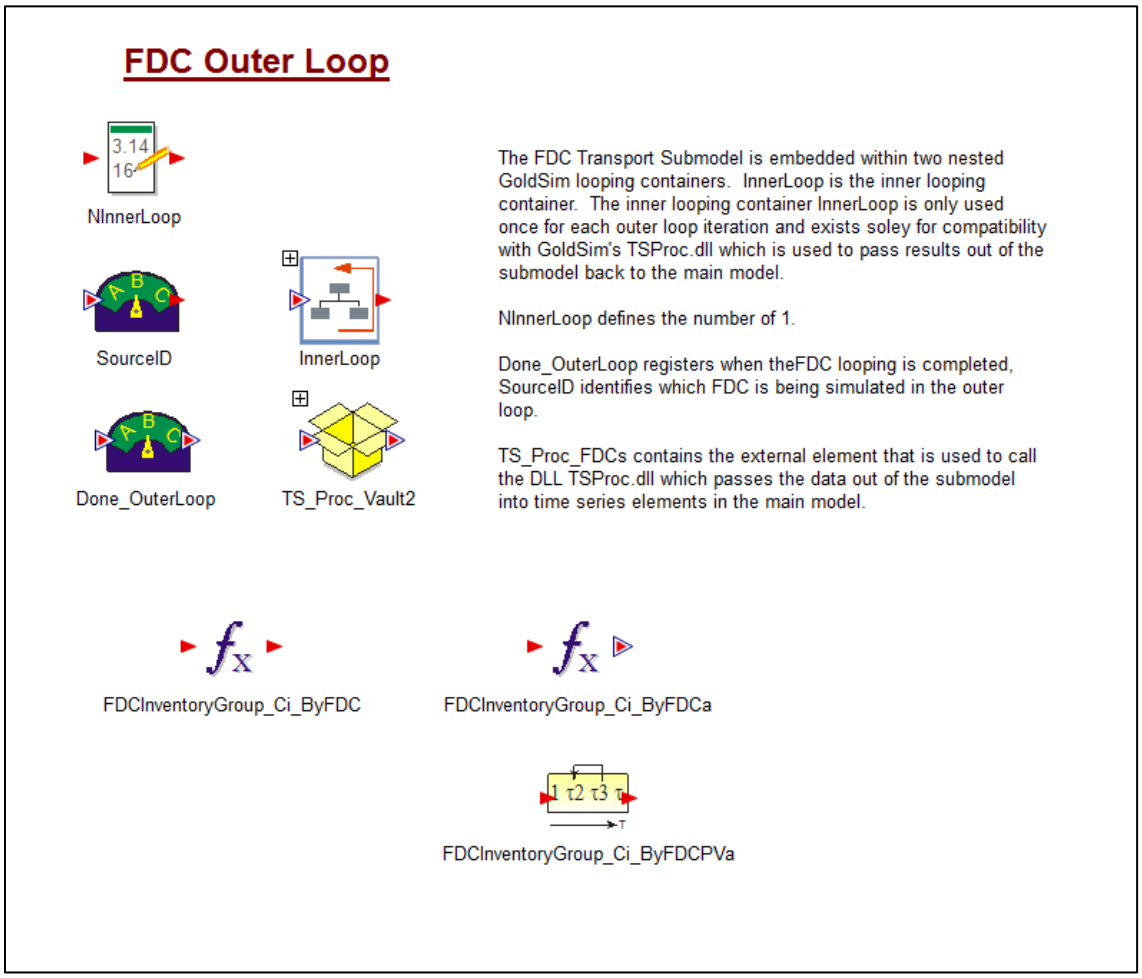

Figure 4.1-6: Contents of Container *InnerLoop*

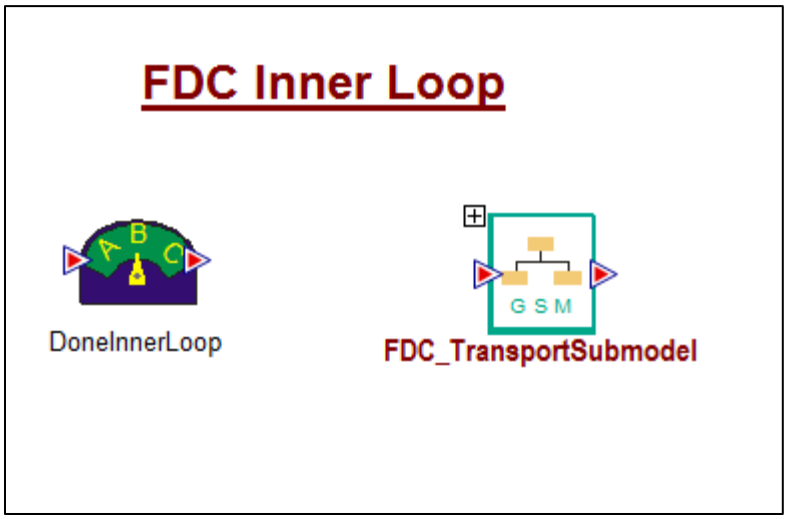

Figure 4.1-7: External Element Controlling *TSProc1.dll*

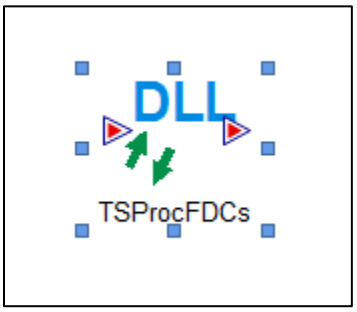

FDC_TransportSubmodel, is comprised of (see Figure 4.1-8) a disposal unit modeling component (*FDCs*). *FDCs* is a conditional container which is only activated when results for a specified FDC are desired. Several other upper level containers are also present in *FDC_TransportSubmodel* (Figure 4.1-8). These containers include *FDC_Transport_Results, Material, and InputData.*

Due to limitations of conditional containers, time series elements cannot be used within the *FDCs* container (Figure 4.1-3). Therefore, the time series elements used to transfer data from the submodel to the main model, via *TSProc.dll*, are assembled in the container *FDC_Transport_Results* (see Figure 4.1-9).

Species elements and reference fluid elements must be defined separately in the main model and submodel. The species element and the base reference-fluid element for the submodel are located in the *Material* container (Figure 4.1-8). Note that cloned versions of the fluid element found in *Material* are located in containers where material-specific diffusion coefficients are assigned.

The other upper level container within *FDC_TransportSubmodel* is *InputData* (Figure 4.1-8) which serves as a transfer site for data passed from the main model to the submodel. The data from the main model is passed directly to the submodel though the submodel-interface in *FDC_TransportSubmodel* shown in Figure 4.1-10. Selector and expression elements located within *InputData* serve an organizational purpose as they capture the data from the interface and reset the variable name to the name from the main model for consistency.

It should be noted that data is also outputted from the submodel through the interface. The output data is then returned to the main model using the software *TSProc.dll* in conjunction with an external properties element (GTG-2010d).

Within the submodels *FDCs* container (as well as the Vault_1 and Vault_4 containers), are located the cell networks and pipe elements used to evaluate the transport of radionuclides through the SDUs and saturated zone. Figure 4.1-11 depicts the organizational scheme within the container *Vault_4* and Figure 4.1-12 depicts the organizational scheme within the container *FDCs*.

Figure 4.1-8: Contents of *FDC_TransportSubmodel*

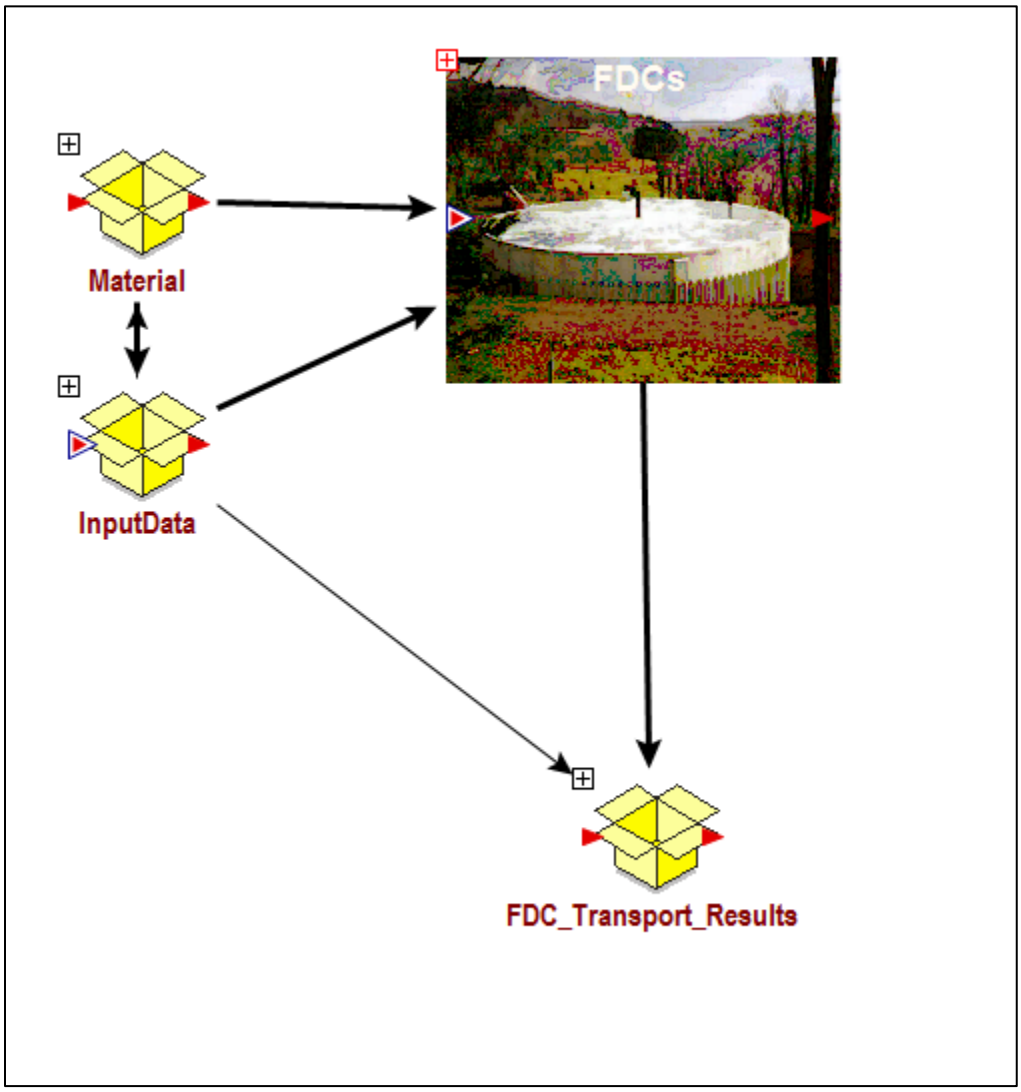

Figure 4.1-9: Typical GoldSim Time Series Element Used in *FDC_Transport_Results*

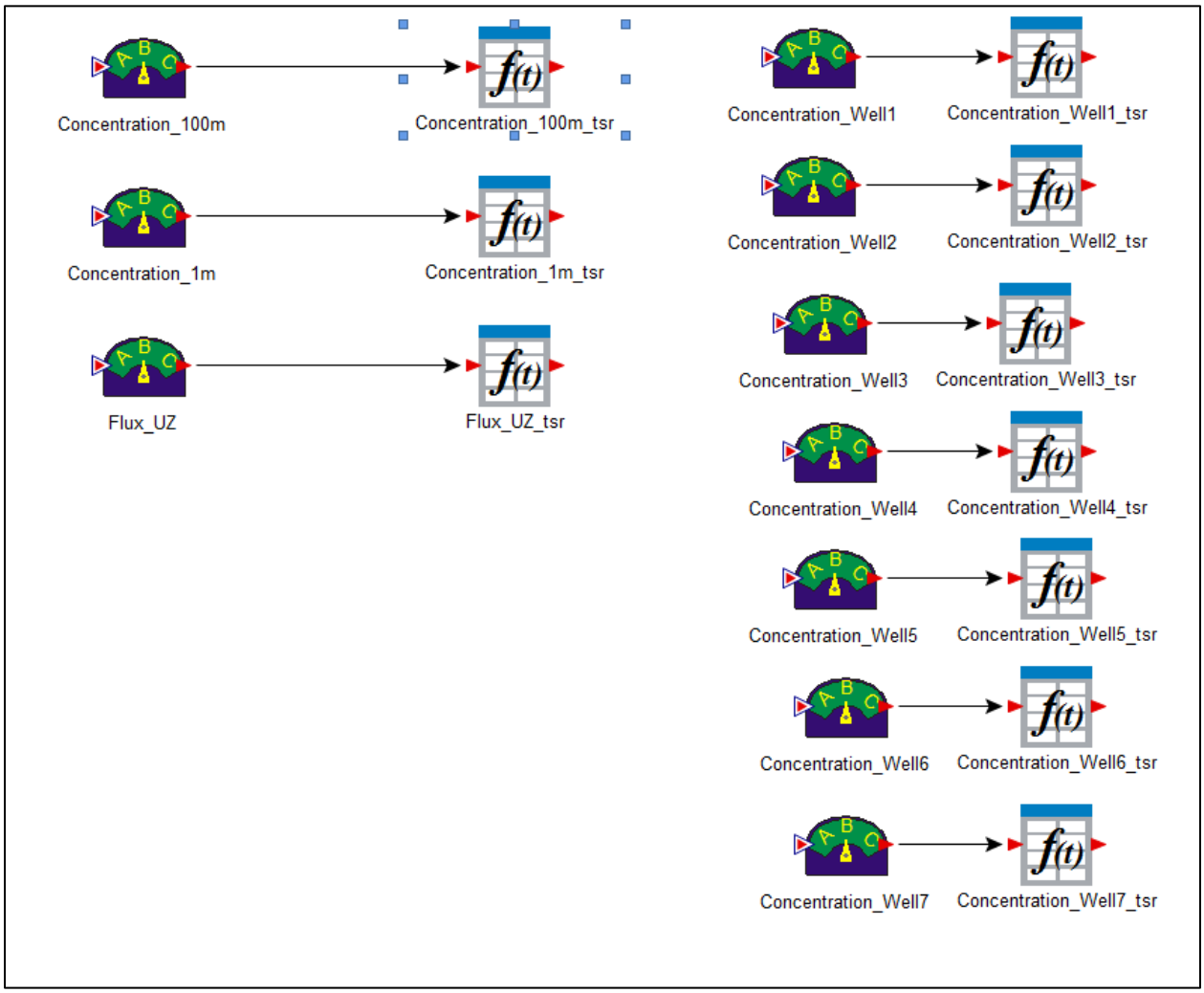

Figure 4.1-10: *FDC_TransportSubmodel* Submodel-Interface

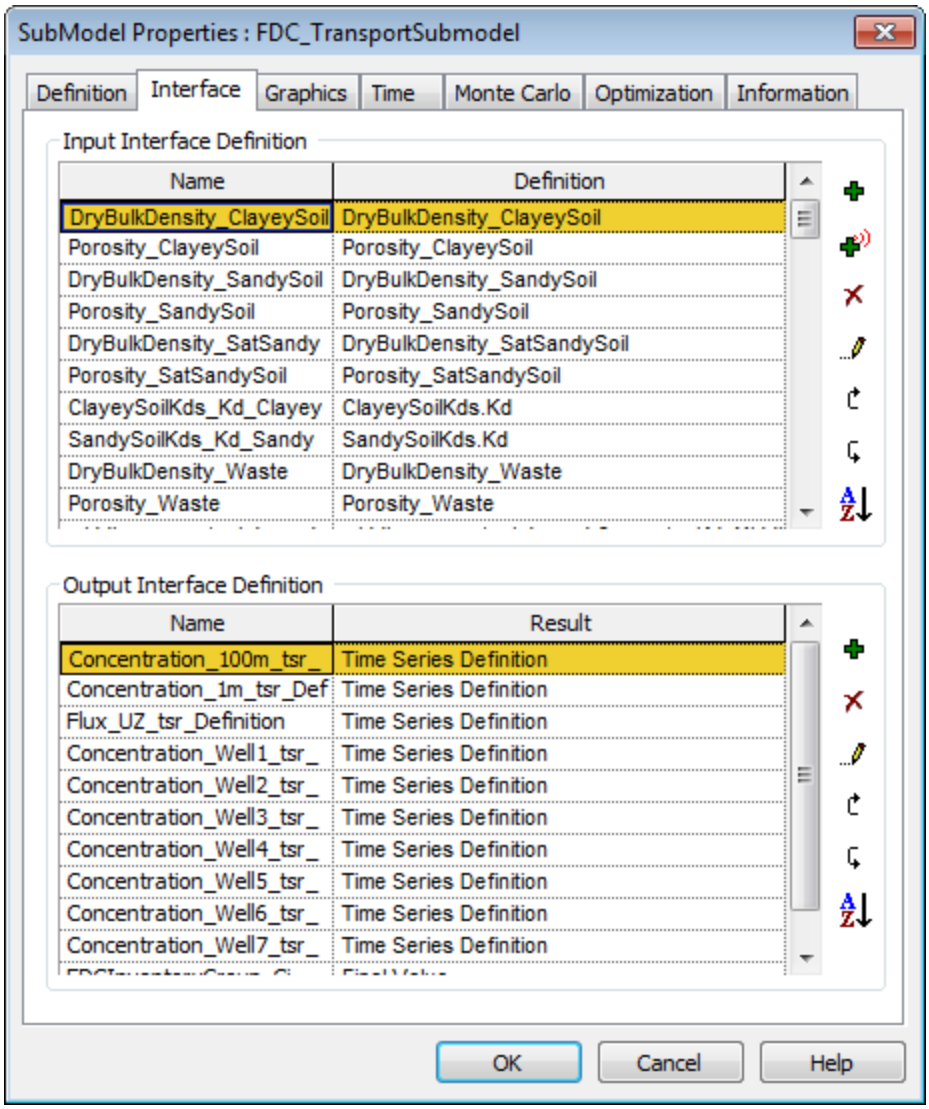

Figure 4.1-11: Contents of the *Vault_4* Container

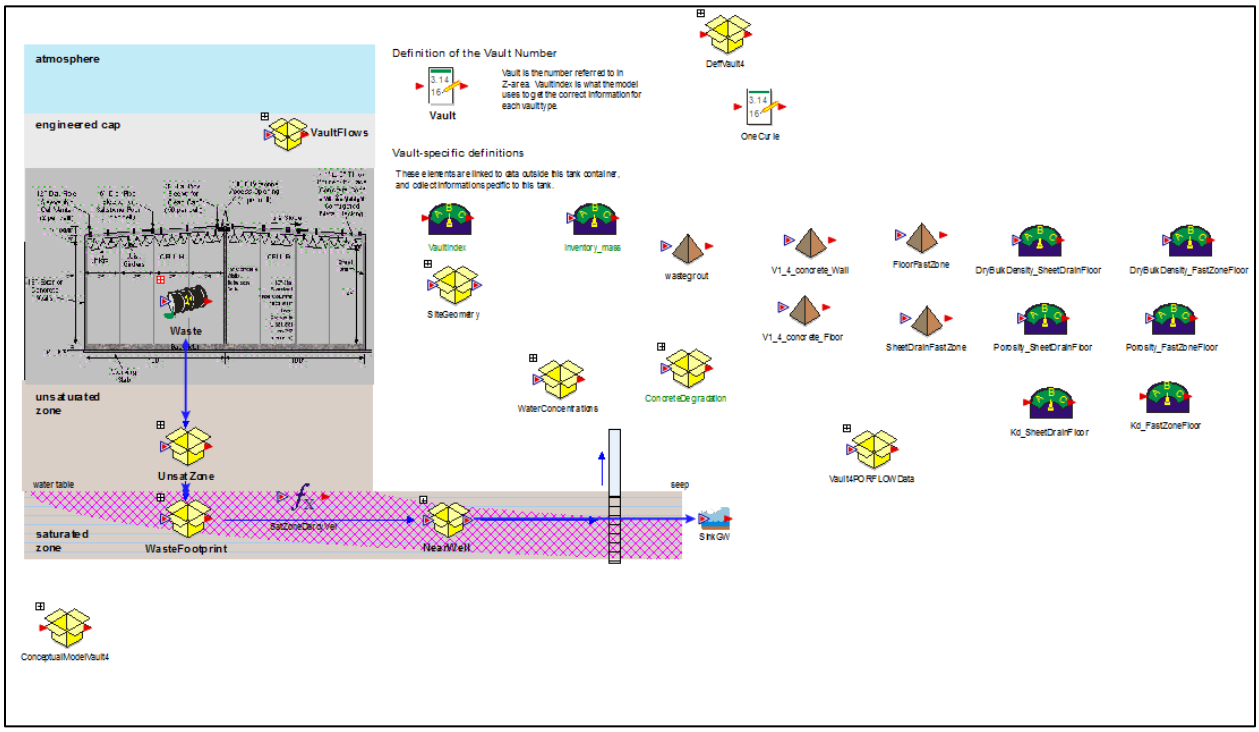

Figure 4.1-12: Contents of the *FDCs* Container

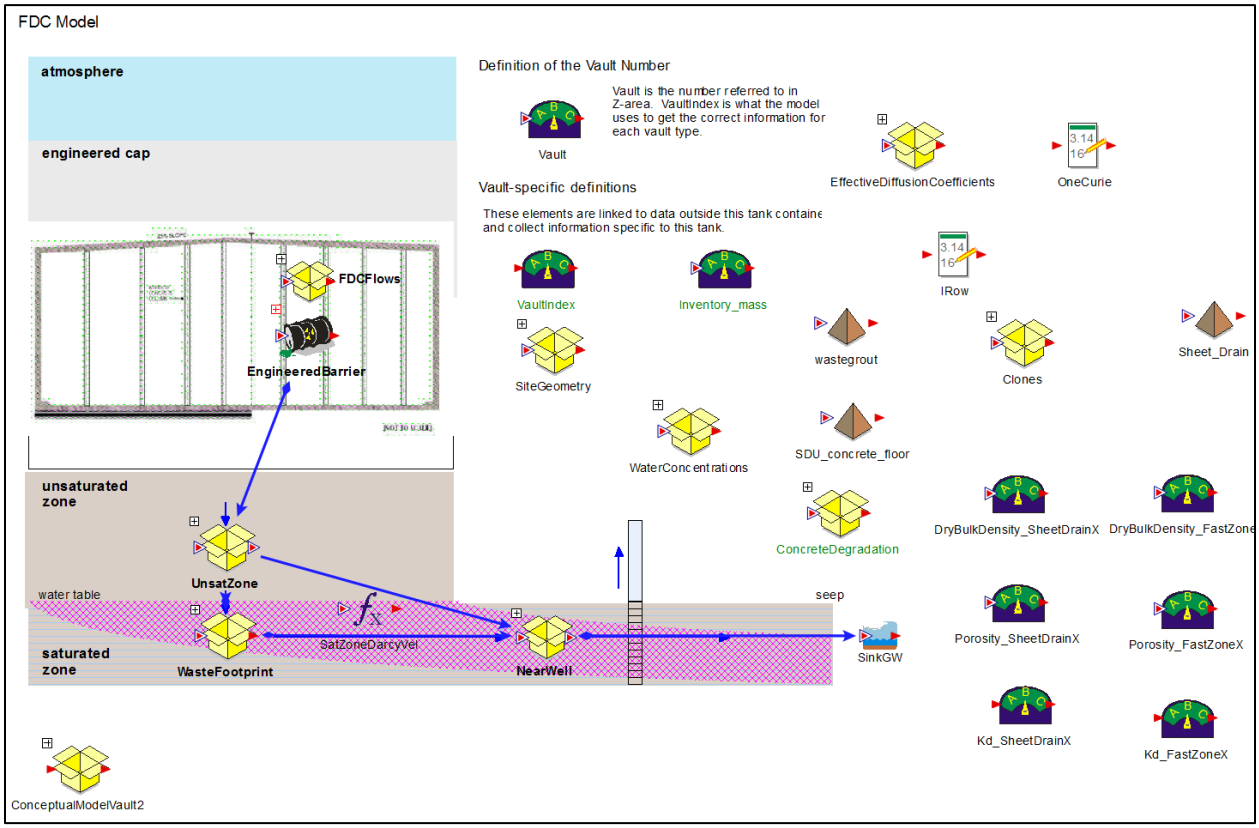

The SDF GoldSim Model containers *Vault_1, Vault_2, FDCs* are comprised of mixing-cell networks and pipe-elements (analytical solutions) that evaluate radionuclide migration from the saltstone (and for SDU 1 and SDU 4, the walls), through the remainder of the engineered barrier, through the backfill and unsaturated zone. The radionuclide releases from the unsaturated zone are applied as boundary conditions to pipe-elements representing the saturated zone where concentrations are evaluated at the 100-meter boundary and IHI Wells.

Radionuclide concentrations at the mid-points of sectors along the 100-meter boundary (Figure 4.1-2) form the basis of the SDF GoldSim Model MOP dose calculations. The SDU components of the SDF GoldSim Model also contain pipe-elements that simulate the transport of radionuclides from SDUs to IHI wells adjacent to specified SDUs (see Figure 4.1-2). It is at these wells that concentrations used in the IHI dose calculations are calculated. The SDU components of the containers *Vault_1, Vault_2, FDCs* are organized in a hierarchy, with the top level of the SDU transport components for Vault 4 shown in Figure 4.1-11 and the FDCs shown in Figure 4.1-12. Model containers, represented as yellow boxes, are used to organize the calculation logic. Using the FDC submodel as an example, a brief description of the upper-level containers and their contents is introduced here:

- The source element *EngineeredBarrier* contains the mixing-cell network that represents: (1) the engineered barrier comprised of the saltstone, sheet-drains, columns, floor components, joints, walls, and backfill and (2) the UZ. Within the engineered barrier and UZ, radionuclide transport is controlled by advection, molecular diffusion, linear sorption, and radionuclide decay. Using the FDC model as an example, the engineered barrier above the floor is comprised of a mixing-cell network that is discretized into 21 layers defined by containers (Figure 4.1-13). The addition of the layer represented by the cells in the *TopCa*p container is a change from the previous version of the model, Version 4.101. The addition of *TopCa*p allows the model to consider the disposal of waste up to the roof. Each layer (found in the containers *CellRow_01* through *CellRow_20*, and *TopCa*p) is represented by a set of containers, comprised of mixing cells, representing the material zones (saltstone [grout], sheet-drains, columns [fast zone], walls, HDPE liners, and backfill) of the engineered barrier (Figure 4.1-14). From the saltstone cells, mass can diffuse or advect between the saltstone cells and the rest of the cell network. Several simplifying assumptions are made in conjunction with the abstraction model used in the SDF GoldSim Model. With exception of the wall-to-floor joint cells in the FDCs, only vertical advection through the engineered barrier (and UZ) is considered in the model abstraction upon which the three SDU models are based. The flow regime is defined by spatially averaged vertical components of Darcy velocity which are read into the model for each material zone including, the inner and outer saltstone zones, the sheet-drains, the columns, the walls, the floor (and for the FDCs, floor, upper mud mat, and lower mud mat), HDPE liners (for the FDCs only), and backfill. Because of the importance of diffusion into the walls and from the walls into the backfill in the SDUs during early times, the abstracted model also considers the influence of molecular diffusion on horizontal radionuclide migration within the model.
- For each layer in the FDC model, there is a *Grout* container comprised of two containers of mixing cells linked in series (Figure 4.1-15), one containing the cells representing the inner zone of saltstone (Figure 4.1-16) and the other representing the outer zone of

saltstone (Figure 4.1-17). The inner zone container (*InnerZone*) found in the GoldSim SDF All-Species Model, Version 5,004, differs from prior versions because it contains a container *SDU6add* that extends the inner zone by three mixing cells. This addition was added to increase the number of cells in the inner zone which takes up a larger proportion of the saltstone in the 375-foot diameter SDUs as compared to the 150-foot diameter SDUs. The inner and outer zone mixing cells are separated by a set of cells located in the *FastZone* container representing the columns (or a potential fast zone) in the FDCs (Figure 4.1-18) and SDU 4. The fast zone in SDU 1 is located in the *Grout* container. The other containers found in each layer container are the *SheetDrain* (Figure 4.1-19), *Wall* (Figure 4.1-20), *HDPE* (Figure 4.1-21), and *Fill* (Figure 4.1-22) containers. Within each layer, the mixing-cells in each container and adjacent containers are connected to each other by diffusive links. In addition, each cell within a layer is connected to the equivalent cells above and below them with an advective link. Note that for the 375-foot diameter SDUs, the HDPE cells are converted to fill cells. The cells in the bottom layer *CellRow_20*, are attached to cells representing the zones below them found in the containers *VaultFloor1*, *VaultFloor2, FastZone, Joint1, Joint2, and Joint 3* (Figure 4.1-13). The Joint 1 and Joint 2 cells are in turn connected to the inner and outer UMM cells. The Joint 3 cells are connected to the top wall-floor cell.

- The *VaultFloor1* and *VaultFloor2* containers (see Figure 4.1-13) are each comprised of one chain of 20 mixing cells that represent the floor beneath the inner saltstone zone and outer inner saltstone zone, respectively. Figure 4.1-23 shows the contents of the Vault 1 container. The containers *VFUMM* and *VFLMM* within *VaultFloor1* and *VaultFloor2*, each contain 5 cells linked in series that represent the upper and lower mud mats, respectively. Similar to the *VaultFloor1* and *VaultFloor2* containers, the *FastZone* container (see Figure 4.1-24) is comprised of one chain of 20 mixing cells that represent the floor, upper mud mat and lower mud mat beneath the column. The *Joint1* and *Joint2* containers (see Figure 4.1-13 and Figure 4.1-25) are comprised of chains of ten mixing cells that represent the floor joints beneath the inner saltstone and outer saltzone zones, respectively. The *Joint3* container (see Figure 4.1-26) is comprised of a chain of six mixing cells that represent the wall-to-floor joint beneath the wall. The joint cells in turn provide a fast zone beneath the wall that flows into the backfill. The joint cells also flow into the top cell in the string of 20 cells linked in series found in the *WallFloor* container. The cells in the *WallFloor* container are arranged in the same manner as the rest of the floor cells. The strings of cells found in the *VaultFloor1*, *VaultFloor2*, *FastZone*, and *WallFloor* containers flow into the set of mixing cells located in the *UnsatZone* container.
- The *UnsatZone* container (Figure 4.1-12) is comprised of one chain of 20 mixing cells linked in series that represent the unsaturated zone beneath the FDC (Figure 4.1-27). Note that 10 of the cells (Cells 9 – 19) are located in the container *UZADD*. The bottom cells found in *VaultFloor1*, *VaultFloor2*, *FastZone*, *WallFloor*, and *Fill* containers flow into the top cell in the set of mixing cells located in the *UnsatZone* container. Outflow from the 20th cell (*UZCell _Out*) in the *UnsatZone* container, defines the radionuclide release to the saturated zone. The benchmarking container contains time-history result elements that depict the simulated radionuclide releases for a subset of species.

- The *WasteFootprint* container (Figure 4.1-12) is comprised of one chain of 10 mixing cells that represents the saturated zone beneath the unsaturated zone (Figure 4.1-28). The waste footprint cells are used to determine the adjacent SDU's contribution to well concentration at the wells used for the IHI dose calculations.
- The *NearWell* container (Figure 4.1-12) is comprised of a pipe-element representing 1-D transport to the 100-meter boundary, plus an additional seven pipe elements describing radionuclide transport from upgradient SDUs through the saturated zone to the seven IHI wells (Figure 4.1-29). Contributions from these pipes are used in conjunction with concentrations from the footprint cells to determine the concentrations at the IHI observation wells.
- The *SiteGeometry* container is comprised of GoldSim elements used to set the geometric dimensions for the FDC and associated natural barriers (unsaturated zone thickness and saturated zone streamtrace distance to the 100-meter boundary).
- The *ConcreteDegradation* container is comprised of GoldSim selector elements which are used to control the K_d values based on E_h and pH transition times read in to the model. The SetColumnKdMatrix container is a looping container that contains the logic to update the K_ds for the segmented columns in the FDCs.

Figure 4.1-13: Contents of the *VaultCells* Container for FDCs

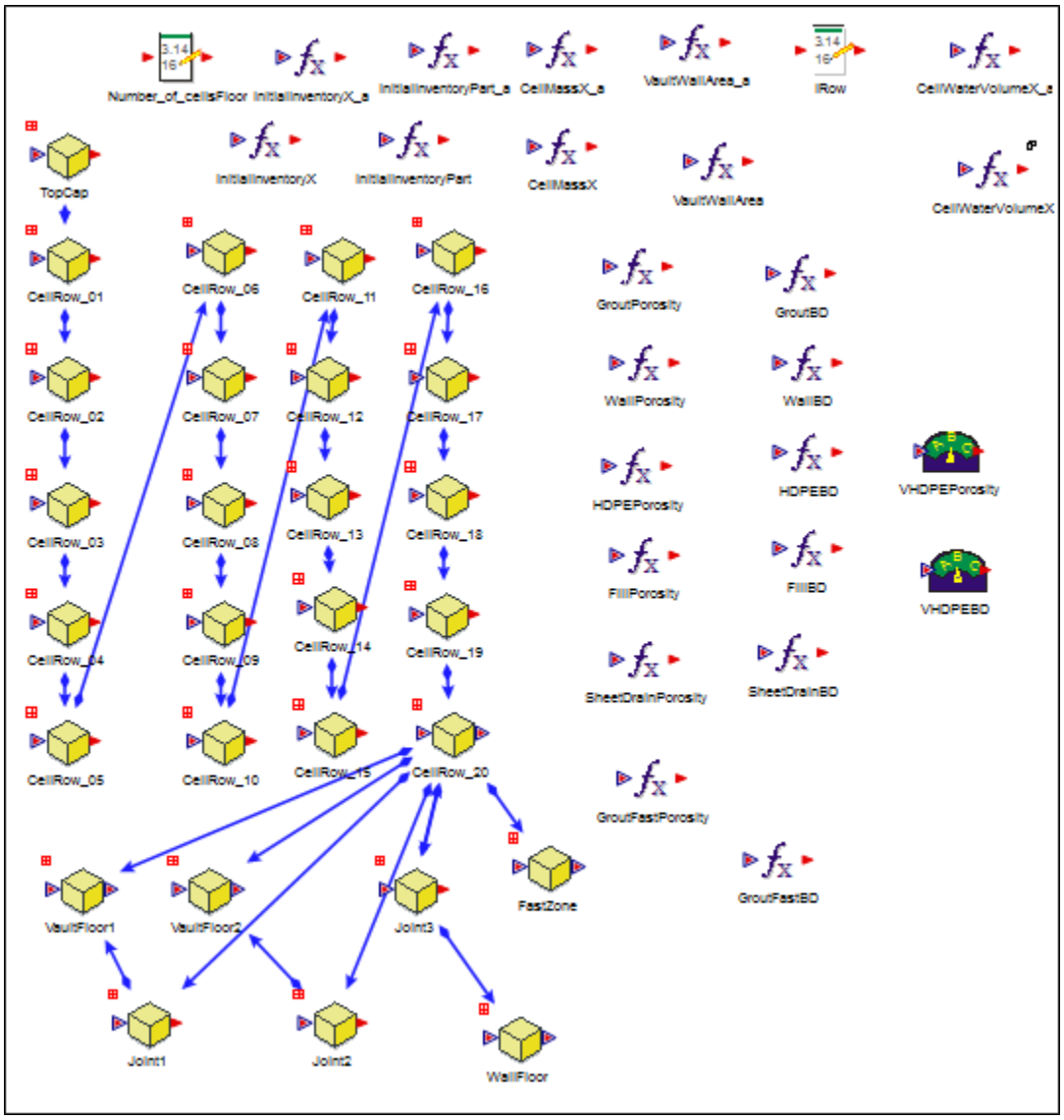

Figure 4.1-14: Contents of the *CellRow_01* Container for FDCs

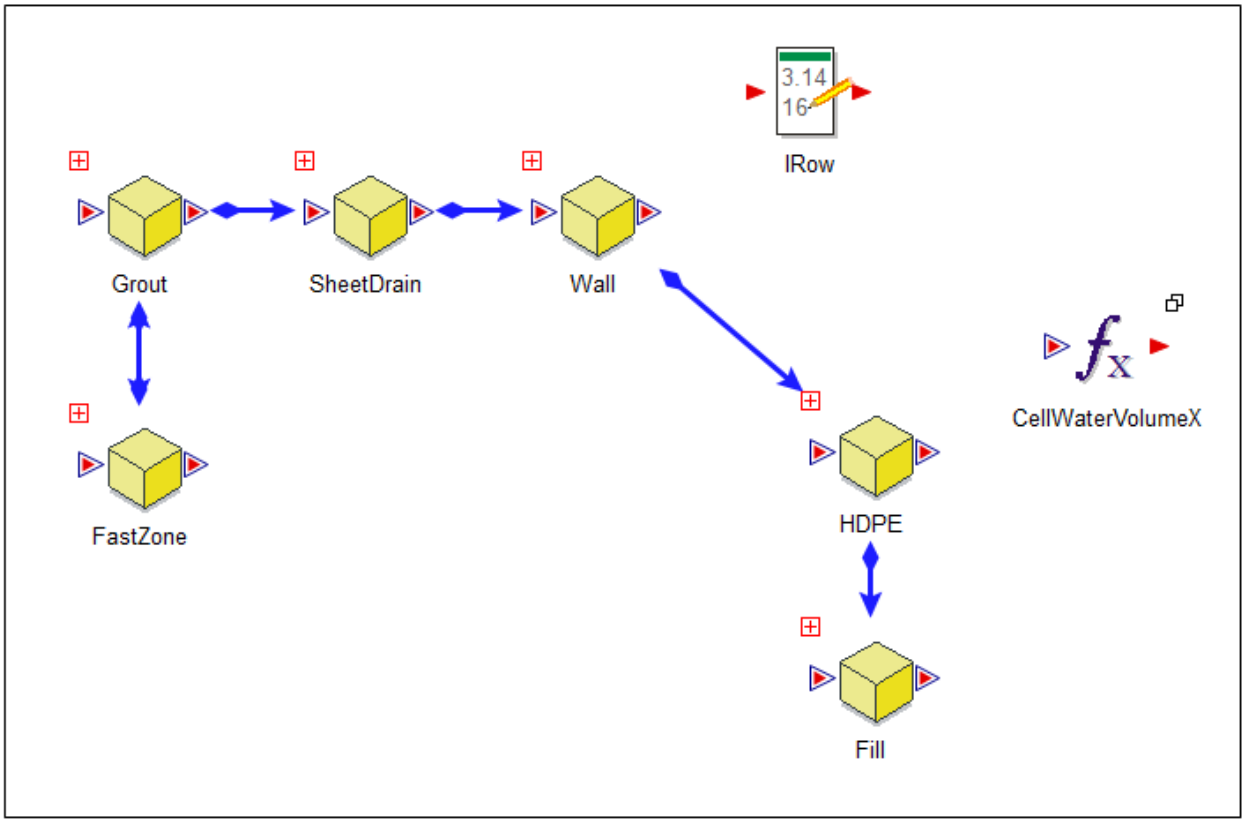

Figure 4.1-15: Contents of the *Grout* Container for FDCs

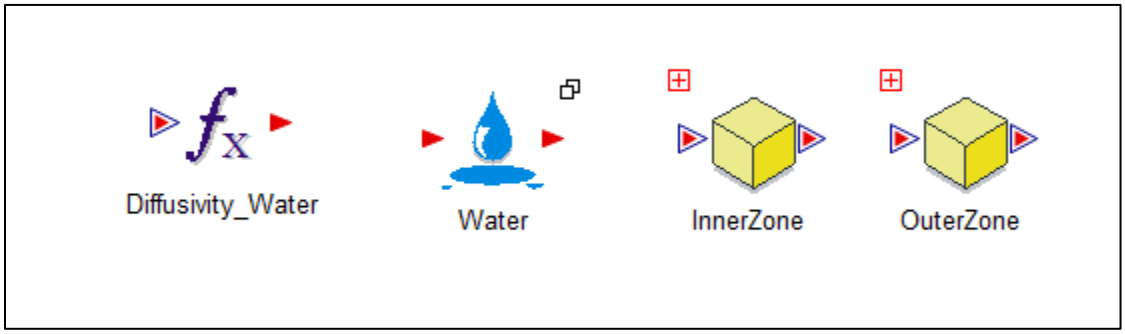

Figure 4.1-16: Contents of the *InnerZone* Container for FDCs

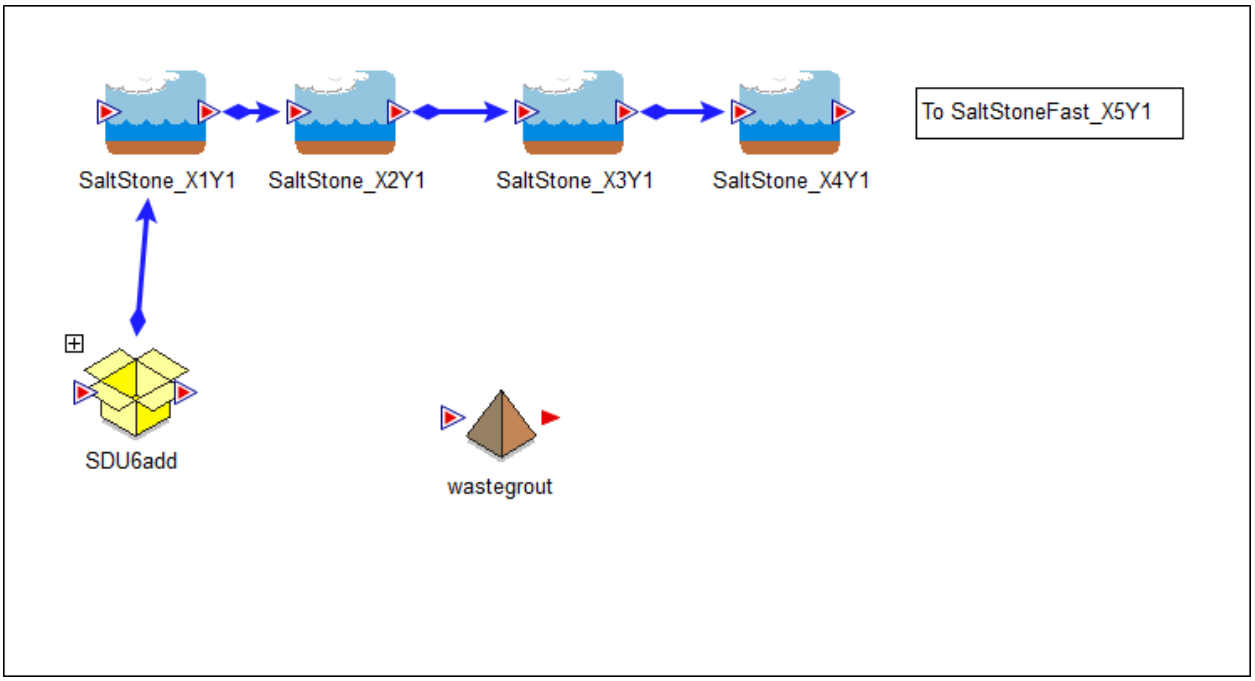

Figure 4.1-17: Contents of the *OuterZone* Container for FDCs

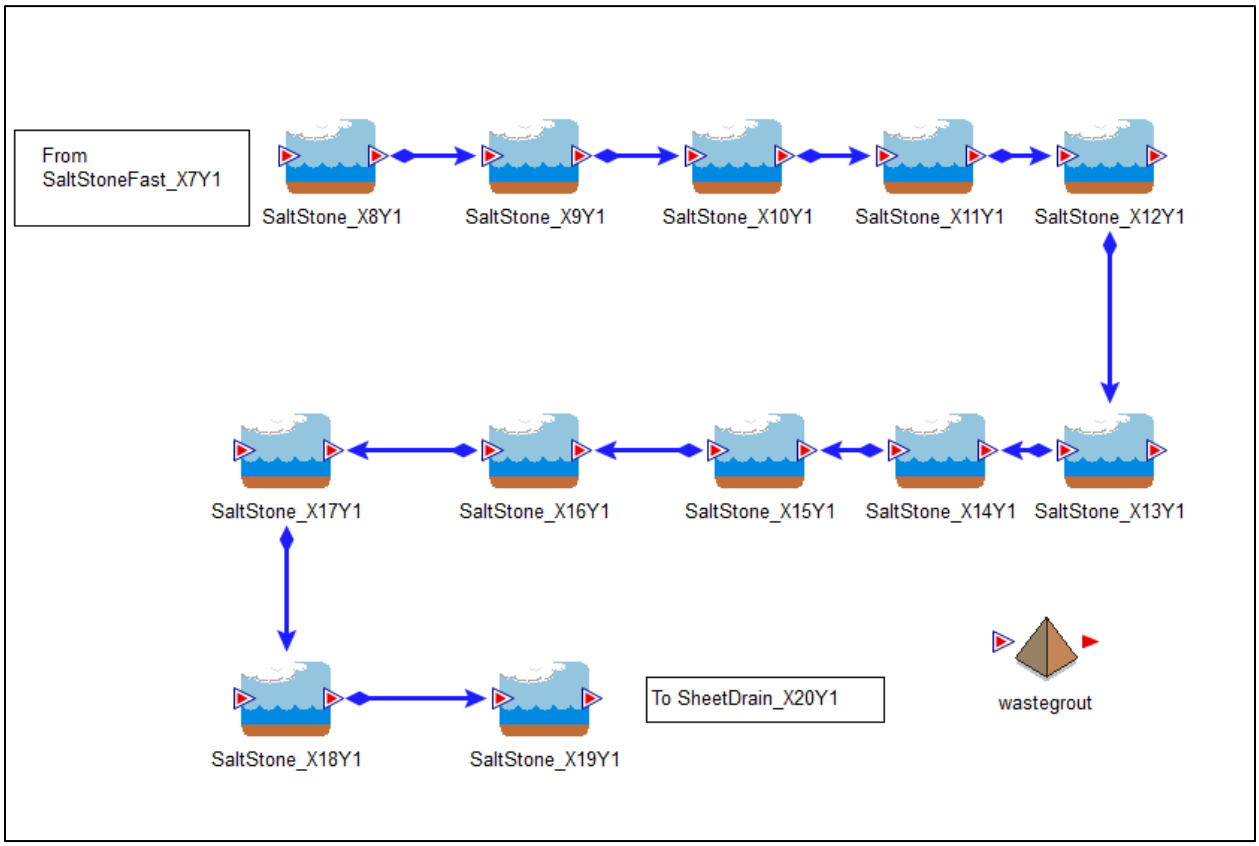

Figure 4.1-18: Contents of the *FastZone* Container for FDCs

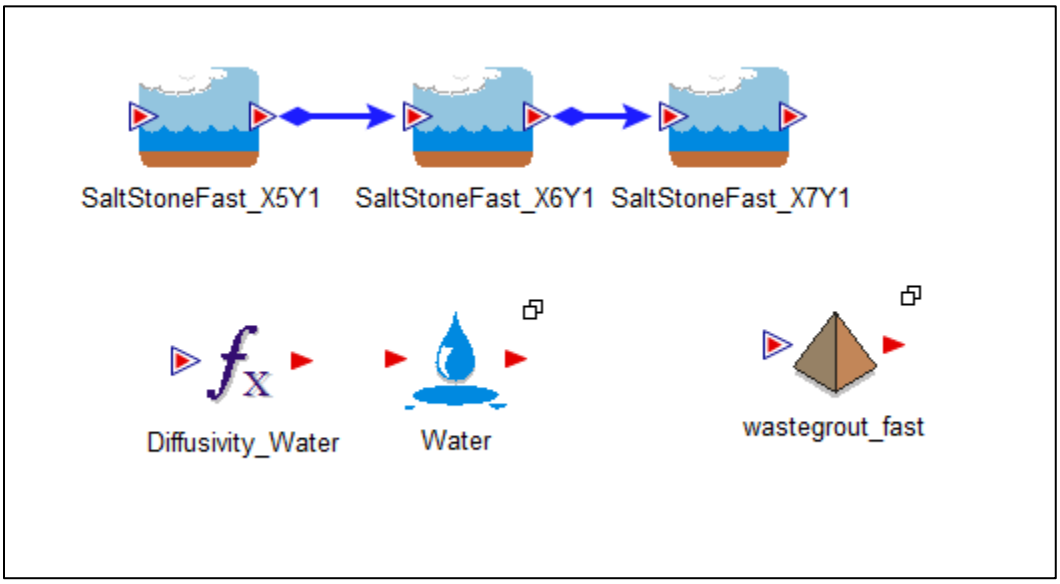

Figure 4.1-19: Contents of the *SheetDrain* Container for FDCs

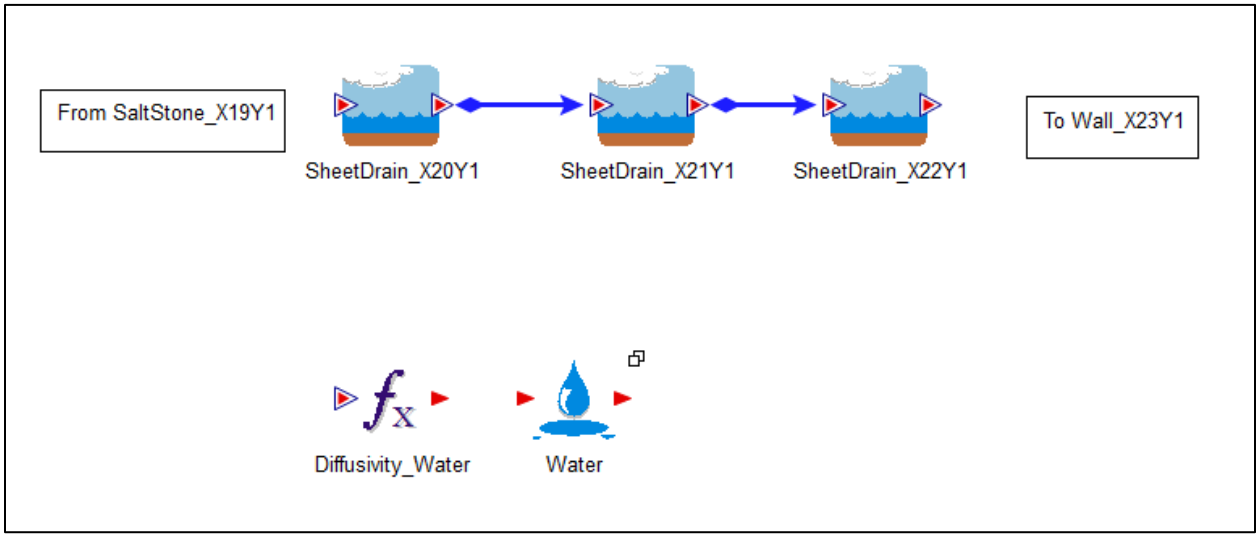

Figure 4.1-20: Contents of the *Wall* Container for FDCs

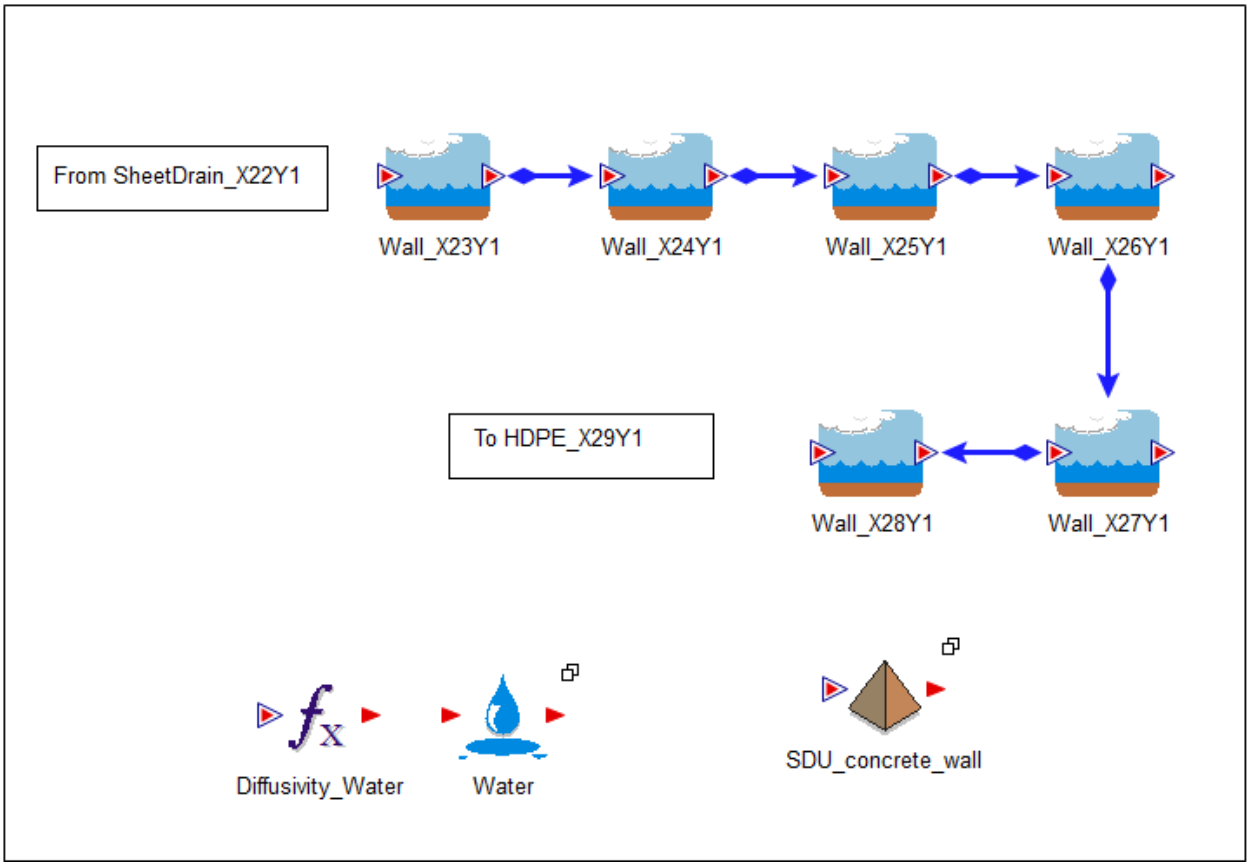

Figure 4.1-21: Contents of the *HDPE* Container for FDCs

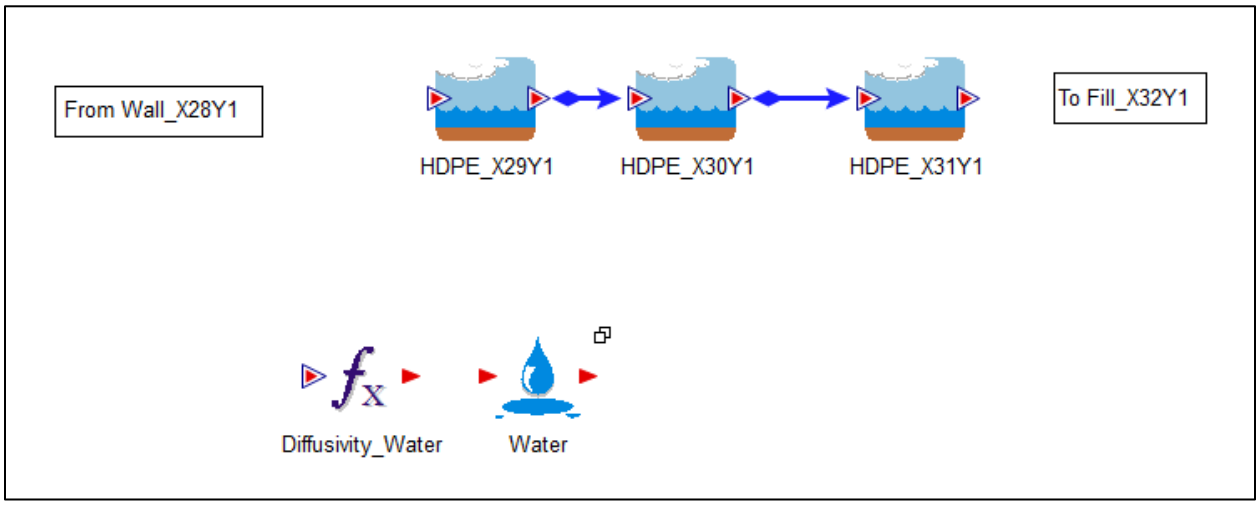

Figure 4.1-22: Contents of the *Fill* Container for FDCs

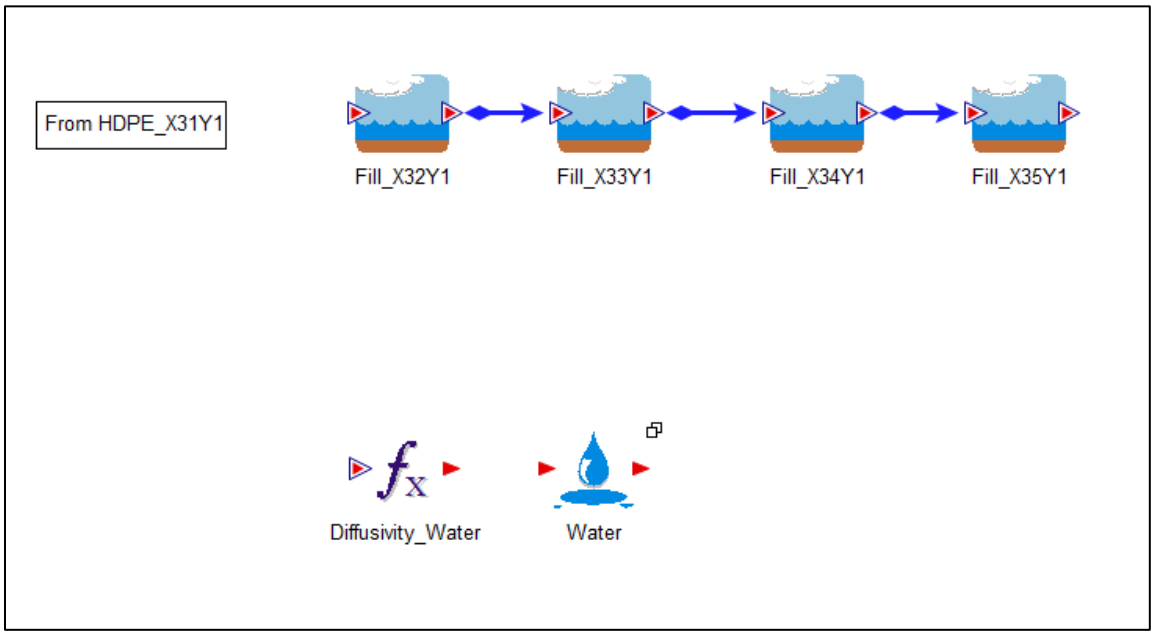

Figure 4.1-23: Contents of the *VaultFloor1* Container for FDCs

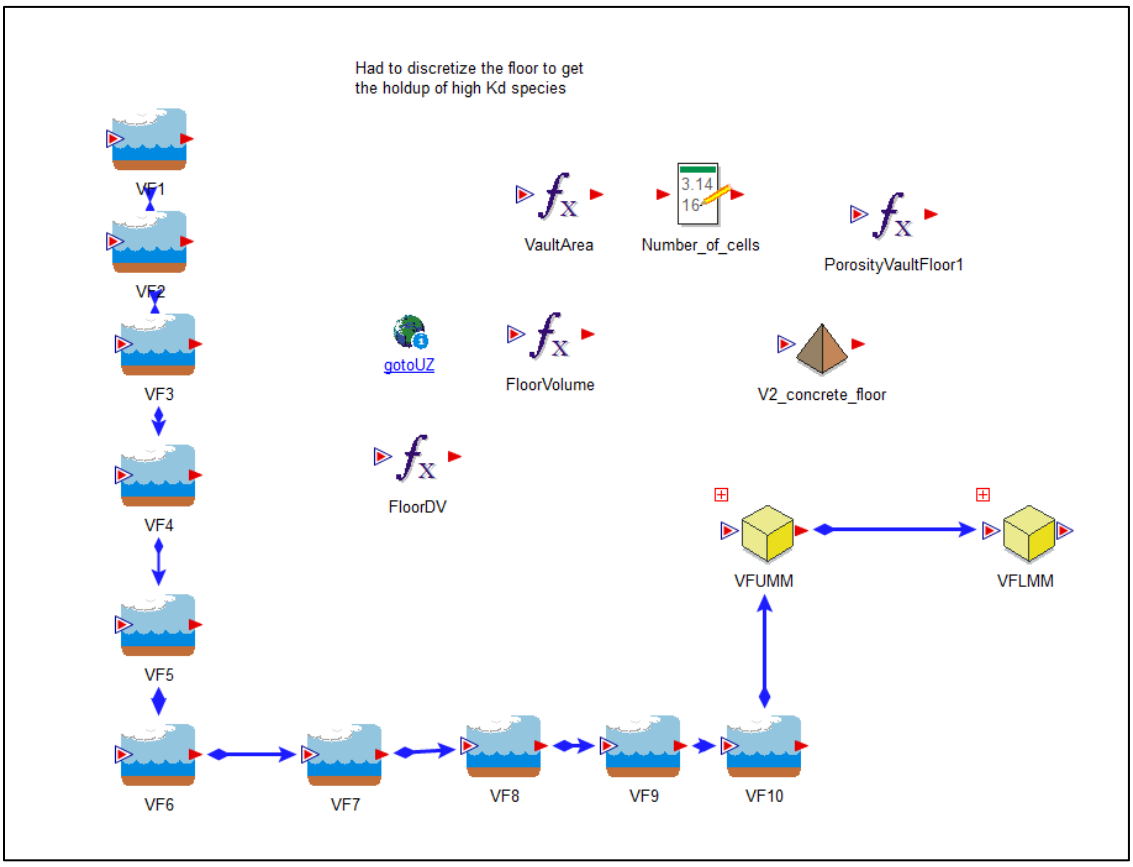

Figure 4.1-24: Contents of the *FastZone* Container for FDCs

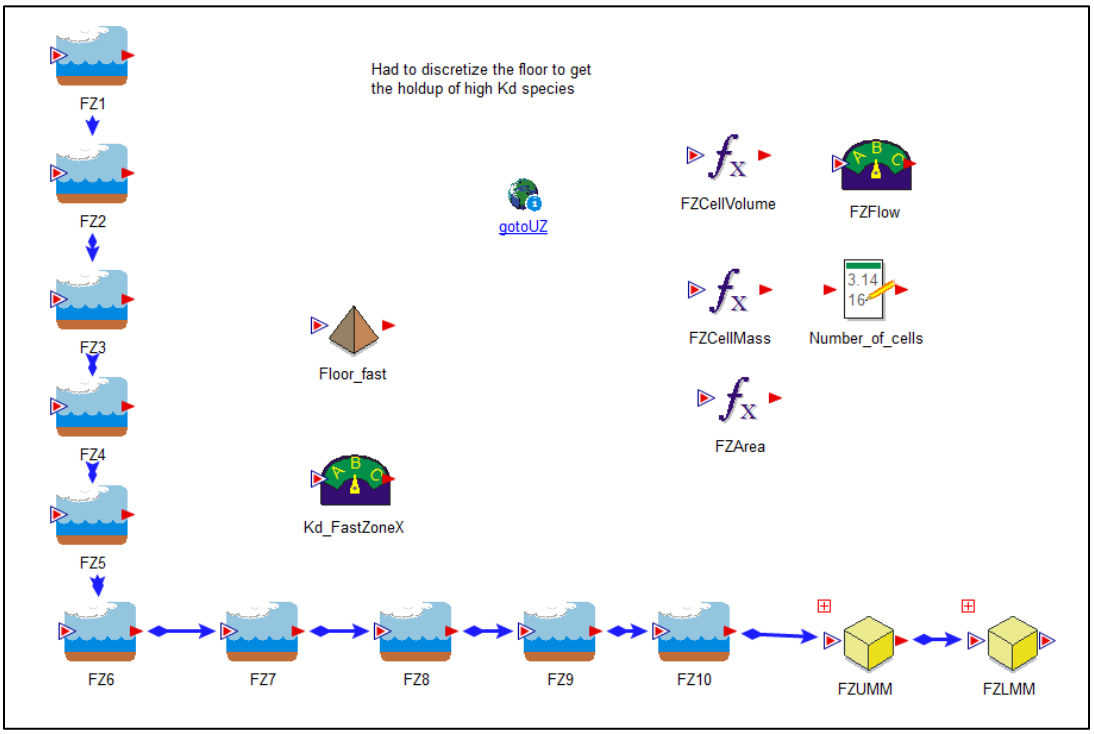

Figure 4.1-25: Contents of the *Joint1 and Joint 2* Containers for FDCs

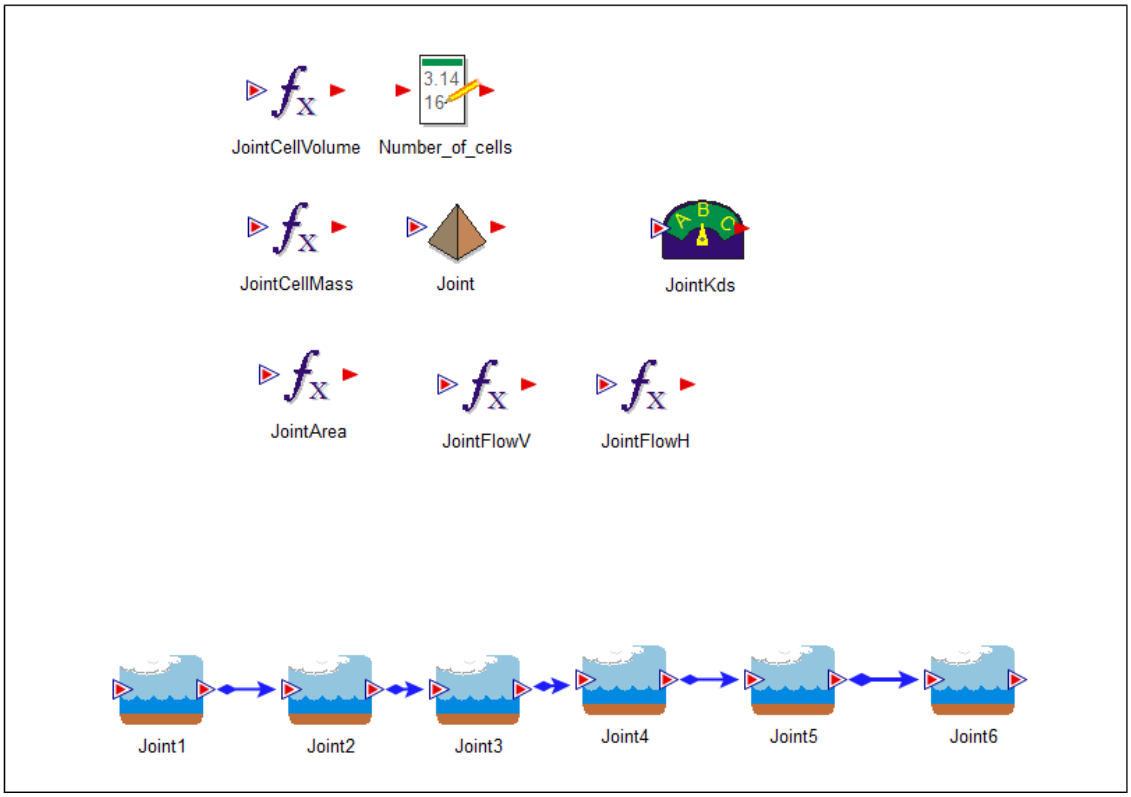

Figure 4.1-26: Contents of the *Joint3* Container for FDCs

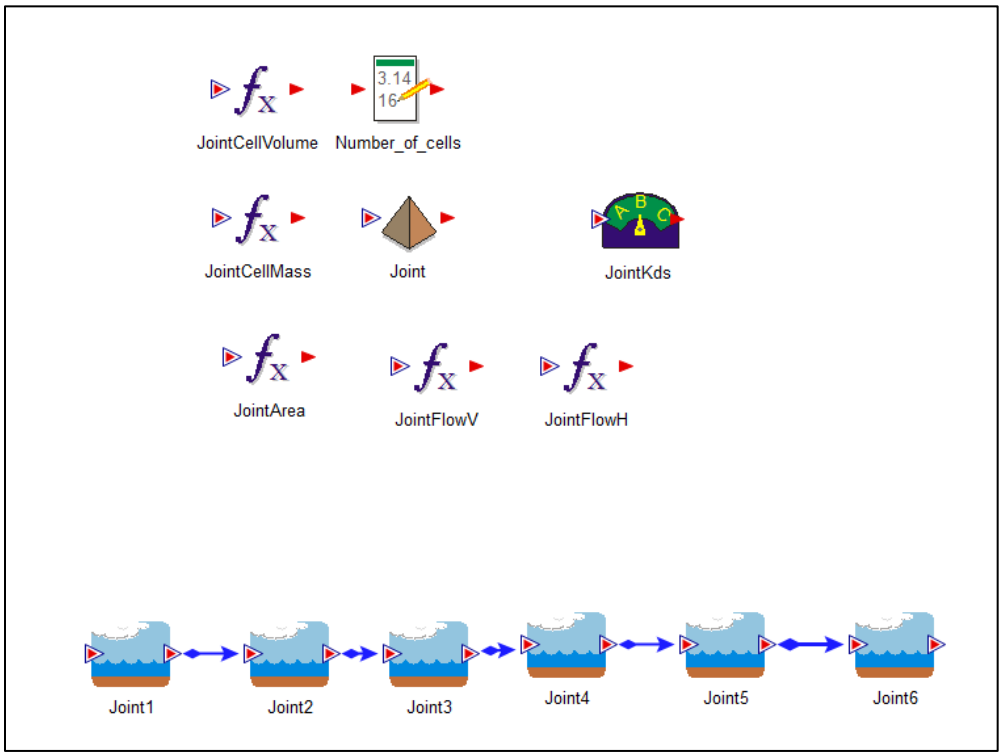

Figure 4.1-27: Contents of the *UnsatZone* Container for FDCs

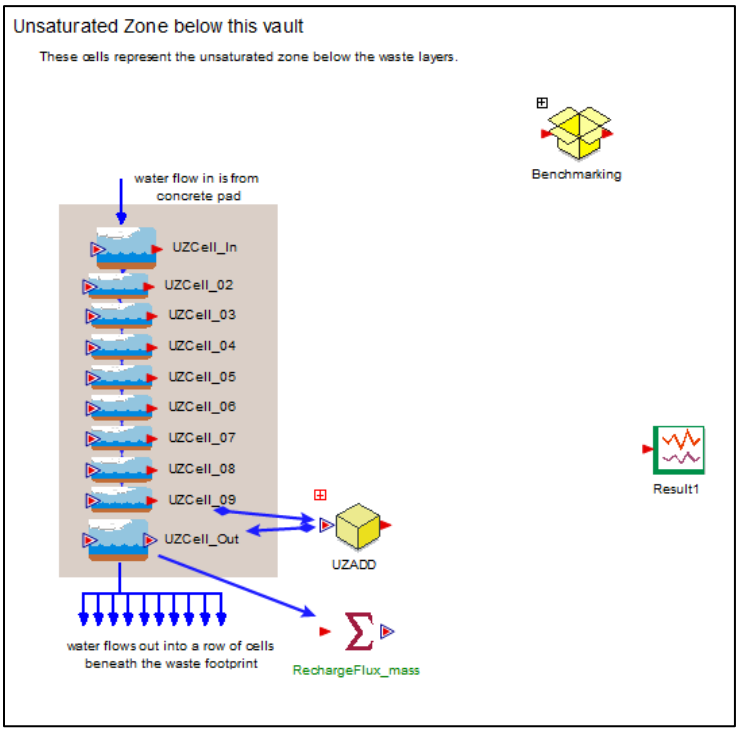

Figure 4.1-28: Contents of the *WasteFootprint* Container for FDCs

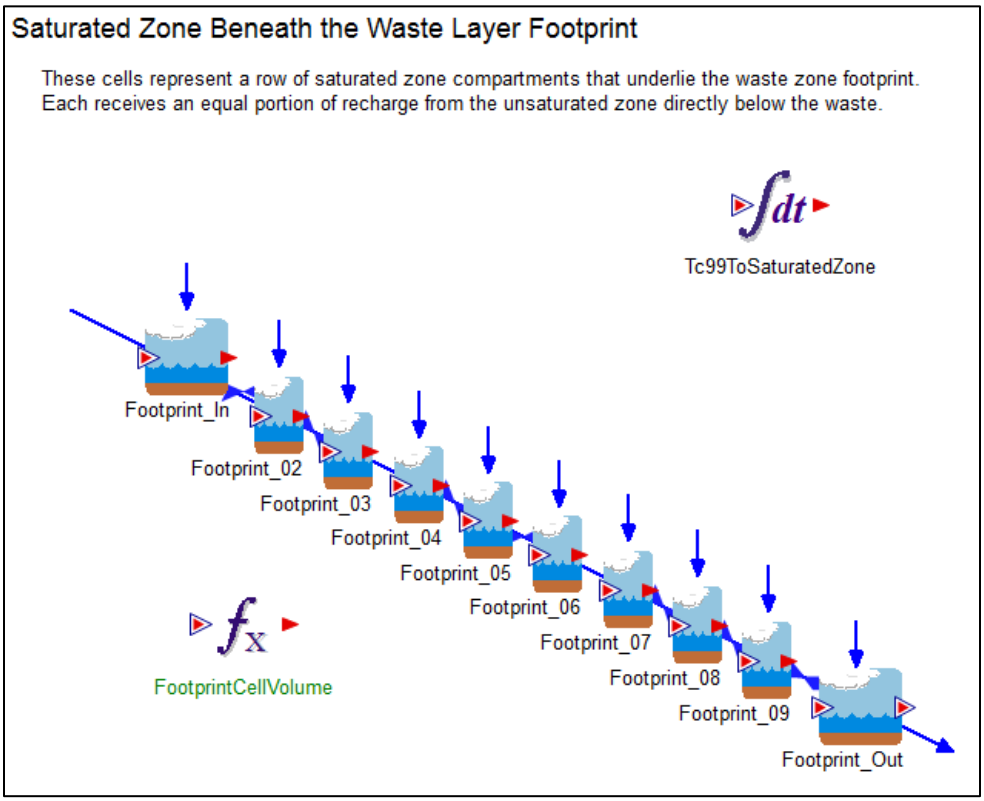

Figure 4.1-29: Contents of the *NearWell* Container for FDCs

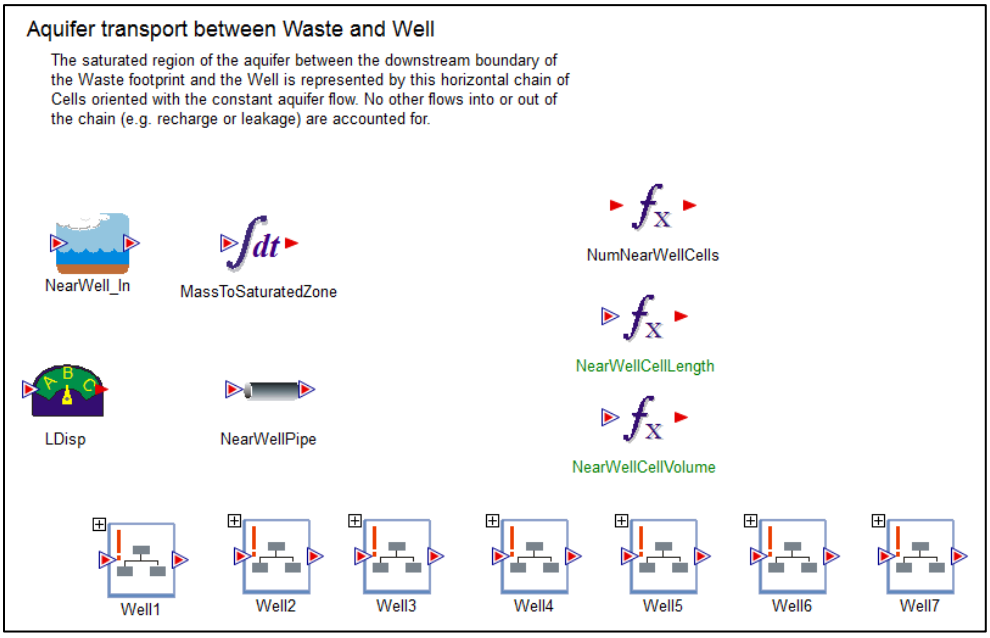

4.2 GoldSim SDF Tc-99 Release Model Organization

As noted in Section 3.2, the generation of Tc-99 release time-histories for the 15 SDUs needed for stochastic sampling of SDU inventories and solubility limits, is a computationally intensive process. The excessive computation time needed to generate the releases effectively limits the pool of samples from which can be randomly assigned to different realizations. In order to reduce the computational effort needed to develop the Tc-99 release time-histories, a standalone GoldSim-based model (the GoldSim SDF Tc-99 Release Model), was developed to generate the Tc-99 release time-histories.

The GoldSim SDF Tc-99 Release Model is comprised of two components, (1) a GoldSim module, which evaluates the migration of Tc-99 transport through the individual SDUs, and (2) a FORTRAN DLL which evaluates cell-by-cell solubility-control transition times. Results, generated by the GoldSim SDF Tc-99 Release Model, are automatically exported to files structured to be read in by the GoldSim SDF All-Species Model.

4.2.1 Structure of the GoldSim SDF Tc-99 Release Model

Like the GoldSim SDF All-Species Model, the GoldSim SDF Tc-99 Release Model is organized into a hierarchy, with the top level of the model shown in Figure 4.2-1. The upper tier of the GoldSim SDF Tc-99 Release Model hierarchy is comprised of five containers, *UserInput*, *Data*, *Material*, *DisposalUnits*, and *ModelOutput* (Figure 4.2-1).

Figure 4.2-1: Upper Tier of the GoldSim SDF Tc-99 Release Model Hierarchy

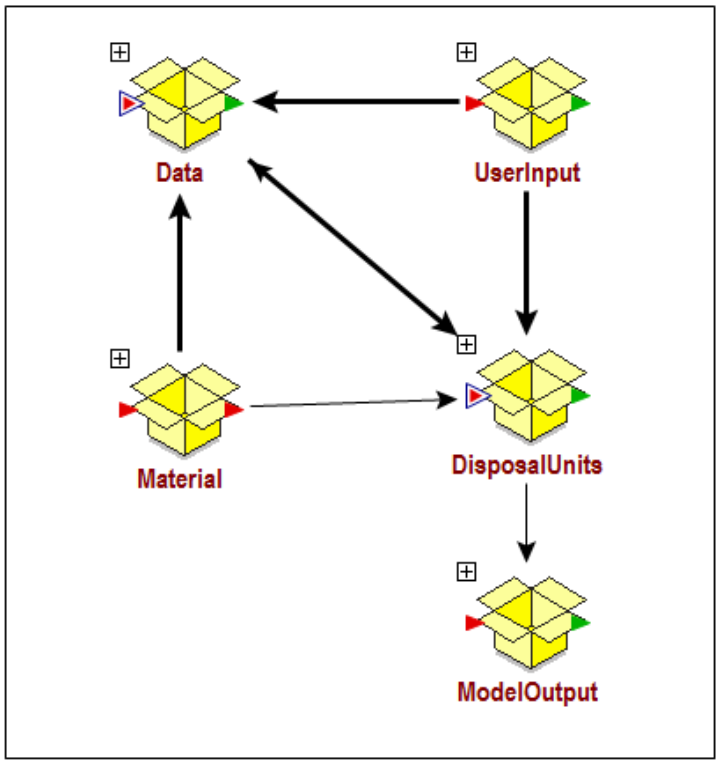

Brief descriptions of the upper-level containers and their contents are presented below:

- *UserInput* contains parameters, optional to the user, that control the setup and execution of the model. These parameters include switches that enable specific transport phenomena to be included or excluded, control the specific sources of contamination, and indicate whether or not a full site-based transport simulation is to be performed or a single SDU simulation is to be performed.
- *Data* contains the modeling parameters describing the geometry, inventory, material properties, and stochastic sampling distributions used in the model. It also contains constants and non-optional control parameters.
- *ModelOutput* contains the time-series elements, the expression elements which evaluate the time-series at specified times, and time histories of these results
- *Material* contains the list of radionuclides simulated in the model and their basic properties (atomic weight, half-lives, etc.) and the original fluid (water) assigned by the model.
- The *DisposalUnits* container is comprised of the elements that calculate the radionuclide transport results, in addition to importing the flow field data, the diffusion coefficient data, and the transition time data, and assigning the SDU specific data.

4.2.1.1 User Input

The transport analysis performed in the GoldSim module, is based on advective-diffusive transport through two sets of GoldSim mixing cells, with all cells in the network linked in series.

Brief descriptions of the user controlled input parameters are presented below:

- *Source_Choice*: the user can choose a specific SDU to be analyzed (see Table 4.1-1) or set this parameter to zero to evaluate all 15 SDUs.
- *Column_Choice*: the user can choose a specific saltstone column to be analyzed or set this parameter to zero to evaluate all saltstone columns in the SDU (this is for checking purposes and should normally be set to zero).
- *ReplaceCleanCap*: set this parameter to “True” (versus “False”) to assign inventory to the clean cap in the 150-foot diameter and 375-foot diameter SDUs.
- *DirectTransferFlux*: set this to “True” (versus “False”) to allow mass in assigned columns to be transferred to the UZ at cell-specific transition times.
- *RemovalPct*: parameter defining the percent of mass in a cell to be transferred to the UZ at the cell-specific transition time (see Eq. 3.2-1).
- *DTFAll*: set this to “True” (versus “False”) to allow mass in in all cells to be transferred to the UZ at cell-specific transition times.
- *InventoryOption_switch*: set this to “True” (versus “False”) to use tank-to-SDU model.

- *TankToFDCRandomizer_Switch_a*: set this to "True" (versus "False") to randomly choose tank emptying and SDU filling order in tank-to-SDU model.

The next few input parameters in *UserInput* are located in the containers *UserInput_XX* where *XX*[1]*=SDU2, SDU6, V1, and V4.*

- *BoundaryReleaseNodes_XX*: set this to "True" (versus "False") to allow mass in assigned columns to be transferred to the UZ for SDU-type XX (*DirectTransferFlux* must also be set to "True").
- *NBRI1_XX*: the number of boundary release nodes to the left of the column zone.
- *NBRI2_XX*: the number of boundary release nodes to the right of the column zone.
- *NBRIO_XX*: the number of boundary release nodes to the left of the outer wall zone.

4.2.1.2 Data

The *Data* container is comprised of five upper-level containers, *Geometry*, *Inventory*, *Materials*, *Miscellaneous*, and *Stochastic*.

Brief descriptions of the contents of these containers are presented below:

- *Geometry*: the *Geometry* container is comprised of five containers holding the data describing the geometry of 150-foot diameter SDUs (*Geometry_SDUType2*), 375-foot diameter SDUs (*Geometry_SDUType6*), Vault 1(*Geometry_Vault1*), Vault 4 (*Geometry_Vault4*), and the UZ (*Geometry_UZ*).
- *Inventory*: the *Inventory* container is comprised of a data element (Tc99Ci) containing the nominal FY2014 SDF SA inventory in curies and a container *Tank_to_FDC* holding the tank-to-SDU inventory calculating logic.
- *Materials*: the *Materials* container is comprised of a data elements defining the material parameters used in the FY2014 SDF SA model including sampling distributions for Tc-99 K_ds and solubilities.
- *Miscellaneous*: the *Miscellaneous* container is comprised of a data and expression elements defining the general parameters used in the model.
- *Stochastic*: the *Stochastic* container is comprised of the sampling logic and stochastic element used to choose the flow field used for each realization (note that the stochastic element was copied from the all-species model to force correlation between the realization numbers and flow fields used in the two models).

4.2.1.3 Material

As noted above the *Material* container contains the *Species* element with its list of radionuclides simulated in the model (Tc-99 only for this model) and basic properties (atomic weight, half-lives, etc.) and the original fluid element (*water*) assigned by the model.

[1] Note: For modeling purposes, *SDU2* is used as a representative 150-foot diameter SDU, *SDU6* is used as a representative 375-foot diameter SDU, and *V1* and *V4* represent Vaults 1 and 4 (i.e., SDUs 1 and 4), respectively.

4.2.1.4 DisposalUnits

The top level of the *DisposalUnits* container (Figure 4.2-2) is comprised of two containers *GlobalData* and *SDU_ReleaseCalculations*. The container *GlobalData* is comprised of data and expression elements defining the SDU specific parameters used in the model. The container *SDU_ReleaseCalculations* contains the elements used to calculate the Tc-99 release-rates to be used by the GoldSim SDF All-Species Model (Figure 4.2-3).

Figure 4.2-2: Contents of *DisposalUnits*

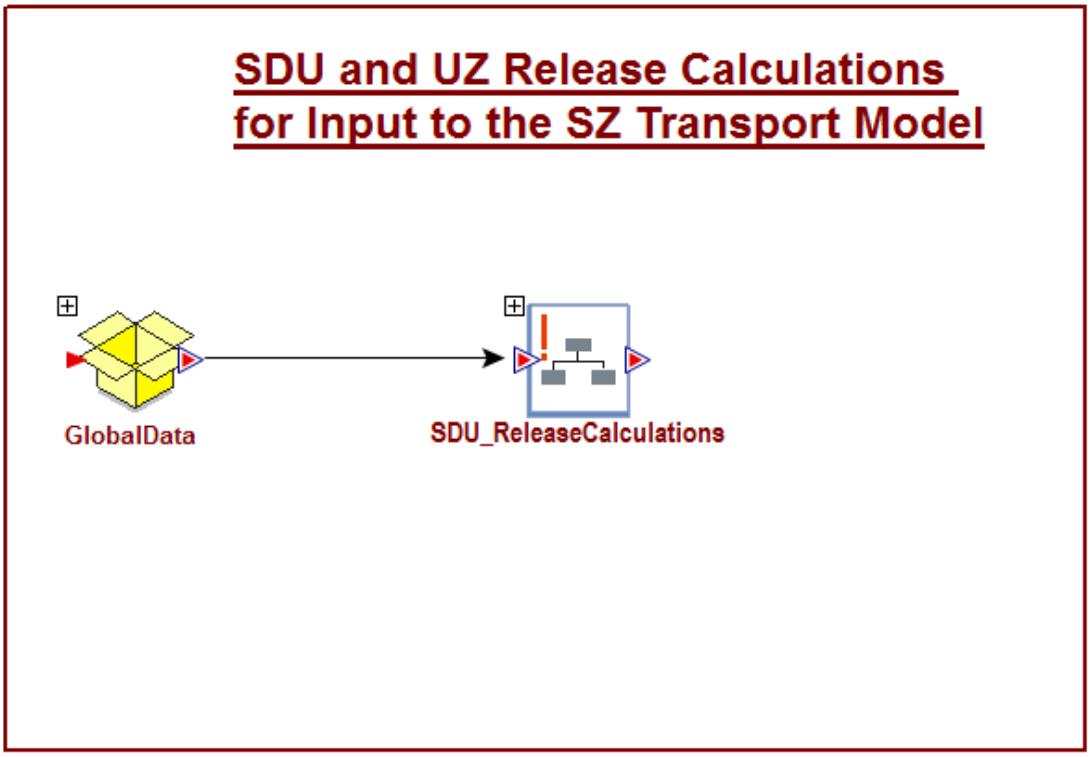

Figure 4.2-3: Contents of *SDU_ReleaseCalculations*

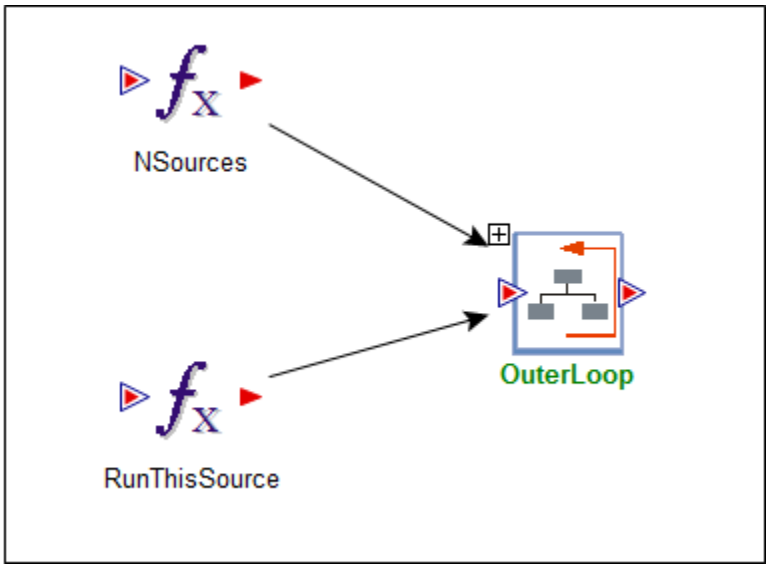

The container *SDU_ReleaseCalculations* contains a set of two nested looping containers, the outer one, *OuterLoop* which loops through the 15 SDUs and the inner one, *InnerLoop* which loops through the FY2014 SDF SA PORFLOW model based column structure Figure 4.2-4).

Figure 4.2-4: Contents of *OuterLoop*

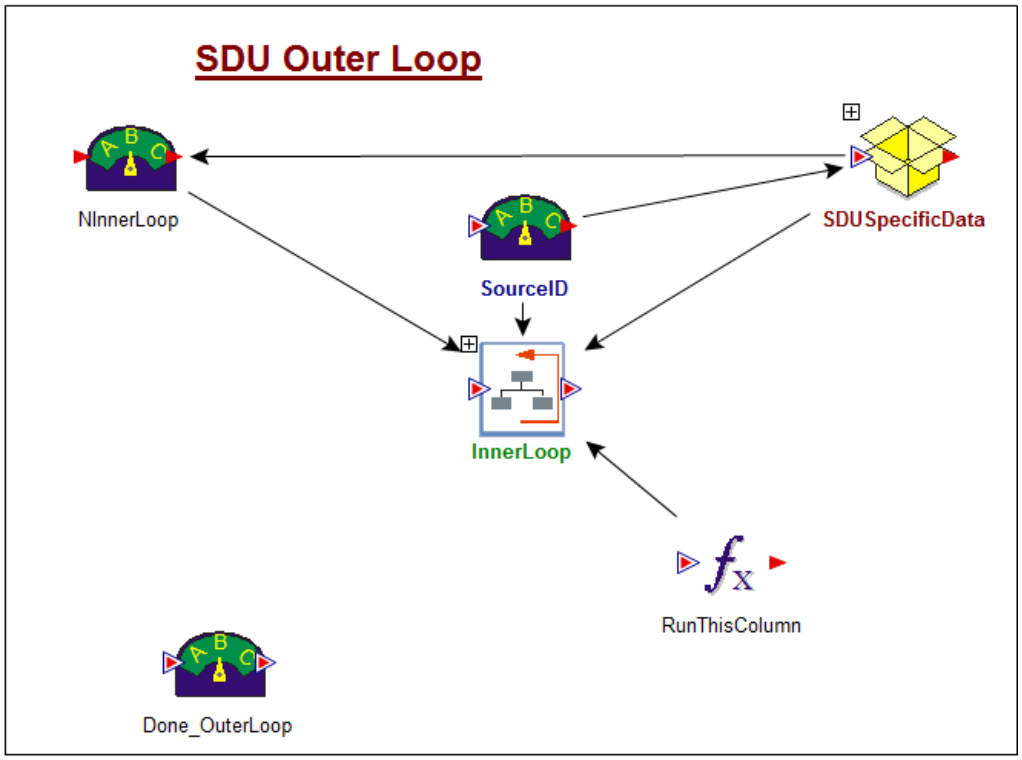

The looping control for *OuterLoop* (Figure 4.2-3) is based on the number of sources, *NSources*, if desired a user-specified source, *RunThisSource* (which is set to zero if all SDUs are evaluated in a run) and the selector *Done_OuterLoop* (Figure 4.2-4) inside the container. The looping control for *InnerLoop* (Figure 4.2-4) is based on the number of columns, *NInnerLoop*, if desired a user-specified source, *RunThisColumn* (which is set to zero if all SDUs are evaluated in a run), and the selector *Done_InnerLoop* (Figure 4.2-5) inside the container. *SDUSpecificData* (Figure 4.2-4) contains the elements that select the SDU specific data as the looping process proceeds.

The contents of the *InnerLoop* container (Figure 4.2-5) include four conditional containers *GenerateTransitionTimes_ctn1*, *GenerateTransitionTimes_ctn2*, *GenerateTransitionTimes_ctn4*, and *GenerateTransitionTimes_ctn6*, the container TS_Proc_SDU, and the submodel container *SDU_TransportSubmodel*. The four conditional containers contain the external (DLL) elements that control the running of the transition time DLL for each SDU-type: Vault 1, 150-foot diameter SDUs, Vault 4, and 375-foot diameter SDUs, respectively. In addition the four conditional containers contain the elements used to pass data to the DLL and capture data from the DLL. Note that the vaults were made conditional to minimize the number of times each container becomes active and runs.

Figure 4.2-5: Contents of *InnerLoop*

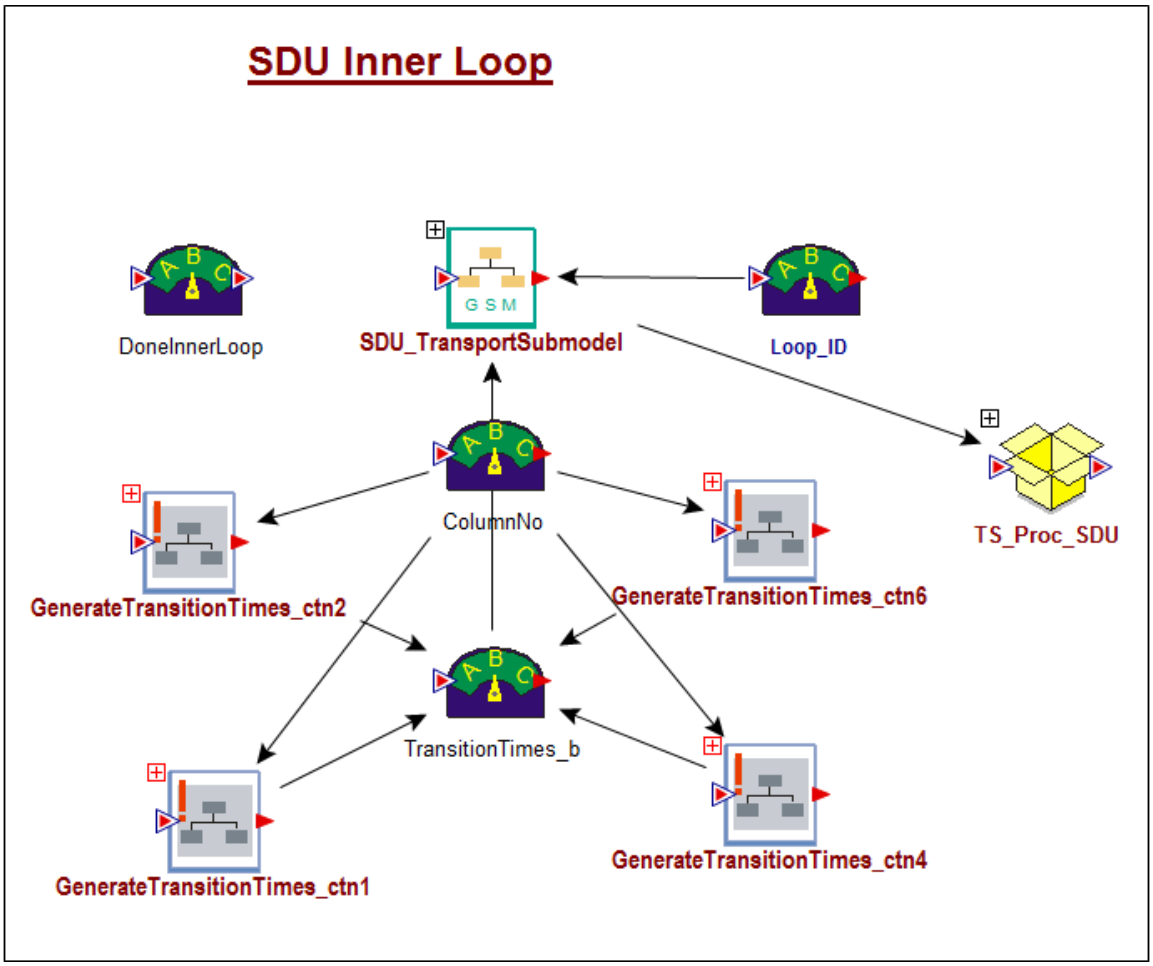

Similarly, the container *TS_Proc_SDU*, contains the external (DLL) elements that control the running of GoldSim's *TS_Proc* DLL which sums the column by column releases controlled by the inner looping container and generated in the submodel, and passes the summed values for each SDU, into a time-series element located outside the nested looping container system.

Within the GoldSim submodel container *SDU_TransportSubmodel* there are four upper level containers, *Material*, *InputData*, *SDU_Abstraction* and *SDU_Transport_Results* (Figure 4.2-6). The *Material* container is equivalent to the similarly named container in the main model, and it includes the list of radionuclides simulated in the model and their basic properties (atomic weight, half-lives, etc.) and the original fluid (water) assigned by the model. Because submodels are independent modules, they need their own fluid (*Water*) and species (*Species*) elements. The *InputData* container is mainly comprised of selector elements that are used to capture data passed from the main model through the submodel (*SDU_Abstraction*) interface. In addition, *InputData*, contains two containers *ReadFlowData* and *Deff_FDCs*, which contain the external (DLL) elements used to control *ReadPORFLOWData.dll* and associated feeds. The external element in *ReadFlowData* is

used to read in the flow data needed by the model and the external element in *Deff_FDCs* is used to read in the time-dependent diffusion coefficients needed. The elements used to simulate the release of Tc-99 from the SDUs are located in the *SDU_Abstraction* container. *SDU_Transport_Results* contains the time-series elements and their feeds used in conjunction with the *TS_Proc* DLL outside the submodel to feed results out of the submodel.

Figure 4.2-6: Contents of the GoldSim Submodel Container SDU_TransportSubmodel

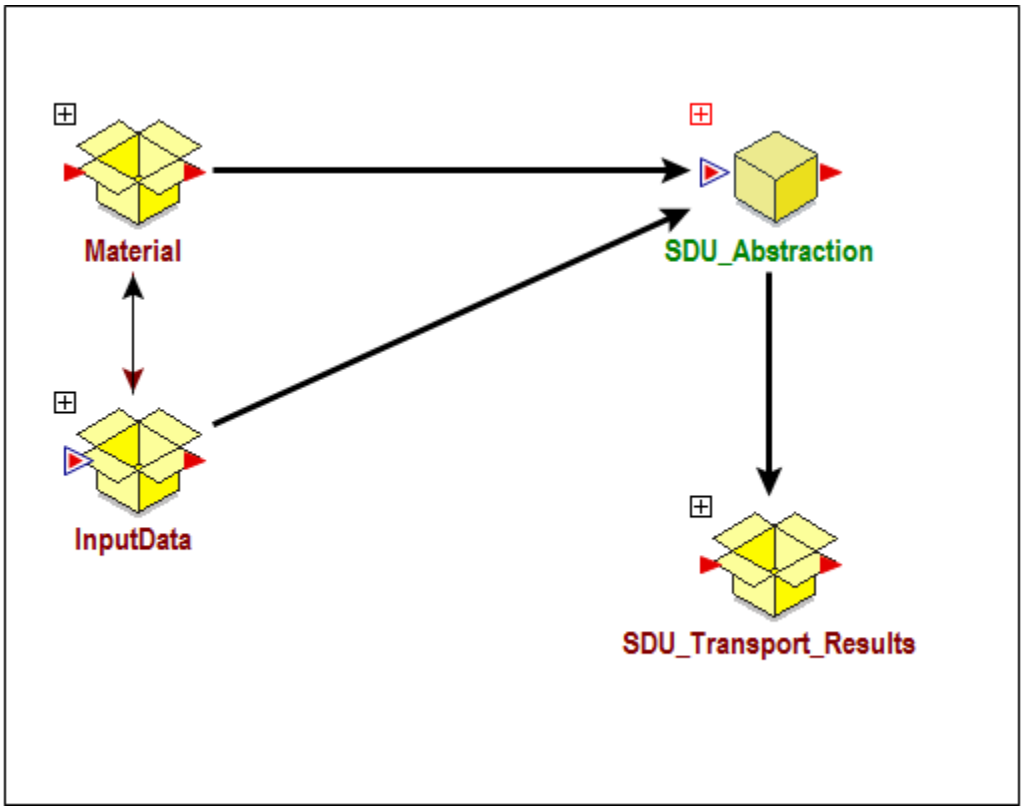

The *SDU_Abstraction* container is comprised of two upper level containers, *Clones* and *SaltStoneRelease* (Figure 4.2-7). The *Clones* container is comprised of all of the elements, except one, defining input parameters for mixing cells. The exception, *RowNo*, defines the cell row (layer) number, which is different for each cell. The elements in *Clones* that are direct feeds to the mixing cells (cell pathway elements) are cloned into the each of the 84 containers holding mixing cells. By use of cloning, any changes made to an element do not have to be repeated 84 times.

The *SaltStoneRelease* container is comprised of two containers (Figure 4.2-8) one holding the elements simulating radionuclide migration through the SDUs (*DisposalUnit*) and one holding the elements simulating radionuclide migration through the unsaturated zone (*UZ*).

The *DisposalUnit* container in turn, contains the *SDUCells* container (Figure 4.2-9) within which 84 containers (Figure 4.2-10) each containing a single mixing cell the mixing cell data feeds (Figure 4.2-11). The reason each mixing cell has its own container is to allow each cell to have its own *Water* element clone and associated solubility control data feed. The 84 cells

represent the saltstone, floor, and when appropriate upper mud mat layers of the PORFLOW model columns. Note, as discussed in Section 3.2.1, each cell has a release mechanism that

Figure 4.2-7: Contents of *SDU_Abstraction*

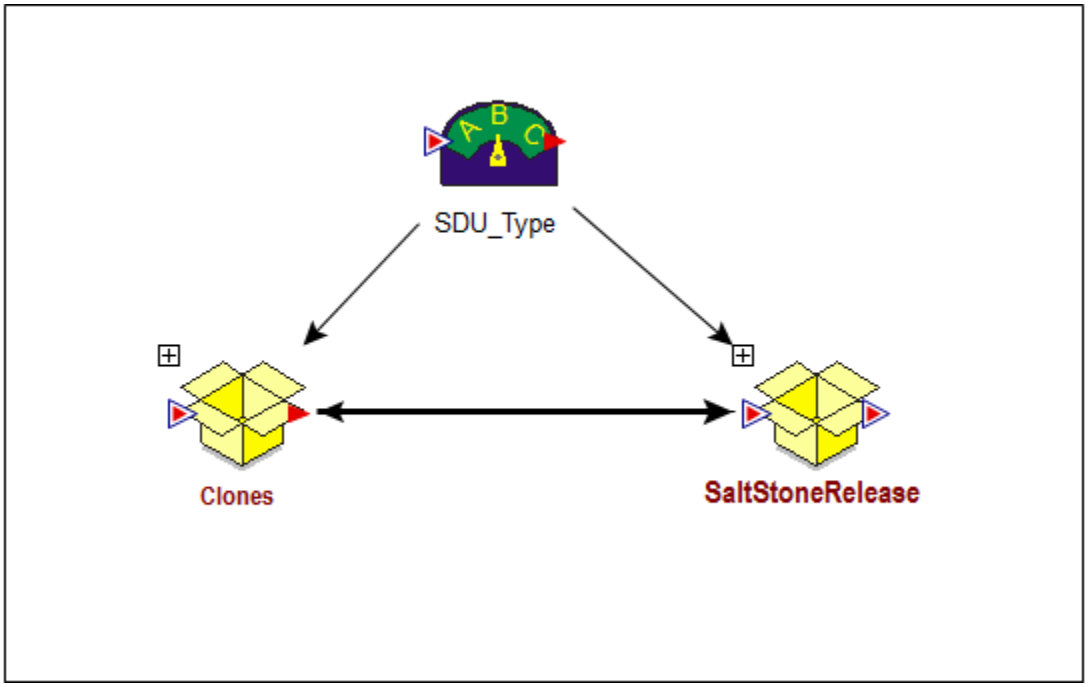

Figure 4.2-8: Contents of *SaltStoneRelease*

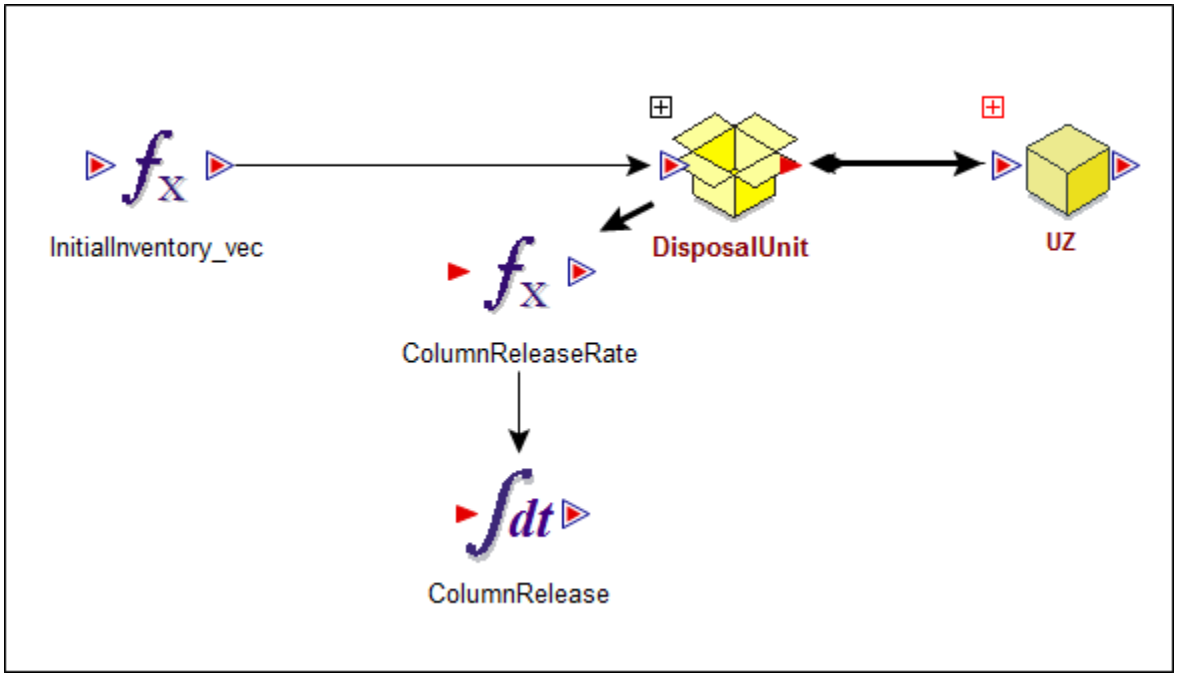

Figure 4.2-9: Contents of *Disposal Unit*

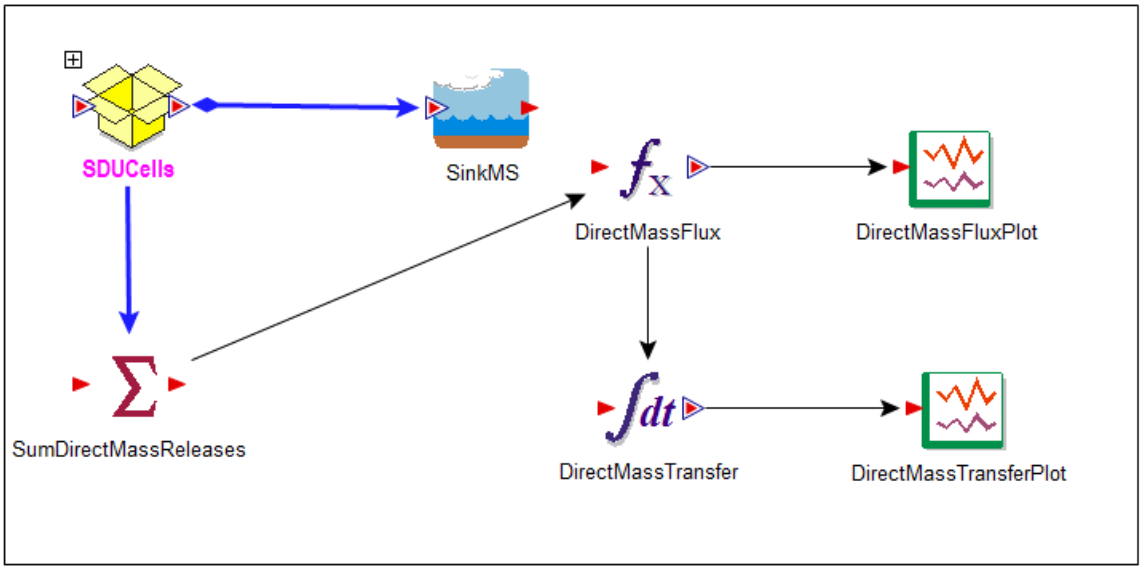

Figure 4.2-10: Contents of *SDUCells*

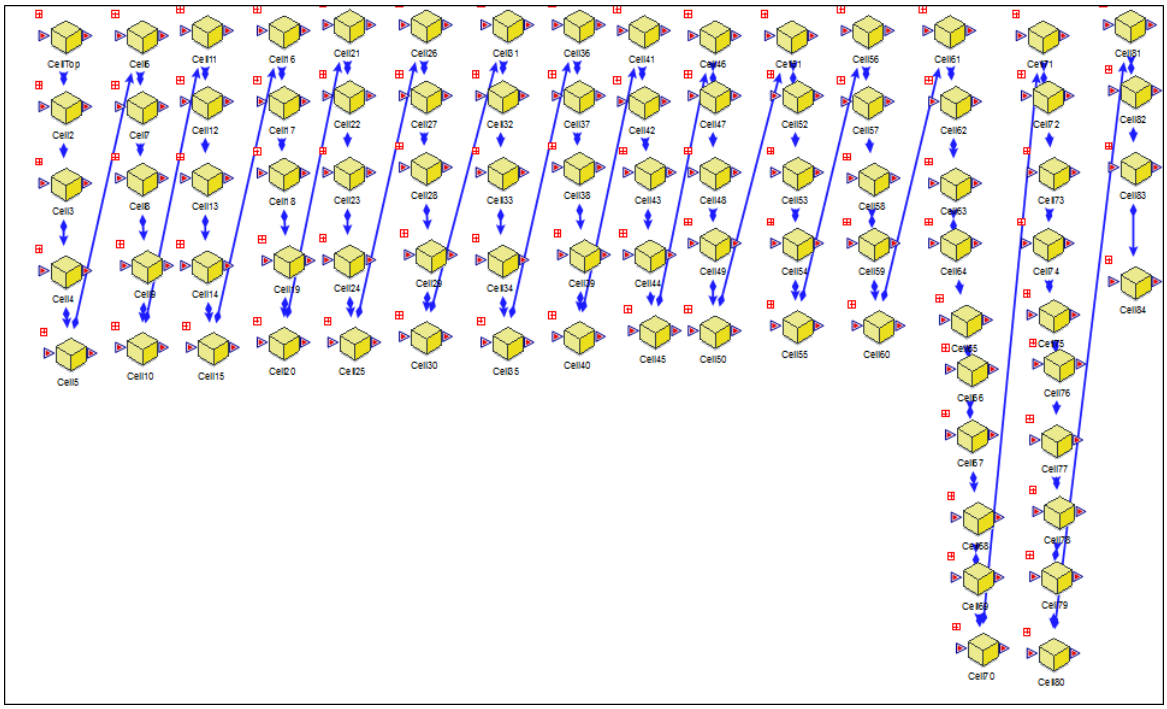

Figure 4.2-11: Contents of Each Container in *SDUCells*

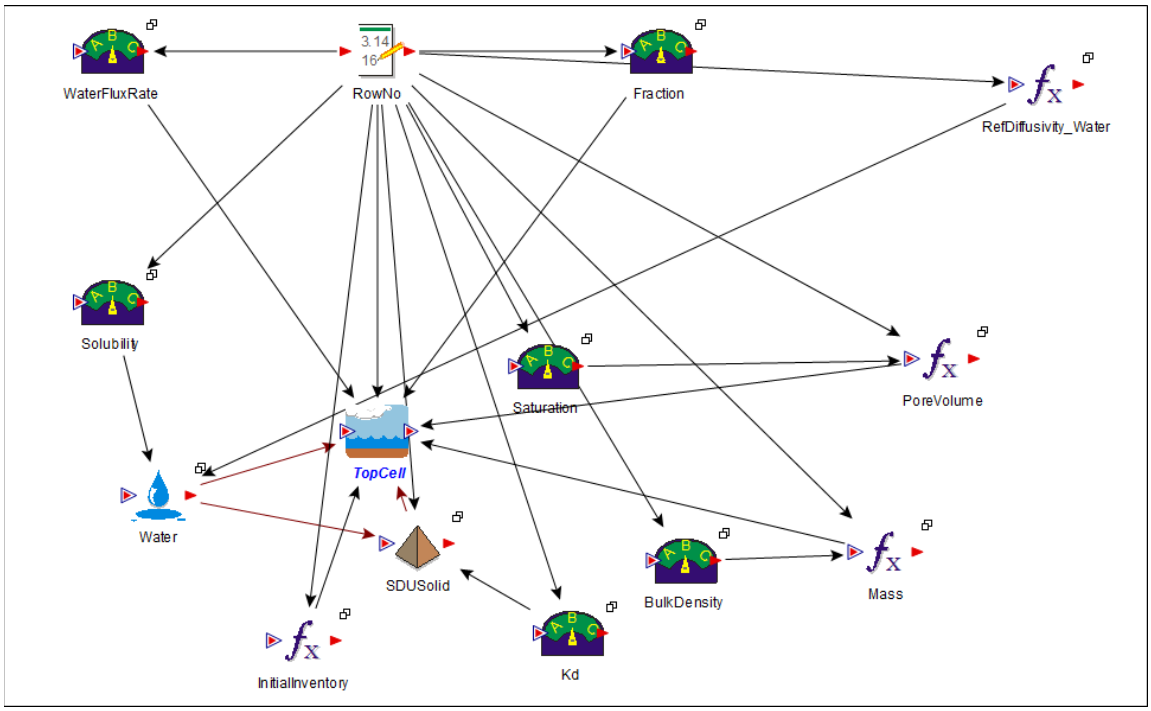

can directly transfer mass to the UZ. This release mechanism, a GoldSim Mass Transfer Link, transfers the radionuclides to a sink cell (see *SinkMS* in Figure 4.2-9) and the sum, of all transfer link release rates, is integrated and added to the top UZ cell as a cumulative input.

The *UZ* container is comprised of two containers, *UZSet1* and *UZSet2*, each containing 10 mixing cells linked in series (Figure 4.2-12). The releases from the last cell in series, *UZCell_Out* is passed on to the main model (Figure 4.2-13).

Figure 4.2-12: Contents of *UZ*

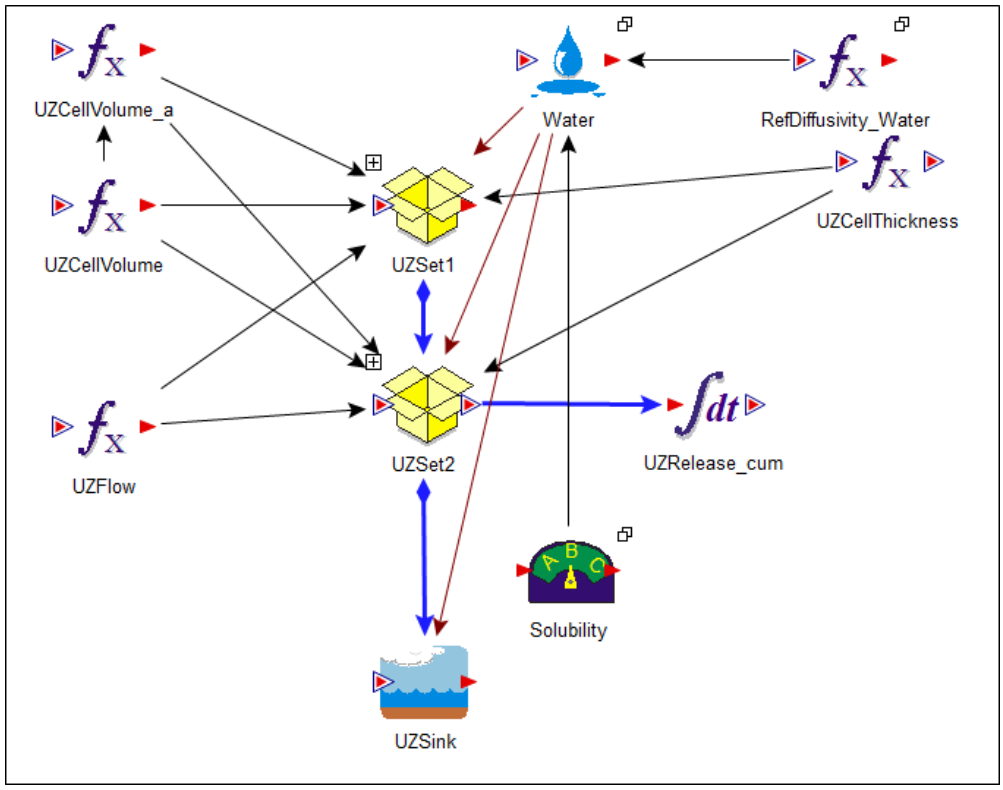

Figure 4.2-13: Contents of *UZSet2*

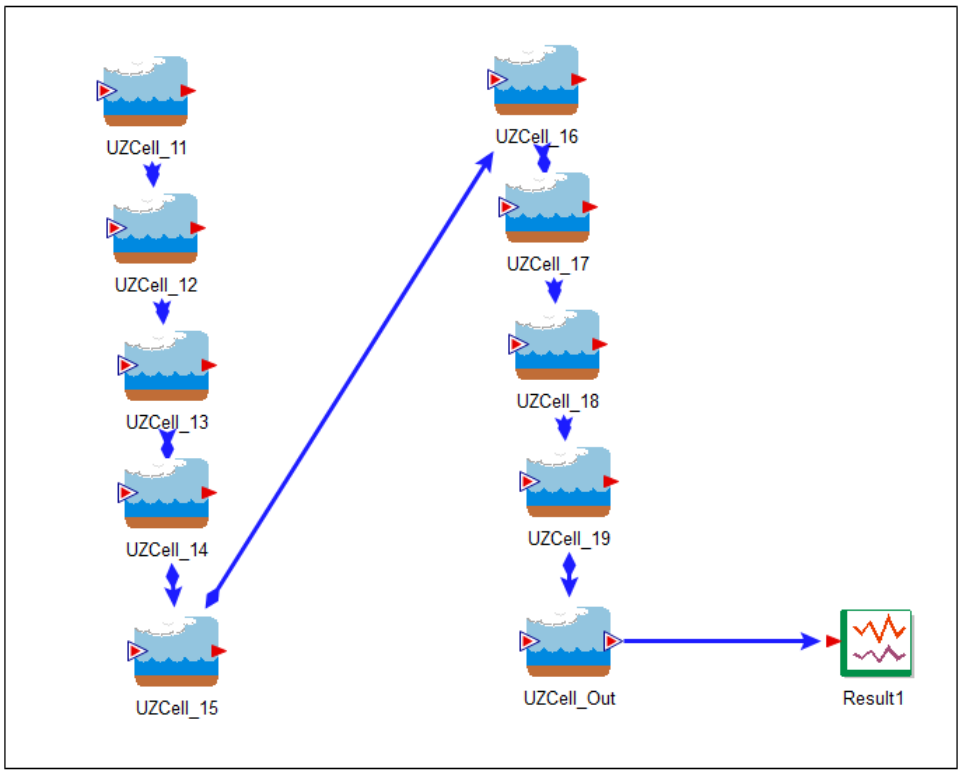

4.2.1.5 ModelOutput

The *ModelOutput* container is comprised of two GoldSim time-series elements that capture the SDU Tc-99 release rates and cumulative releases from the submodel. In addition, the container includes expression elements that evaluate the time-series at each time step and time history elements that can be viewed. Note that the container *SDUReleaseOutputs* contains time history elements that automatically export release-rate time histories for each SDU to text files that are imported by the all-species model.

4.2.2 Transition Time Dynamic Link Library

In the GoldSim SDF Tc-99 Release Model, solubility-control transition times are generated by subroutines contained in the FORTRAN DLL, *TransitionTime.dll* (SRR-CWDA-2014-00033). *TransitionTime.dll* reads in PORFLOW generated velocity files then uses the data to follow the oxygen fronts vertically through each column and horizontally along each row of cells. The front velocities are a function of the time-dependent flow rate and the rate at which the oxygen reacts with the slag, using up the grout or concrete materials reduction capacity. The software then selects the minimum transition time (time the slag reducing capacity is consumed) from the vertical and horizontal analyses, and sets the minimum time as the transition time to be used in the SDF GoldSim Model. GoldSim external (DLL) elements (see *TTA* in Figure 4.2-14) provide the interfaces (one for each SDU-type) between the GoldSim model and the DLL. From GoldSim, the DLL is called using GoldSim's external function which passes the instructions through its input interface to the dynamically allocated variable *gsmin()* in *TransitionTime.dll*. The DLL then reads the data files and assigns the requested data to the 1-dimensional variable array *gsmout()*. The structure of the vector-variable, is controlled by the output interface of the external function element. The required structure of the external function interface and the general structure of the DLL are described in Appendix C of GTG-2010c. The data passed through the external element's interface to control the DLL (*TransitionTime.dll*) aredescribed in Table 4.2-1.

Table 4.2-1: Instruction Data Passed to *TransitionTime.dll*

Number	Variable Name	Variable Meaning
1	FileExt	File Extension Number
2	SDU	SDU Type
3	IRLZ	Realization Number
4	Column	Column Evaluated
5	NColPF	Number of columns in PORFLOW model
6	NLayPF	Number of layers in PORFLOW model
7	Column1	First column in window
8	Column2	Last column in window
9	Layer1	First layer in window
10	Layer2	Last layer in window
11	NumberOfColumns	Number of saltstone columns
12	NCWALL	Number of wall columns
13	NumSSRows	Number of saltstone layers
14	NumFloorRows	Number of floor layers
15	NumUMMRows	Number of UMM layers
16	NCLN	Number of clean grout layers

17	OxygenConc_a	Oxygen concentration at boundaries
18	SLAGRedCap1_a	Slag reduction capacity in saltstone
19	SLAGRedCap2_a	Slag reduction capacity in concrete
20	Rhob1	Saltstone bulk density
21	Rhob2	Floor bulk density
22	Rhob3	UMM bulk density
23	Por1	Saltstone bulk porosity
24	Por2	Floor bulk porosity
25	Por3	UMM bulk porosity
26	ISLUMM	Realization has slag in the UMM
27	NOSLAG	Realization has slag in the wall
28	CFZ1	First Column of Fast Zone
29	CFZ2	Last Column of Fast Zone
30	NWJLay	Number of joint layers
31	ICheck	Print debug data
32	Blank	A zero indicating that no more data is requested

The feeds for the data passed through to the DLL are found in the containers *TTADLLData* (Figure 4.2-15) and *TTADLLData_a* (Figure 4.2-16). The transition times generated by the DLL, are captured by a data element found in *TransitionTimeContainer*. Additionally, time series of column-averaged vertical Darcy velocities are captured by time-series elements found in *VelocityContainer*. The control data passed from the GoldSim model to the DLL tells the DLL which control data file to read, and the control file, along with data passed into the DLL, tells the DLL which file to read and where it is located. A typical control input file, *TTAdata.in*, is presented in Figure 4.2-17.

Figure 4.2-14: GoldSim External Element Used for Reading in Flow Transition Time Data

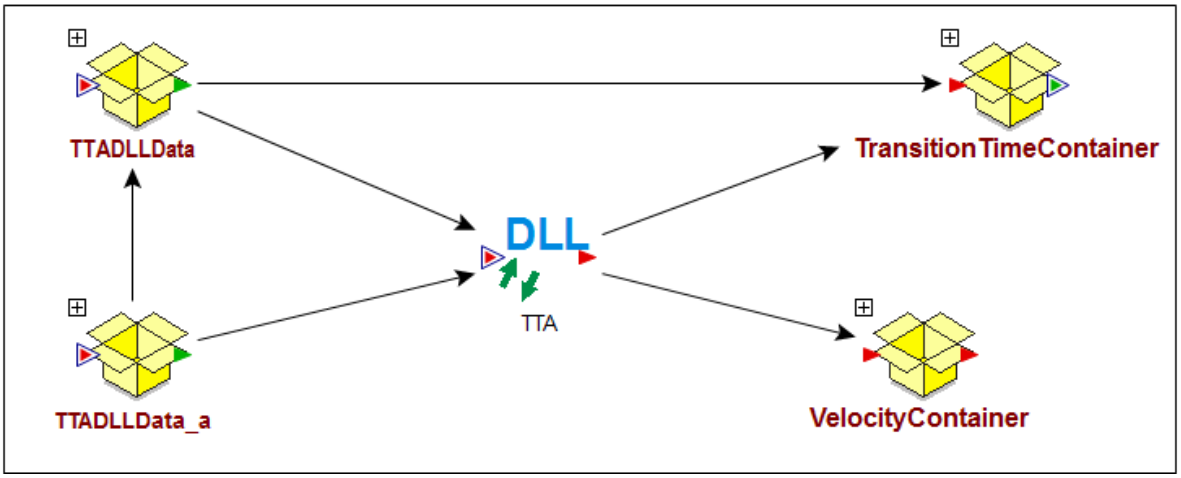

Figure 4.2-15: Contents of the GoldSim Container *TTADLLData*

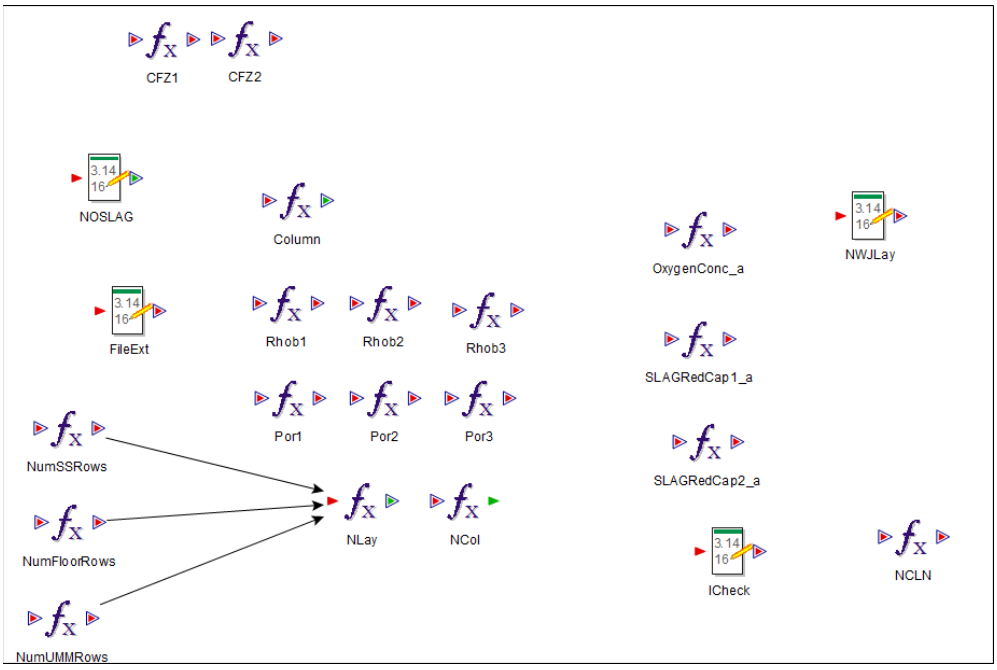

Figure 4.2-16: Contents of the GoldSim Container *TTADLLData_a*

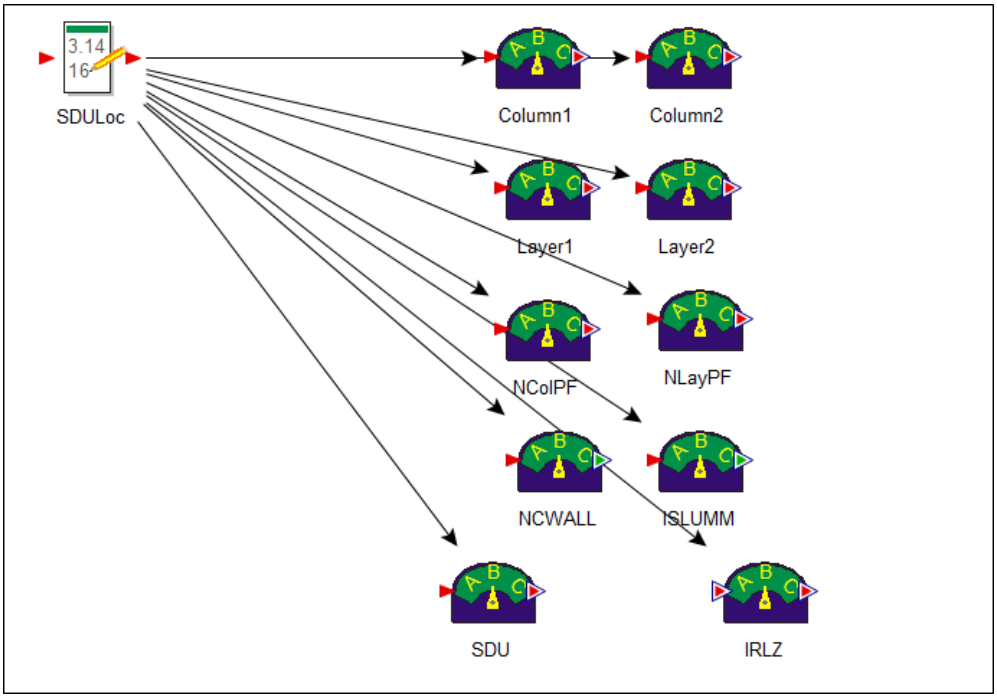

Figure 4.2-17: *TransitionTime.dll* Control File *TTAdata.in*

```
C:\SaltstoneData1\Vx\SDUx_Geom.in
C:\SaltstoneData1\Vx\RLZyyy\Flow\goldsim.tab
C:\SaltstoneData1\Vx\RLZyyy\Flow\FLOW_TI0z.sav
20        25
20        25
20        25        41
```

5.0 MODEL BENCHMARKING AND ALTERNATIVE CONCEPTUAL MODEL RESULTS

The SDF GoldSim Model is a probabilistic model designed to perform parameter uncertainty and parameter sensitivity analyses used to help evaluate the potential for radionuclide migration from the SDUs to the accessible environment. The probabilistic model used for the FY2014 SDF SA and future Special Analyses was constructed using the GoldSim systems analysis software and represents an enhancement to previous versions. A description of the probabilistic model and the enhancements provided for the upcoming Special Analysis, is presented in Section 3. The probabilistic model uses an abstraction of the SDF PORFLOW Model to perform radionuclide transport simulations. Dose calculations for the SDF GoldSim Model are performed using the same dose calculations that were used to determine the PORFLOW dose results.

Use of the abstraction model reduces the analysis time needed for multi-realization processes, such as Monte Carlo sampling or Latin Hypercube Sampling (LHS). In order for the probabilistic model abstraction to be used in lieu of the SDF PORFLOW Model, its validity must be tested by comparing the abstraction model results with SDF PORFLOW Model results for the Evaluation Case. A reasonable degree of agreement between the two models is necessary to give confidence that the trends produced in the probabilistic analysis reflect the trends that would occur if the SDF PORFLOW Model is run repeatedly in a probabilistic mode.

Because of these simplifications associated with the abstraction use in the GoldSim model (i.e., reduction in dimensionality, coarser spatial and temporal discretization, abstractions of nonlinear processes, etc.), a perfect match between GoldSim and PORFLOW results is not expected, but basic features of breakthrough curves reflecting processes such as material degradation and changes in chemical environments should be similar.

The following sections describe the approach used to benchmark the SDF GoldSim Model to the SDF PORFLOW Model and the results of that benchmarking.

5.1 Benchmarking Results

The benchmarking analysis was comprised of four phases. The first phase focused on how well the abstraction model (i.e., the SDF GoldSim Model) can approximate the PORFLOW-generated radionuclide releases from the SDUs. Radionuclide releases to the saturated zone from the two models were compared. The second phase focused on how well the abstraction model approximates the radionuclide transport behavior in the saturated zone. PORFLOW-to-GoldSim model comparisons of radionuclide concentrations within specified sectors along the 100-meter boundary (Figure 4.1-2) form the basis of how well the abstraction model approximates in the dilution/attenuation processes in the saturated zone. Breakthrough curves representing the radionuclide concentrations over time for each of the several sectors form the basis of this comparison.

The third phase of the benchmarking process focuses on examining how well the abstracted model approximates the MOP dose results. The fourth phase of the benchmarking process focuses on examining how well the abstracted model approximates the IHI dose results at the seven wells analyzed in the PORFLOW and GoldSim models.

5.1.1 Mass Releases to the Saturated Zone

The FY2014 SDF SA Evaluation Case, which is used in the benchmarking process, represents an alternate scenario, which includes 375-foot diameter SDUs, and updates to the time-based degradation of the SDU components, including the grout, wall, floor and mud mats, simulated to help answer specific questions asked by the NRC.

Note that when comparing breakthrough curves generated by the PORFLOW model and the GoldSim abstraction of the model, the simplifying assumptions of the abstraction are reflected in the differences between the resultant breakthrough curves. The major attributes of the GoldSim abstraction, which allow it to be computationally more efficient include:

- the degree of refinement of the discretized system,
- the spatial averaging of the flow fields in the abstraction,
- the assumption that the advective migration of contaminants controlling the dose calculations is dominated by the vertical component of the velocity field, and
- the assumption that the transport integral to the dose calculations is dominated by releases from the bottom of the SDUs.

Within the GoldSim abstraction model the PORFLOW finite-element model (and associated grid) is replaced by a coarser network of mixing cells representing the saltstone mass, the structure, and the surrounding backfill (see Section 4.1.1). Other features, such as the floor, the UZ, and joints, are represented by one-dimensional strings of mixing cells, linked in series. The coarser grid structure will influence the degree to which the releases from the two models can match. In addition, while the PORFLOW model uses a heterogeneous flow field with velocities varying from cell-to-cell, the abstraction utilizes a uniform flow field derived from the PORFLOW model flow field. Within individual model structures, like the UZ, a single spatially averaged flow rate, determined from the heterogeneous PORFLOW model flow field, is used. As described below, with respect to specific benchmarking comparisons, the horizontal component of flow in the UZ can have a moderate influence on the initial timing of breakthrough curves and the less important early time releases. This effect is accentuated by the lower vertical components of UZ velocities below the center of the SDUs. The differences between breakthrough curves from the two models are associated with the spatial averaging of the velocities used in the GoldSim model and the abstraction's assumption of a uniform vertical flow field beneath the SDU. This effect is more prominent in the smaller SDUs (SDU 1 and the 150-foot diameter SDUs) than the SDUs with larger footprints (SDU 4 and the 375-foot diameter SDUs). Because of the influences of the column zone on the saltstone flow domain, the saltstone is divided into two rectangles (central and outer) for SDUs 1 and 4 and two cylinders (inner and outer cylinder) for the other SDUs. Each zone has its own spatially averaged uniform velocity derived from the PORFLOW flow model outputs.

Also, note that the Tc-99 GoldSim model is also subject to additional simplifying assumptions including the assumption that the horizontal component of diffusion is not a controlling factor in contributing to peak dose. In addition, the GoldSim model uses the "shrinking core" model from the FY2013 SDF SA as opposed to the "shrinking core" model

from the FY2014 SDF SA, which assumes that transient dissolution within a computational cell (element) is a function of the degree of slag oxidation within the cell. The FY2013 SDF SA "shrinking core" model, which is utilized in the present GoldSim model, assumes a step-function approach to release, wherein all precipitate in a cell instantaneously dissolves at the time that the last remaining slag is oxidized.

The criterion for acceptability of the simplified GoldSim results as an analogue for the PORFLOW results, is based upon a comparison between PORFLOW and GoldSim model peak values. A difference of 25% or less was considered acceptable, although under specific conditions a greater difference was considered appropriate. For example, more flexibility was given to the differences in spike releases from the Tc-99 model due to the differences between the instantaneous-dissolution assumption (GoldSim) versus the time-dependent dissolution assumption (PORFLOW). In general, peak differences were less than 20% and usually much less, especially when the release peaks fell within the simulation time range. The timing of peaks was also considered important, but acceptability was based the individual simulations and cause of deviations when they occurred. Note that a 12.5% temporal deviation was the worst case.

The species evaluated during the benchmarking represent the most important dose contributors noted in the PORFLOW simulations: I-129, Cs-135, Ra-226, and Tc-99. Note that in the Tc-99 release model transition-time analysis, the upper mud mat reduction capacity is the same for the 150-foot diameter and 375-foot diameter SDUs. This is not true for the PORFLOW simulations where the upper mud mat is initially oxidized in the 375-foot diameter SDUs. This may have a small effect on timing of the releases.

5.1.1.1 SDU 1

A comparison of the PORFLOW SDF Model and SDF GoldSim Model mass releases of Cs-135, I-129, Ra-226, and Tc-99, as presented in Figures 5.1-1 through 5.1-5, indicate that the GoldSim model produces an acceptable approximation of the releases from SDU 1 generated by the PORFLOW model. Table 5.1-1 summarizes the peak values for these releases.

Table 5.1-1: GoldSim and PORFLOW Model Peak Unsaturated Zone Release Comparisons for SDU 1 within 20,000 years

Radionuclide	PORFLOW Peak Release (g/yr)	PORFLOW Time of Peak Release (yr)	GoldSim Peak Release (g/yr)	GoldSim Time of Peak Release (yr)	Peak Release Percent Difference GoldSim vs PORFLOW
I-129	3.9E-01	~5,500	4.2E-01	~5,500	9%
Cs-135	2.3E-02	~10,000	2.0E-02	~9,000	-12%
Ra-226	4.2E-08	20,000	4.5E-08	20,000	6%
Tc-99	4.3E-01	~13,500	4.2E-01	~13,000	-2%

The SDF GoldSim Model I-129 release presented in Figure 5.1-1, closely replicates the PORFLOW model release with the GoldSim mode having a 9% higher peak and a similar peak-arrival timing. The variation in the PORFLOW and I-129 breakthrough curves for SDU 1 at 1,000 years, depicted in Figure 5.1-1, can be attributed to the differences in the spatial distribution of the UZ flow-fields used by the two models. The PORFLOW model

uses spatially explicit cross-sectional flow fields generated during PORFLOW flow model simulations.

Figure 5.1-1: SDU 1 I-129 Release to the Saturated Zone

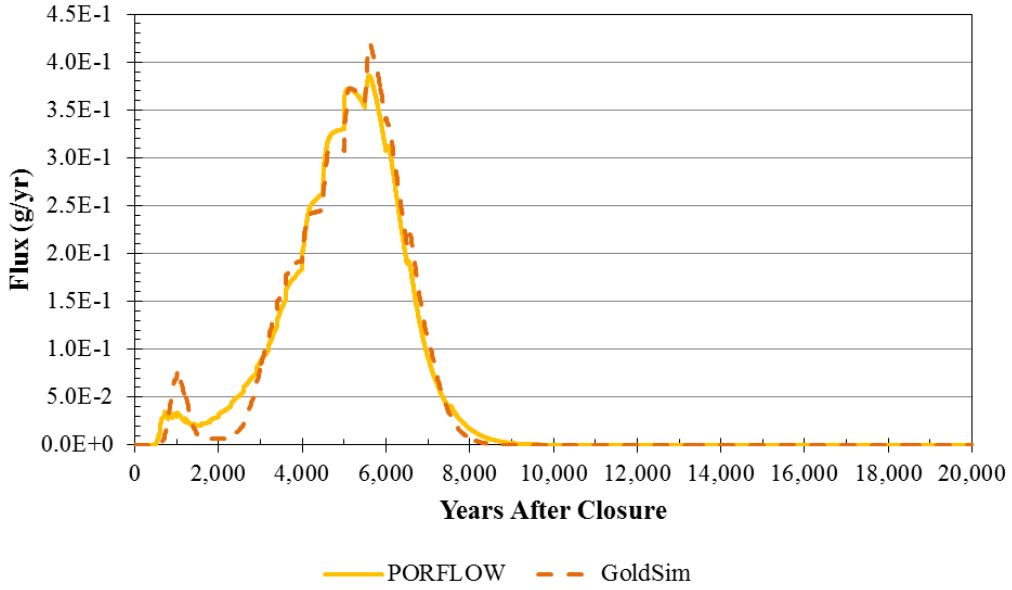

In contrast, the GoldSim model utilizes zone-specific (i.e., the UZ) uniform flow rates based upon spatial averaging of the vertical component of flow based on flow-fields generated by PORFLOW. As seen in Figure 5.1-2, this early PORFLOW model release, which emanates from the wall, is controlled by the inwardly directed horizontal component of flow, which causes the release to migrate to the center of the SDU and disperse as it migrates vertically downwards. The left edge of the figure represents the middle of SDU 1 and cells with greater discretization indicate the outer wall, roof, and floor. The Y-Axis provides the distance from the bottom of the floor of the SDU (in cm) and the X-Axis provides the distance from the middle of the SDU (also in cm). The directional vectors describing the flow field are presented in Figure 5.1-3. Note also that the vertical component of flow in the UZ decreases from the edge of the SDU to the middle of the rectangular structure. In the GoldSim model, the early release from the wall advects directly downwards from the floor beneath the wall. An additional component in the fill adjacent to the wall is also transported downwards to the UZ. Figure 5.1-4 presents the breakdown of the GoldSim model I-129 releases from different components of SDU 1, along with the UZ release breakthrough curve. As can be seen in the figure, the early-time (~1,000 years) UZ-release breakthrough curve is dominated by the mass release from the wall (and the floor beneath it). This pattern of release from the wall is similar to that seen in the PORFLOW model concentration-contour plot presented in Figure 5.1-2.

Figure 5.1-2: SDU 1 I-129 PORFLOW Model Release to the Saturated Zone at 1,000 Years

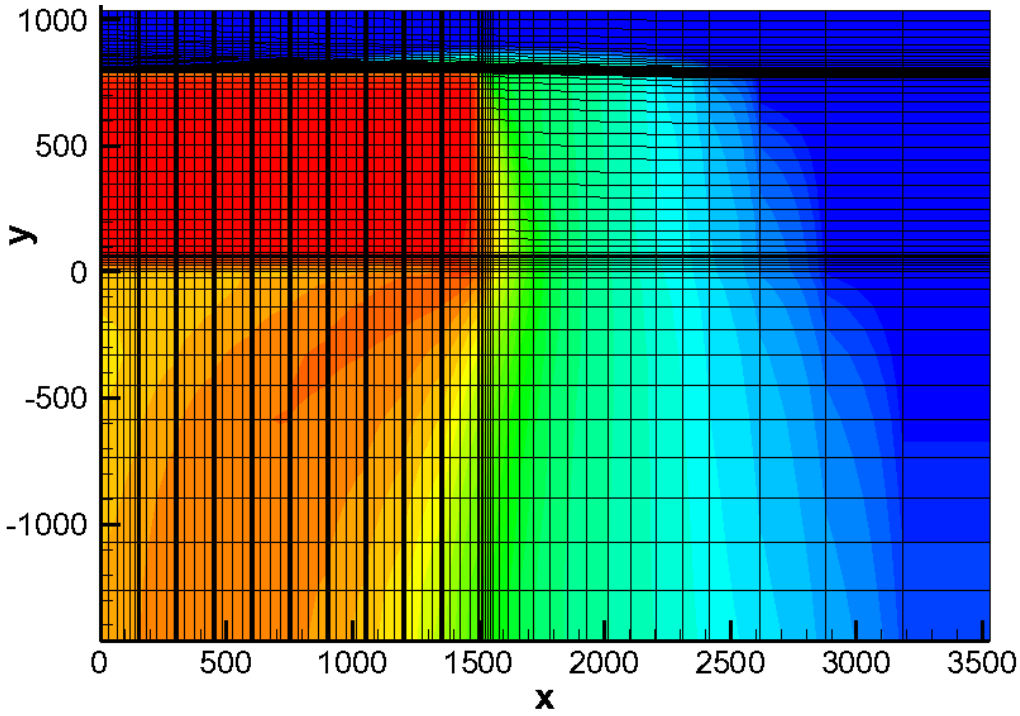

Figure 5.1-3: SDU 1 Flow Field at 1,000 Years

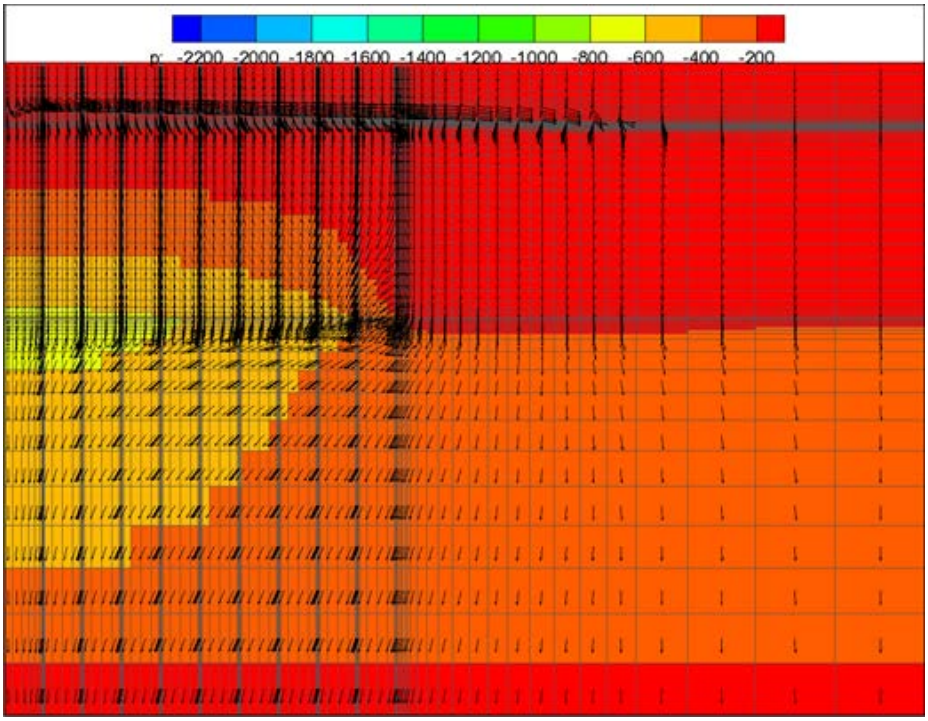

Figure 5.1-4: UZ and Vault Component I-129 Releases for SDU 1 (GoldSim)

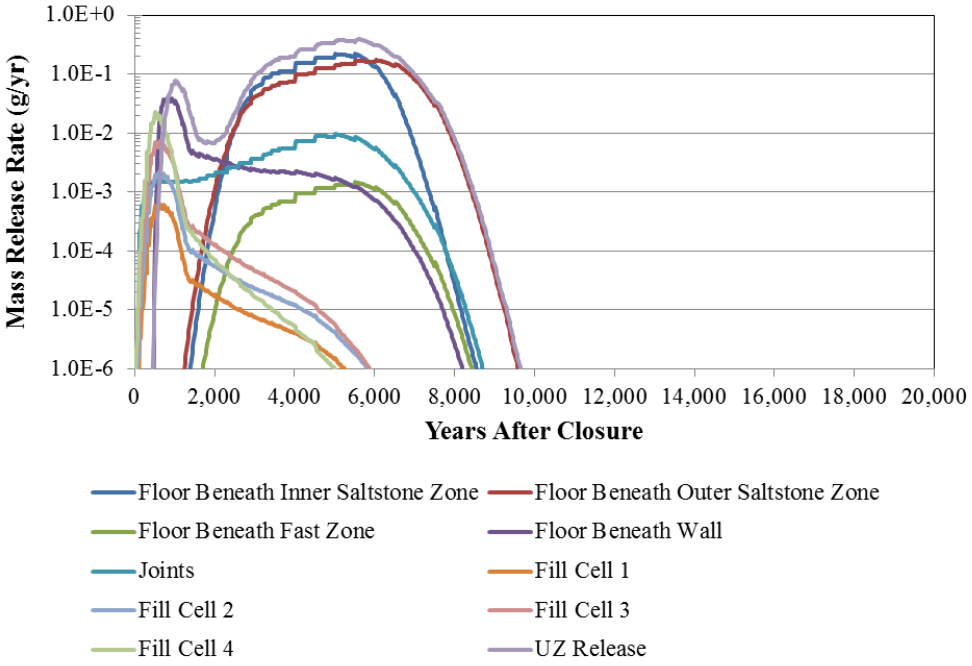

The SDF GoldSim Model Cs-135 release presented in Figure 5.1-5, acceptably replicates the PORFLOW model release in shape but the GoldSim breakthrough curve arrives sooner (the peak is near 9,000 years as opposed to approximately 10,000 years) and is slightly more dispersed with a peak value that is 12% lower than the PORFLOW peak. The difference in peak arrival time between the Cs-135 breakthrough curves can be attributed to the simplification (by velocity averaging) of the UZ flow fields used by the SDF GoldSim Model. The differences between the PORFLOW- and GoldSim-generated breakthrough curves are also accentuated by cesium's higher K_d (relative to iodine).

Figure 5.1-5: SDU 1 Cs-135 Release to the Saturated Zone

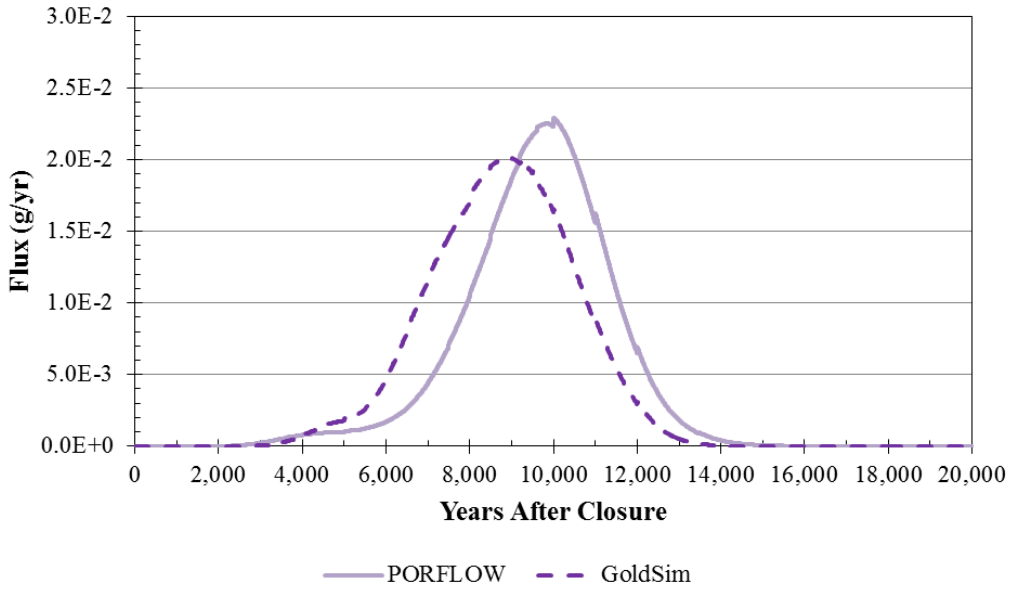

The Cs-135 concentration profile at 7,250 years, as generated by the PORFLOW model, is presented in Figure 5.1-6. This figure shows a vertical cross section of SDU 1. The influence of the horizontal component of flow over time is readily seen in Figure 5.1-6, with the center of mass migrating towards the middle of the SDU. Figure 5.1-7 shows the flow vectors and depicts the horizontal component of flow in the UZ immediately beneath the SDU, which causes the Cs-135 to migrate towards the UZ below center of the SDU. In the UZ, the vertical flow rate (as generated by the PORFLOW flow model) in the UTRA-UZ below the outer area of the SDU is up to 5 to 10 times greater depending on the time step, than under the middle of the SDU. The GoldSim model utilizes a uniform flow field in the UZ based on the spatial averaging of the vertical component of the PORFLOW generated flow field. This heterogeneity in the flow field beneath the SDU controls the PORFLOW breakthrough curve presented in Figure 5.1-5. The GoldSim model utilizes a uniform flow field based on the spatial averaging of the vertical component of the PORFLOW generated flow field. This simplified model generates a breakthrough curve that arrives sooner and is more dispersed. Note that the spatial differentiation in the flow field beneath the SDU dissipates at later times as the SDU cementitious material degrades, and vertical flow becomes the dominant component of the PORFLOW flow fields (see Figure 5.1-7).

Figure 5.1-6: SDU 1 Cs-135 PORFLOW Model Release to the Saturated Zone at 7,250 Years

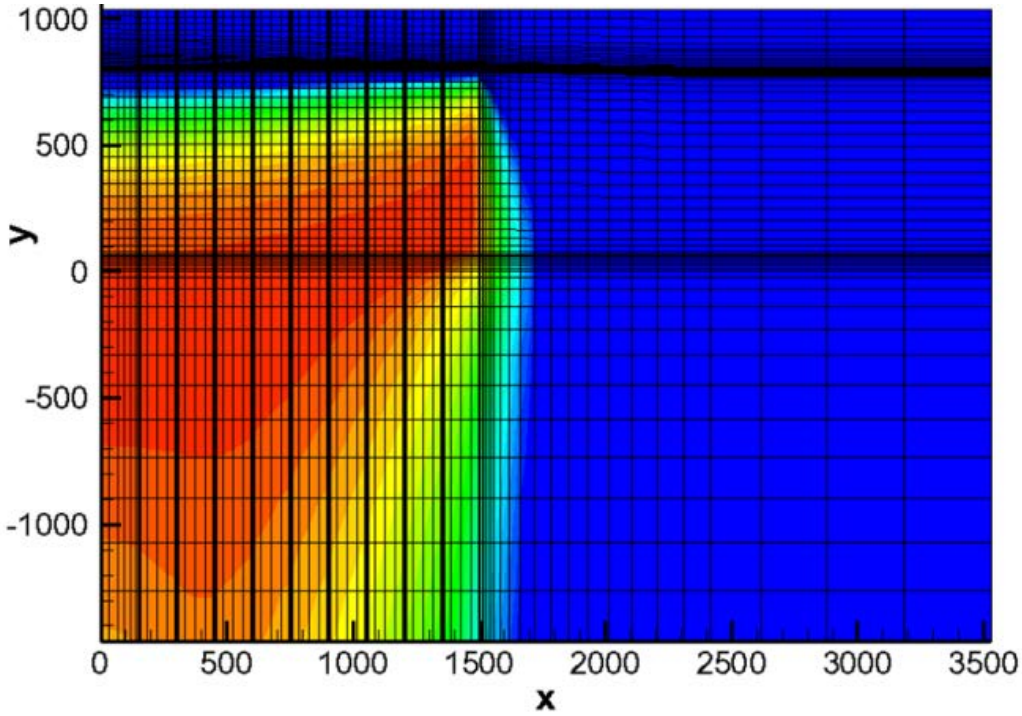

Figure 5.1-7: SDU 1 Flow Field at 18,900 years

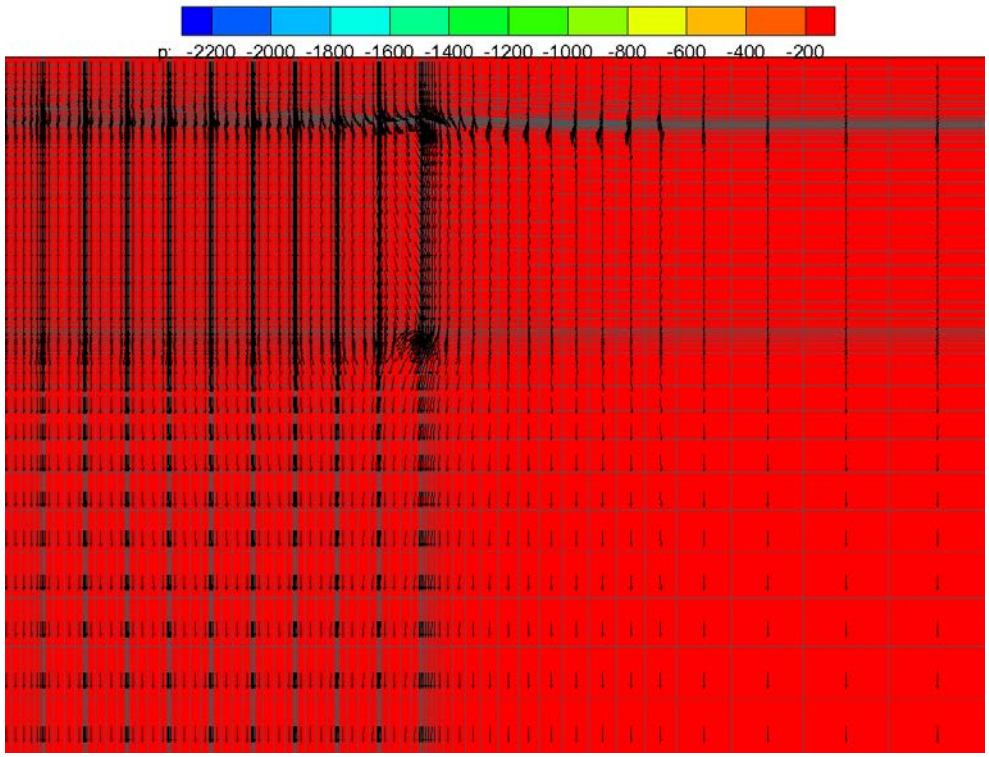

The similarity in the flow field data is reflected in the closeness of the Ra-226 breakthrough curves (Figure 5.1-8). Also note that for SDU 4 and SDU 6 (see Sections 5.1.1.2 and 5.1.1.4) which are dominated earlier by vertical flow, the Cs-135 timing of the breakthrough curve peak generated by the GoldSim model is similar to the timing generated by the PORFLOW model. At later times, when the vertical component of flow becomes dominant, as depicted in Figure 5.1-7, relatively steady releases such as the Ra-226 (from the ingrowth from U-234) generate PORFLOW and GoldSim breakthrough curves which are quite similar as shown in Figure 5.1-8.

Figure 5.1-8: SDU 1 Ra-226 Release to the Saturated Zone

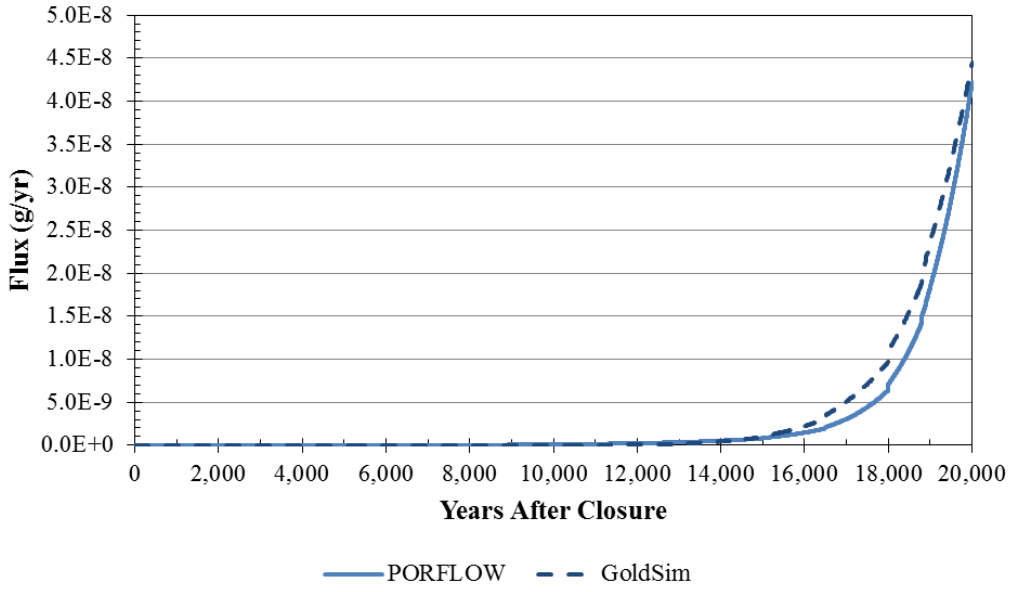

With respect to Tc-99 releases from SDU 1 (Figures 5.1-9 and 5.1-10), the GoldSim model predicts a greater release of Tc-99 at early times, than the PORFLOW model. This early-time difference in the breakthrough curves can be attributed to the difference between the GoldSim "shrinking core" model (which is the same as the "shrinking core" PORFLOW model from the FY2013 SDF SA) and the "shrinking core" PORFLOW model from this FY2014 SDF SA. In the FY2014 SDF SA "shrinking core" model, precipitated Tc-99 within each cell dissolves at a linear rate as oxidation of the slag occurs. In the FY2013 SDF SA (and within the present GoldSim model), all of the precipitated Tc-99 in a particular cell dissolves instantaneously at the time when the last of the slag has been oxidized. The difference between the breakthrough curves generated by the two different conceptualizations of the "shrinking core" models can be readily seen by comparing Figures 5.1-9 and 5.1-10 with Figures 5.1-11 and 5.1-12, which are GoldSim model benchmark comparisons with the SDF PORFLOW Model from the FY2013 SDF SA. [SRR-CWDA-2013-00062]

Figure 5.1-9: SDU 1 Tc-99 Release to the Saturated Zone

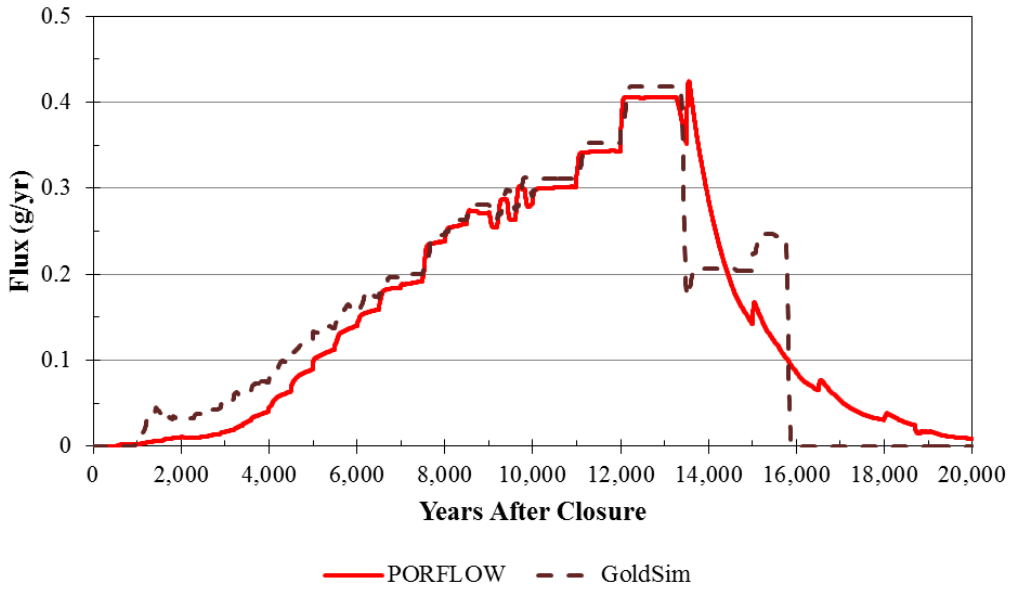

Figure 5.1-10: Semi-Log Plot of SDU 1 Tc-99 Release to the Saturated Zone

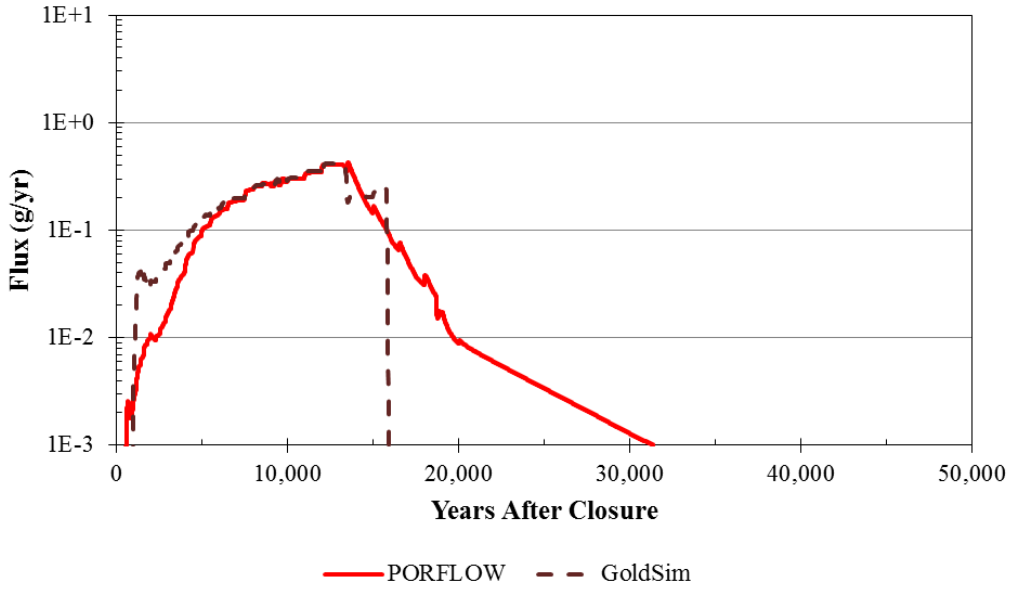

Figure 5.1-11: SDU 1 Tc-99 Release to the Saturated Zone (FY2013 SDF SA)

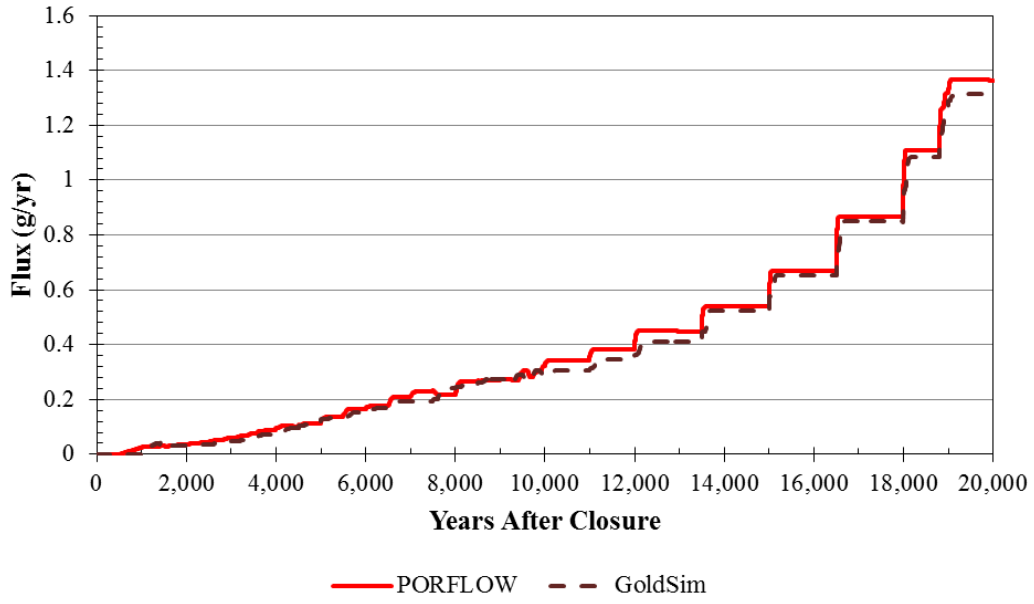

Figure 5.1-12: Semi-Log Plot of SDU 1 Tc-99 Release to the Saturated Zone (FY2013 SDF SA)

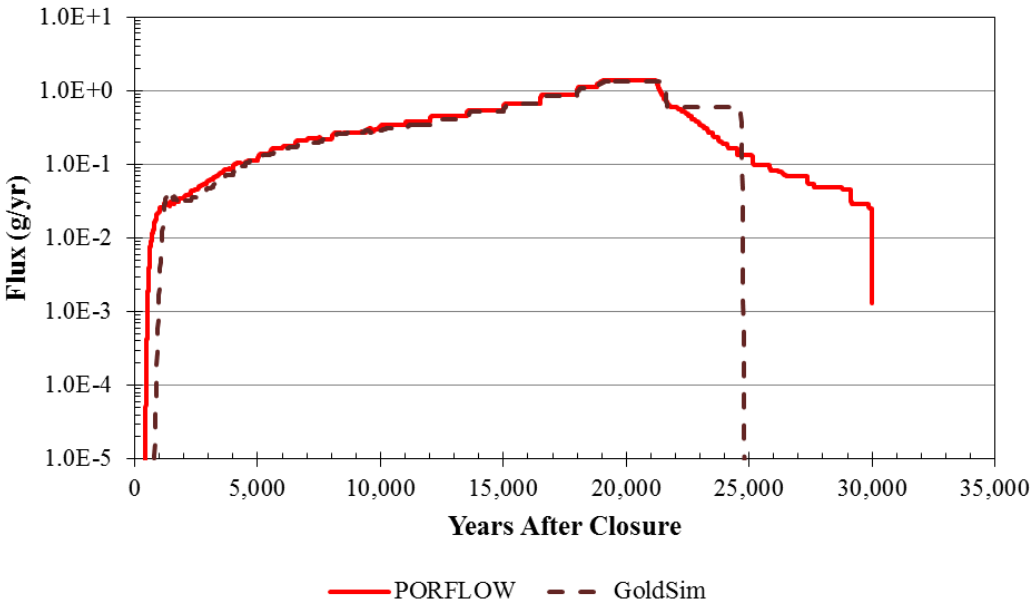

The low-release tail, at the end of the PORFLOW breakthrough-curve, depicted in Figures 5.1-10 and 5.1-12, emanates from a Tc-99 precipitate buildup in oxygen shadow zones[2] near saltstone boundaries. The shadow zone is caused by a delay in slag oxidation, just inside the wall (and in zones adjacent to roof-support columns in SDU 4). The contour plot from the

2 A shadow zone is an area where oxidation is less complete or occurs at a slower rate relative to adjacent areas, normally due to localized lower flow rates.

SDF PORFLOW Model for SDU 1 slag concentration at 30,000 years is presented in Figure 5.1-13. The Tc-99 concentration at the same time is presented in Figure 5.1-14. The buildup of mass is associated with the horizontal components of diffusion and advective transport in the PORFLOW model. The simpler GoldSim Tc-99 abstraction transport model assumes vertical advection dominates the transport processes. However, since the GoldSim Tc-99 abstraction model captures the important trends of the PORFLOW mass release breakthrough curve, it serves as an acceptable representation of the system.

Figure 5.1-13: SDU 1 Slag Concentrations at Saltstone/Wall Contact (28,500 Years)

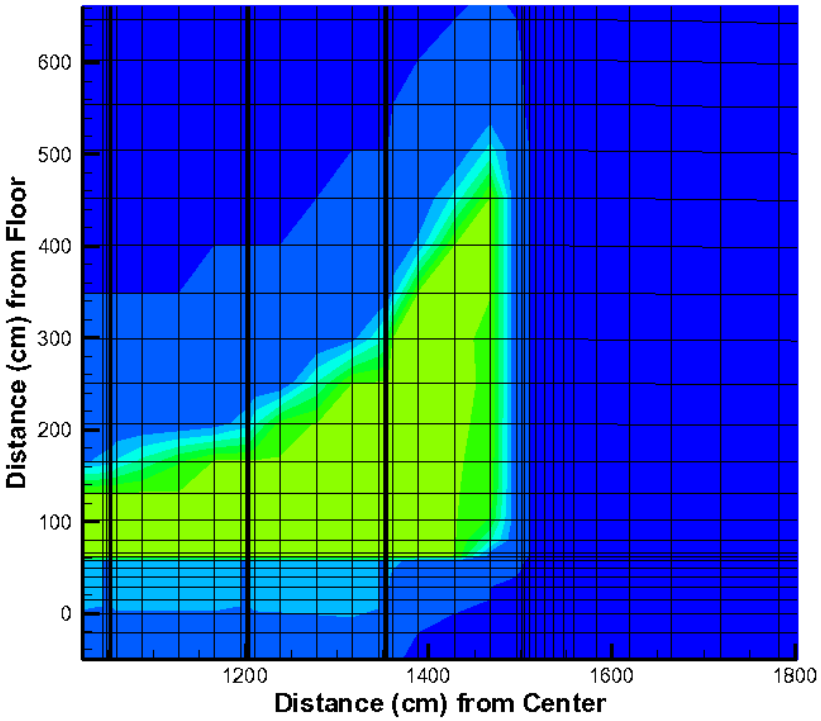

Figure 5.1-14: SDU 1 Tc-99 Concentrations at Saltstone/Wall Contact (28,500 Years)

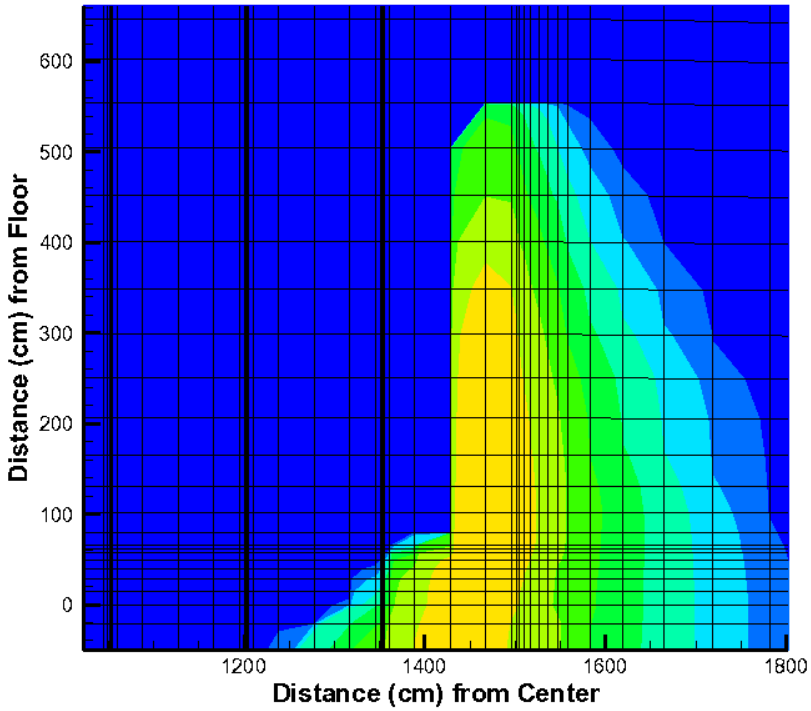

5.1.1.2 SDU 4

Similar to results for SDU 1, the SDU 4 SDF PORFLOW Model and SDF GoldSim Model mass releases presented in within this section indicate that the GoldSim model produces an acceptable approximation of the releases from SDU 4 generated by the PORFLOW model. Table 5.1-2 summarizes the peak values for releases from SDU 4.

Table 5.1-2: GoldSim and PORFLOW Model Peak Unsaturated Zone Release Comparisons for SDU 4 within 20,000 years

Radionuclide	PORFLOW Peak Release (g/yr)	PORFLOW Time of Peak Release (yr)	GoldSim Peak Release (g/yr)	GoldSim Time of Peak Release (yr)	Peak Release Percent Difference GoldSim vs PORFLOW
I-129	1.7E+00	~3,500	1.7E+00	~3,600	-2%
Cs-135	1.2E+00	~5,100	1.3E+00	~5,100	6%
Ra-226	1.8E-05	20,000	1.5E-05	20,000	-16%
Tc-99	2.6E+00	~16,500	2.7E+00	~16,500	-6%

Figure 5.1-15 compares PORFLOW and GoldSim model I-129 releases and shows that the GoldSim model abstraction is an acceptable analog for the PORFLOW model. The peak release level for the GoldSim model is 2% lower than for the PORFLOW model and the GoldSim model arrives about 100 years later (Table 5.1-2).

Figure 5.1-15: SDU 4 I-129 Release to the Saturated Zone

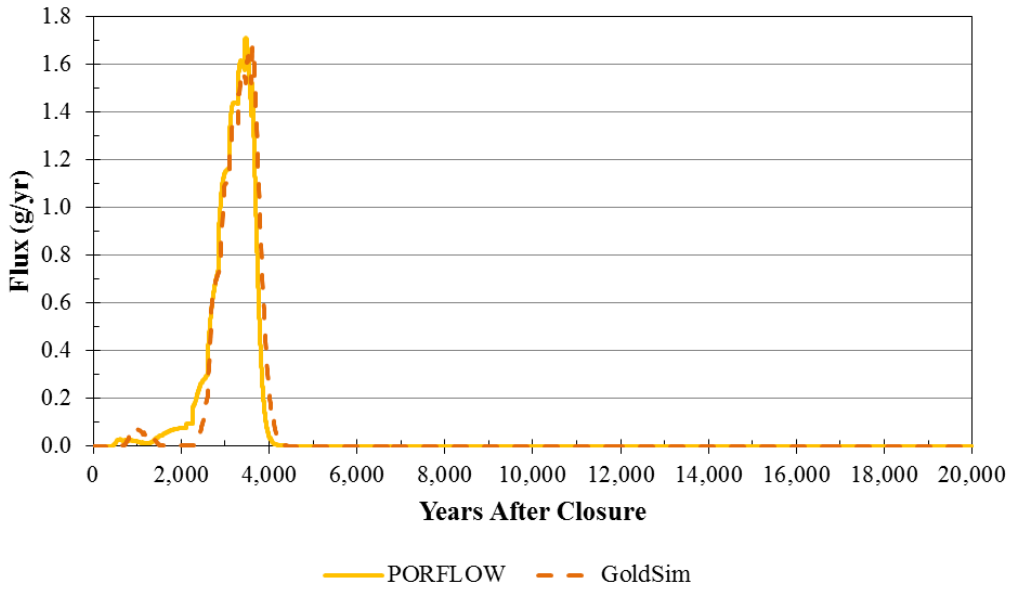

Unlike the results for the Cs-135, release from SDU 1 (Figure 5.1-5), the release from SDU 4 (Figure 5.1-16) shows no significant difference in breakthrough timing between the PORFLOW and GoldSim Model results. This is because releases from SDU 4 move into the unsaturated zone where flow is more dominantly vertical, and the vertical component of flow does not vary as much from the SDU centerline outward.

Figure 5.1-16: SDU 4 Cs-135 Release to the Saturated Zone

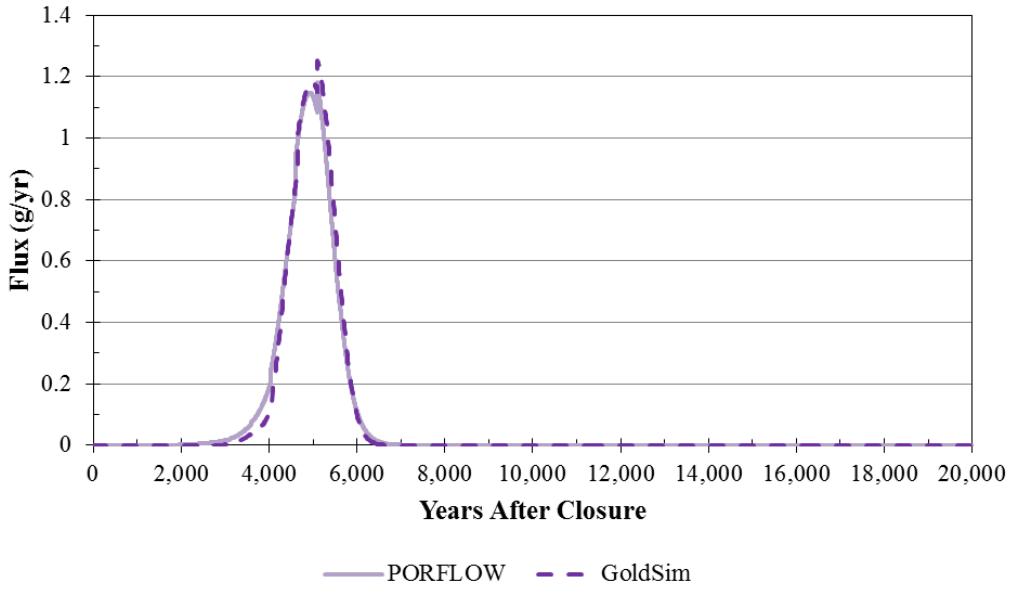

Figure 5.1-17 is a contour plot of the Cs-135 concentrations in and below SDU 4 at 4,250 years after closure. As can be seen, the concentrations tend to be spread out more evenly from the center axis out, as opposed to converging to a narrower band (as shown for the SDU

1 releases in Figure 5.1-6). The symmetry of the releases from the two saltstone zones seen in Figure 5.1-17 is also seen in Figure 5.1-18 (green = inner zone, red dashed = outer zone) which presents the GoldSim model breakthrough curves for the UZ and the various components of the unit.

Figure 5.1-17: SDU 4 Cs-135 PORFLOW Model Release to the Saturated Zone at 4,250 Years

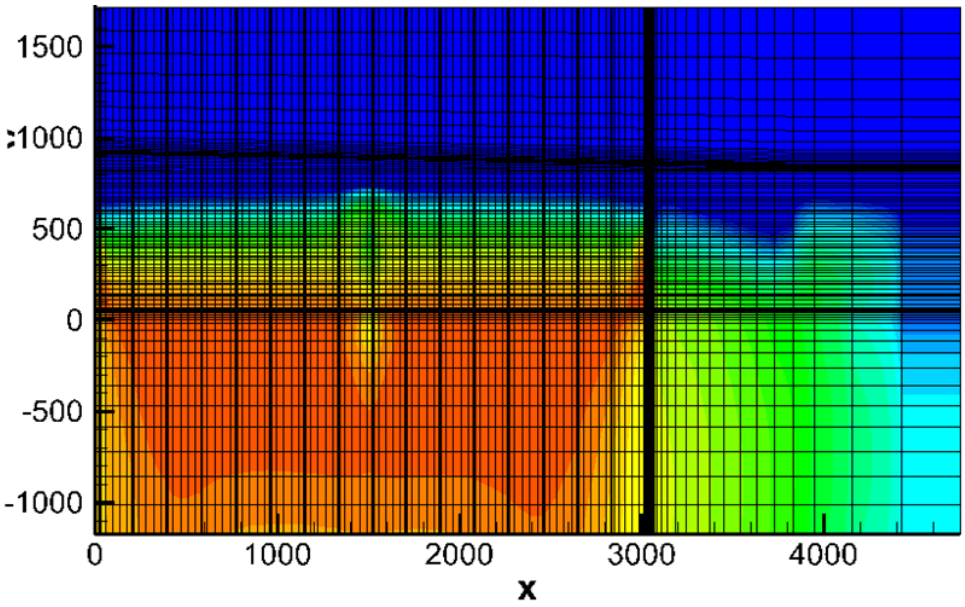

Figure 5.1-18: UZ and Vault Component Releases for SDU 4 (GoldSim)

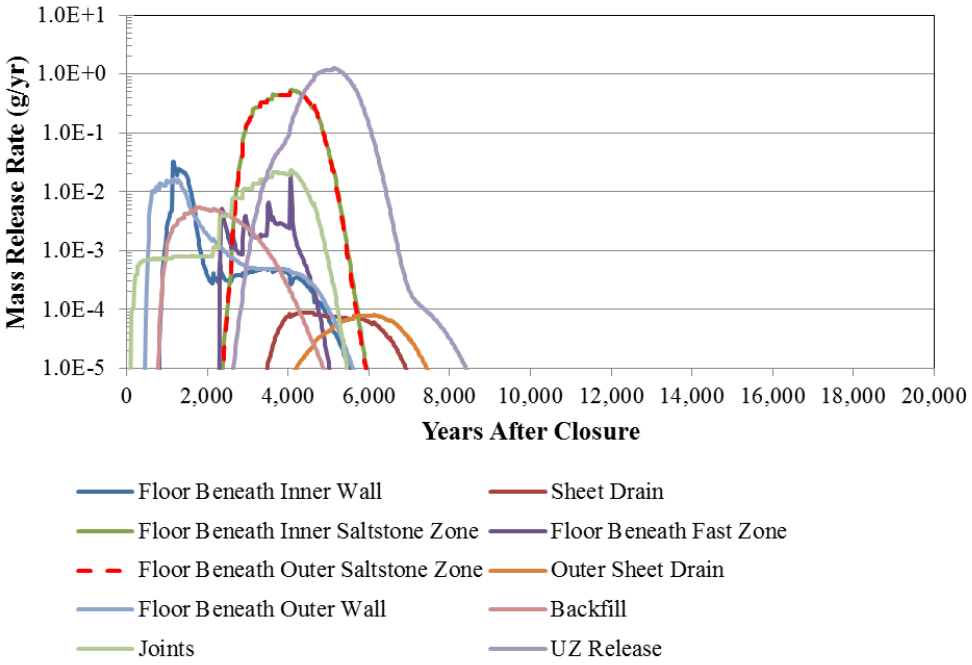

A comparison of Figure 5.1-19 to Figure 5.1-8 shows that the Ra-226 curves do not match quite as well as in the SDU 1 comparison, but when viewed in a semi-log plot the similarity of the trends of the curves is readily seen (Figure 5.1-20). The earlier arrival of the breakthrough curve in the PORFLOW results seen in Figure 5.1-20 is associated the higher vertical velocity in the UZ beneath the outside of the saltstone. This pattern of release is visible in Figure 5.1-21, which shows the PORFLOW model concentrations of Ra-226 generated by ingrowth from Th-230. A similar pattern is also seen for the concentrations of Ra-226 generated by ingrowth from U-234 as depicted in Figure 5.1-22. Note, that these figures are examined because during early time the Ra-226 release is controlled by ingrowth from U-234 and Th-230. With respect to Ra-226 releases from SDU 1, a similar effect can be seen at very low concentrations in the early stages of the concentration front breakthrough, but by the time the Ra-226 release reaches discernable levels (see Figure 5.1-8), the influence of the horizontal flow has obfuscated the effect. As with the Cs-135 and I-129 benchmarking results, the 16% difference between the PORFLOW and GoldSim peaks and peak timings show the abstraction model to be acceptable.

Figure 5.1-19: SDU 4 Ra-226 Release to the Saturated Zone

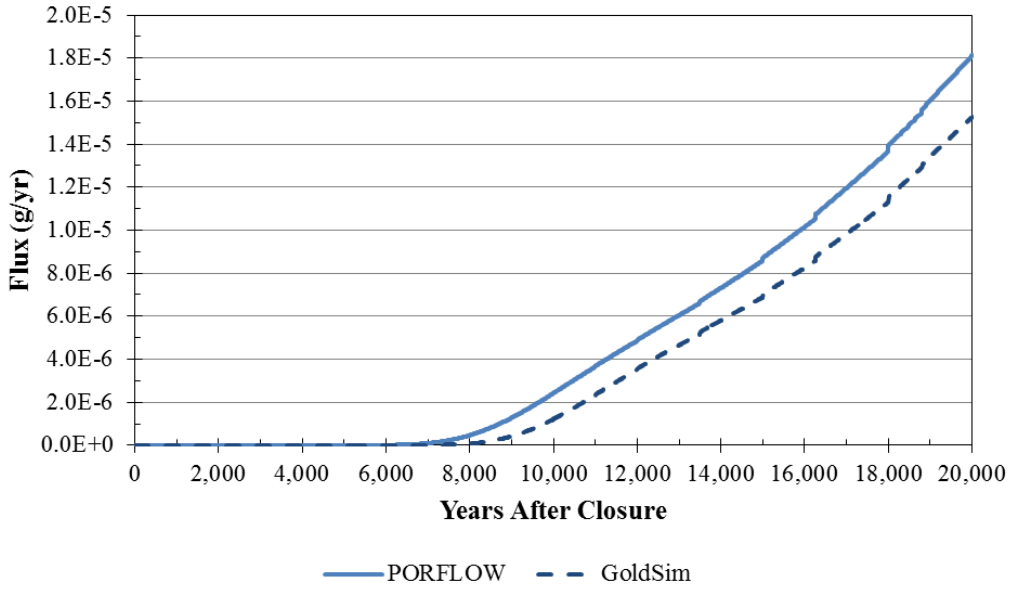

Figure 5.1-20: Semi-Log Plot of SDU 4 Ra-226 Release to the Saturated Zone

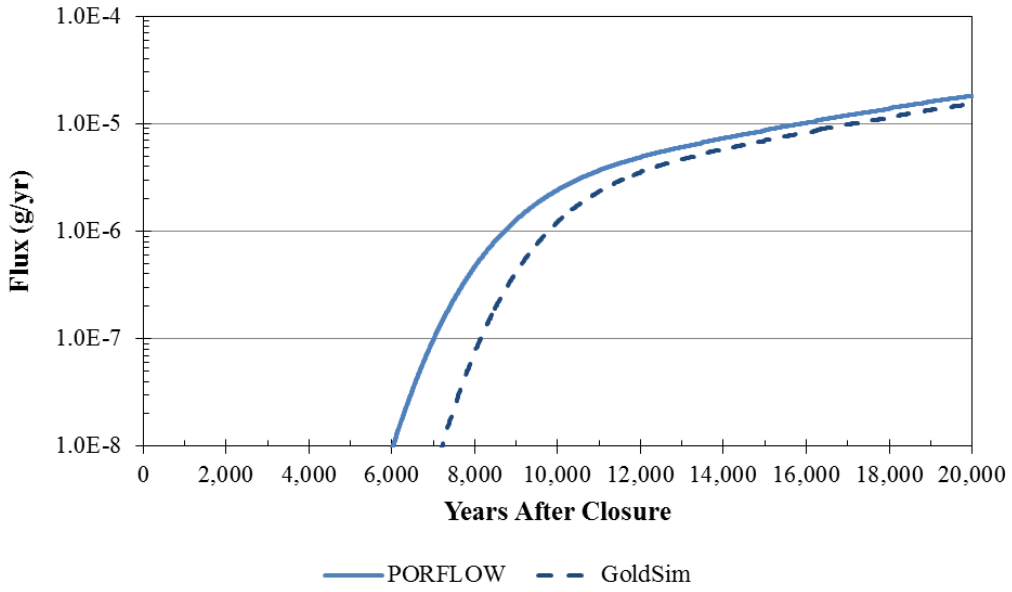

Figure 5.1-21: SDU 4 Ra-226 (from Th-230) PORFLOW Model Release to the Saturated Zone at 4,250 Years

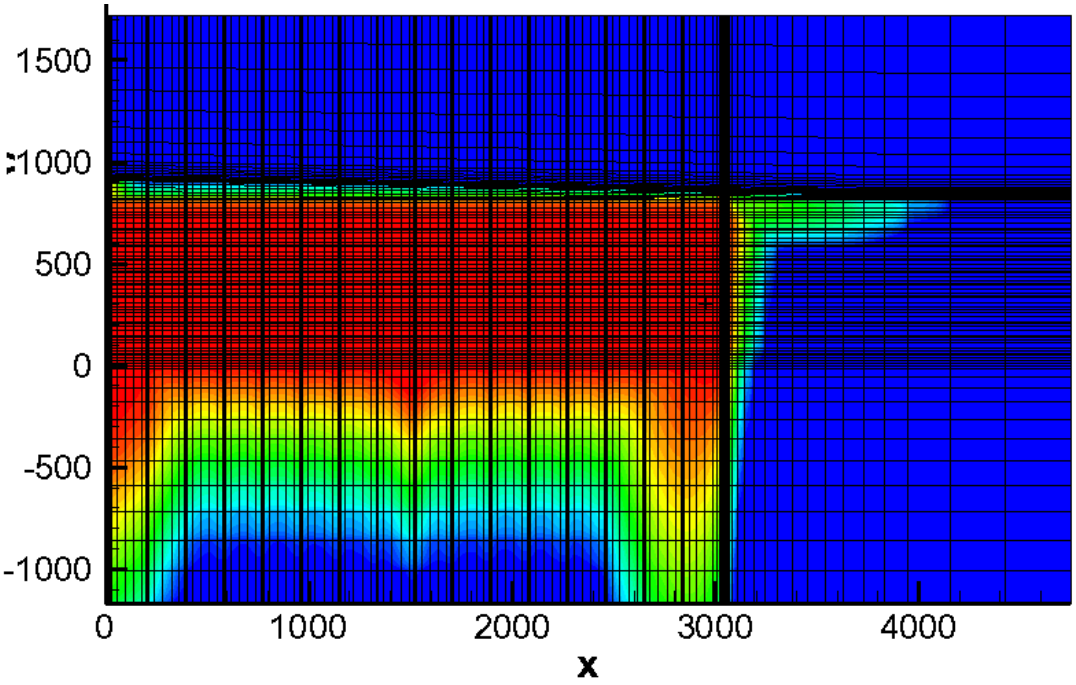

Figure 5.1-22: SDU 4 Ra-226 (from U-234) PORFLOW Model Release to the Saturated Zone at 4,250 Years

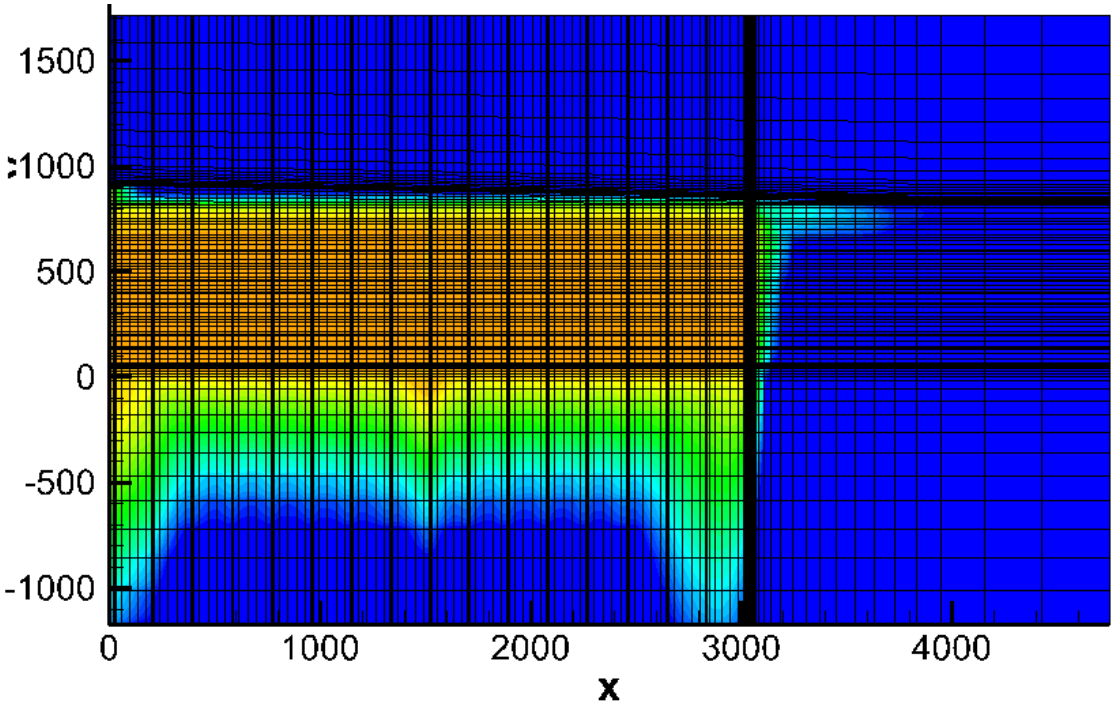

Similar to the SDU 1 results, the low-release tail seen in the SDU 1 Tc-99 release is also present in the SDU 4 results (Figures 5.1-23 and 5.1-24). For SDU 4, the low-release tail at the end of the PORFLOW breakthrough-curve depicted in Figure 5.1-24, emanates from Tc-99 buildup (oxygen shadow) zones two adjacent to the walls and one generated by the spatially-continuous planar representation of structural columns in the PORFLOW model. The Tc-99 buildup adjacent to the outside wall and the oxygen shadow (as indicated by the non-oxidized slag) controlling it are presented in Figures 5.1-23 and 5.1-24, respectively. Since the Tc-99 abstraction model captures the major trends of the PORFLOW mass release breakthrough curve, the SDF GoldSim Model provides an acceptable representation of the system.

Figure 5.1-23: SDU 4 Tc-99 Release to the Saturated Zone to 20,000 Years

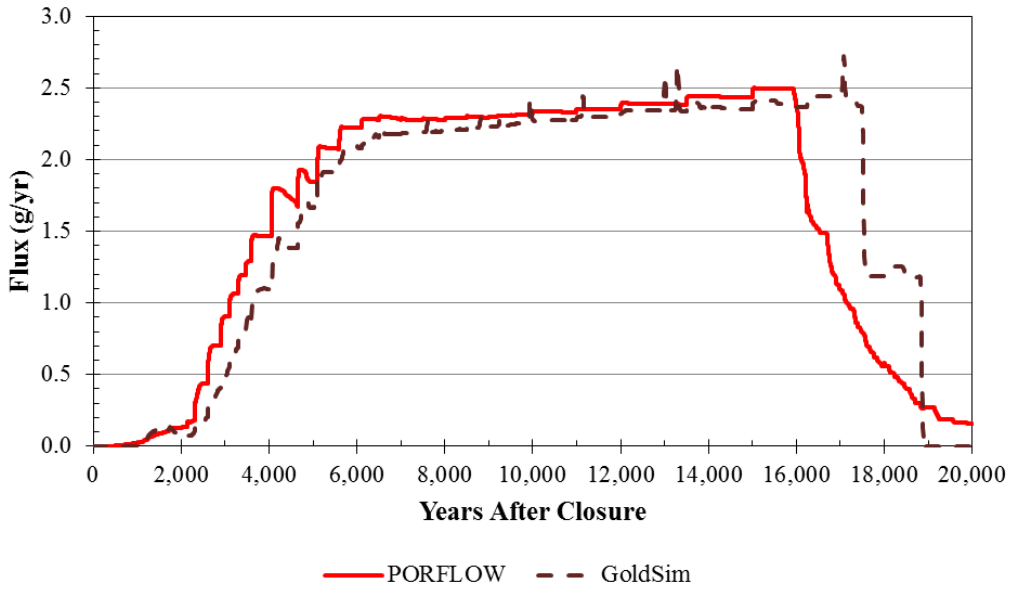

Figure 5.1-24: Semi-Log Plot of SDU 4 Tc-99 Release to the Saturated Zone to 50,000 Years

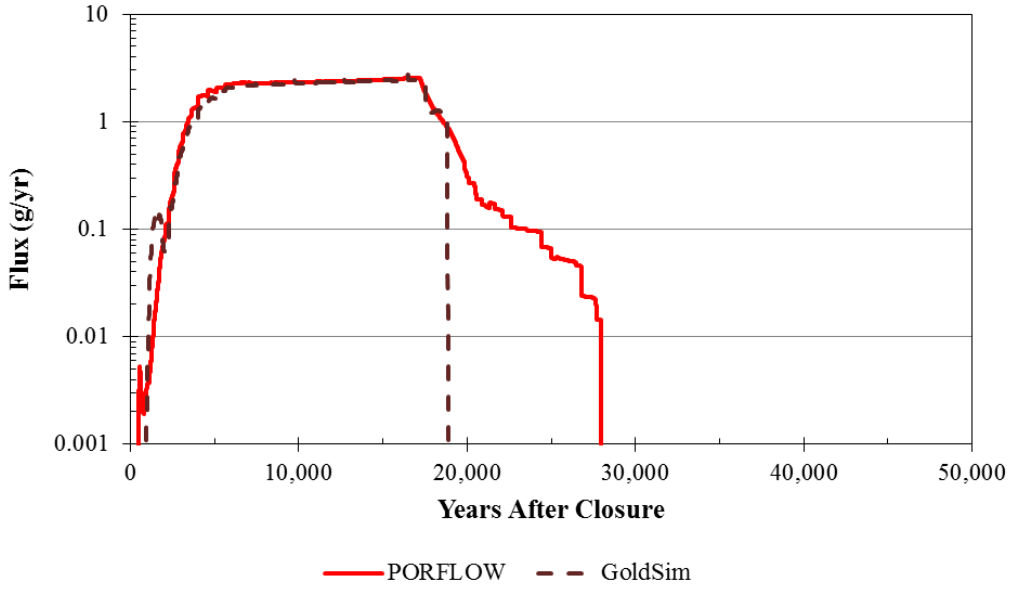

Figure 5.1-25: SDU 4 Tc-99 Concentrations at Saltstone/Wall Contact (20,000 Years)

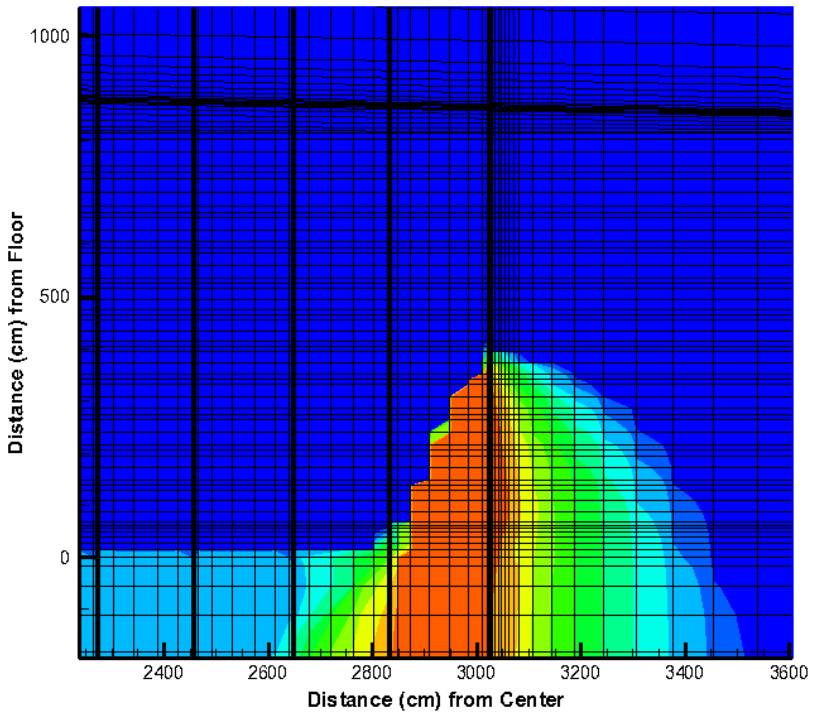

Figure 5.1-26: SDU 4 Slag Concentrations at Saltstone/Wall Contact (20,000 Years)

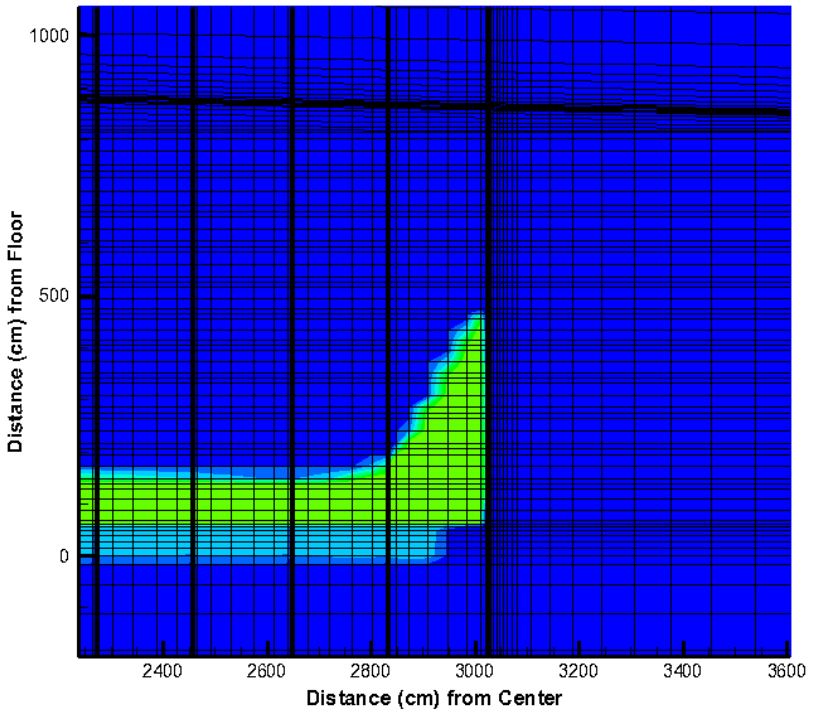

5.1.1.3 150-Foot Diameter SDUs (SDU 3A)

The mass releases from the 150-foot diameter SDUs, for the SDF PORFLOW Model and the SDF GoldSim Model, are presented below. Again, these figures indicate that the GoldSim model produces an acceptable approximation of the releases and trends generated by the PORFLOW model. Table 5.1-3 summarizes the results.

Table 5.1-3: GoldSim and PORFLOW Model Peak Unsaturated Zone Release Comparisons for 150-Foot Diameter SDUs within 20,000 years

Radionuclide	PORFLOW Peak Release (g/yr)	PORFLOW Time of Peak Release (yr)	GoldSim Peak Release (g/yr)	GoldSim Time of Peak Release (yr)	Peak Release Percent Difference GoldSim vs PORFLOW
I-129	1.5E-01	~6,600	1.4E-01	~6,600	-10%
Cs-135	1.6E-03	~12,000	1.4E-03	~10,500	-11%
Ra-226	3.6E-05	20,000	3.8E-05	20,000	5%
Tc-99 (0-20,000 years)	4.4E-01	~19,000	4.0E-01	~19,000	-7%
Tc-99 (0-50,000 years)	9.8E+01	~30,500	7.9E+01	~31,000	-20%

A comparison between the SDF PORFLOW Model and the SDF GoldSim Model I-129 breakthrough curves as presented in Figure 5.1-27 shows that the GoldSim model is an acceptable abstraction for the PORFLOW model with a 10% difference in peak values and similar peak breakthrough times. The slightly different shape of the two I-129 breakthrough curves is also attributed to the simplification of the flow fields in the abstraction (see Section 5.1.1.1). By comparing the GoldSim model generated I-129 release from the wall (passing through the lower mud mat) with the UZ release as presented in Figure 5.1-28 it can be seen that the greater early release (prior to 4,000 years) predicted by the GoldSim model is mostly associated with the release from the wall. In the GoldSim model only diffusion from the saltstone monolith into the wall is considered. Flow into the saltstone from the lower portion of the wall reduces the release from the wall giving the GoldSim model an acceptable conservative early-time release. Comparing the lower mud mat releases below different zones of the saltstone monolith with the UZ release (see Figure 5.1-28), it can be seen how quickly the poorly-sorbed I-129 from the saltstone migrates through the unsaturated zone.

Figure 5.1-27: SDU 3A I-129 Release to the Saturated Zone

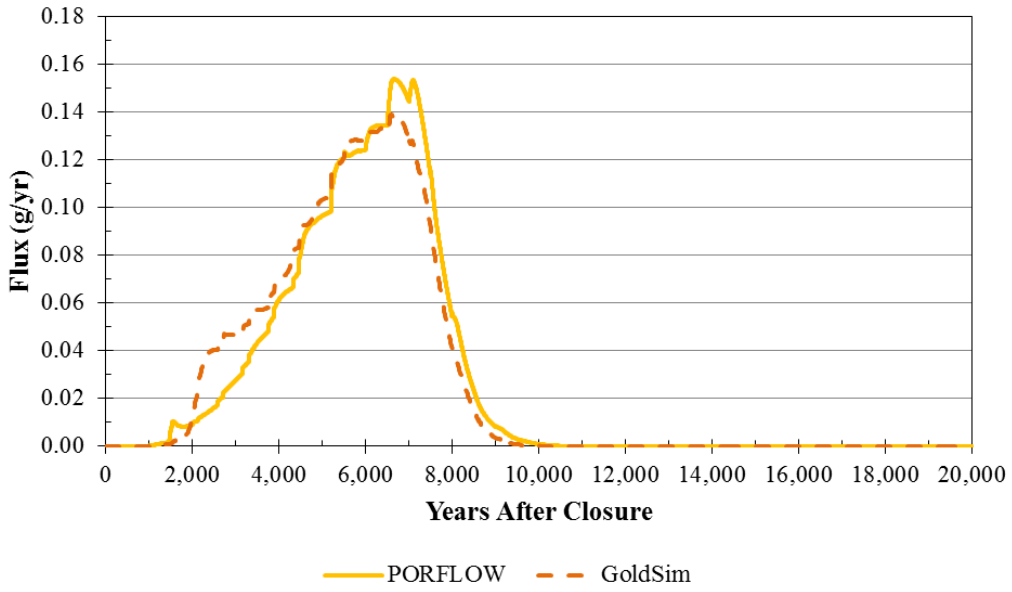

Figure 5.1-28: UZ and SDU Component I-129 Releases for SDU 3A (GoldSim)

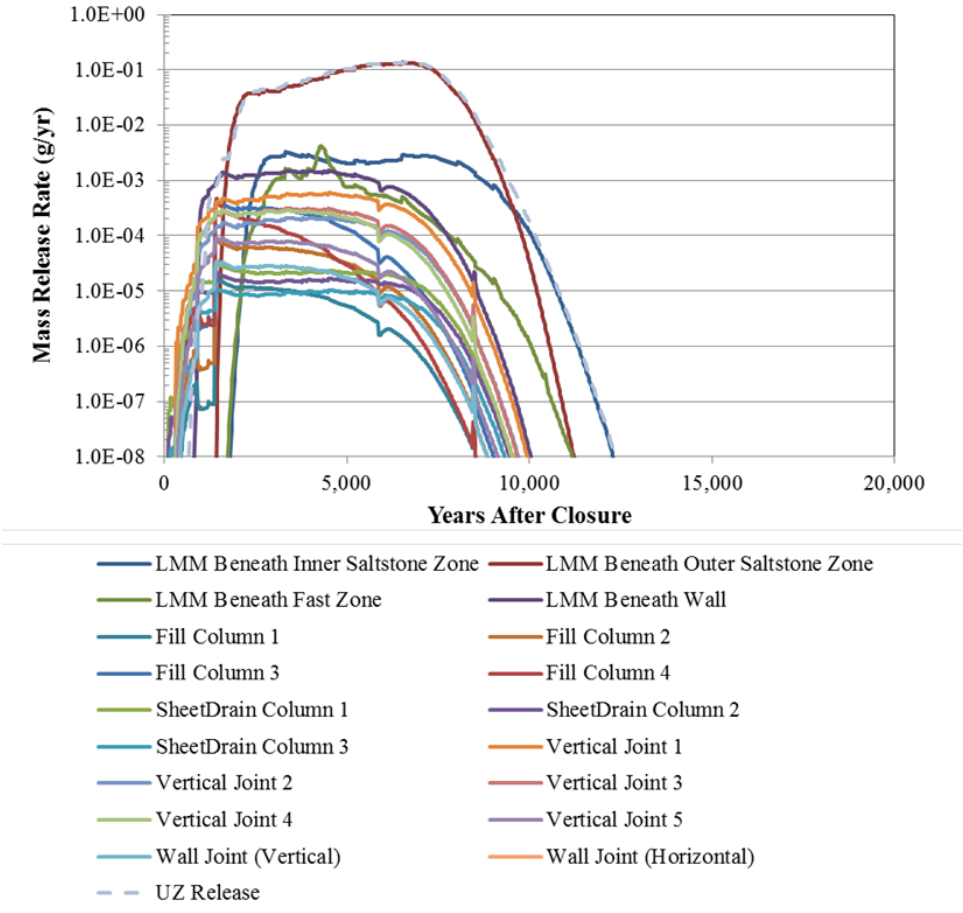

Similar to SDU 1, Figure 5.1-29 shows that the PORFLOW generated breakthrough curve for Cs-135 released from SDU 3A lags behind the GoldSim model generated curve. Examination of the SDU 3A concentration profile at 11,000 years (Figure 5.1-30) indicates that the peak Cs-135 release generated by PORFLOW is controlled by the convergence of the release plume (outside the support-column zone) to an area adjacent to the support-column zone. This pattern is reflective of the flow field beneath the SDU, as depicted in Figure 5.1-31. The convergence of the plume to an area adjacent to the support-column zone, as opposed to direct vertical migration at a spatially averaged flow rate, enhances the difference between the PORFLOW and GoldSim model results. Note that in GoldSim model the Cs-135 release through the floor beneath the outer zone of saltstone dominates the release from the SDU. Figure 5.1-32 presents breakthrough curves from different components of the system. Again, it can be seen that Cs-135 release from the wall area in the GoldSim model fosters a conservative slightly higher release at early time. The Cs-135 comparison shows an 11% difference in peak values and occurs about 1,500 years earlier in the GoldSim model. This is an acceptable abstraction for the PORFLOW model.

Figure 5.1-29: SDU 3a Cs-135 Release to the Saturated Zone

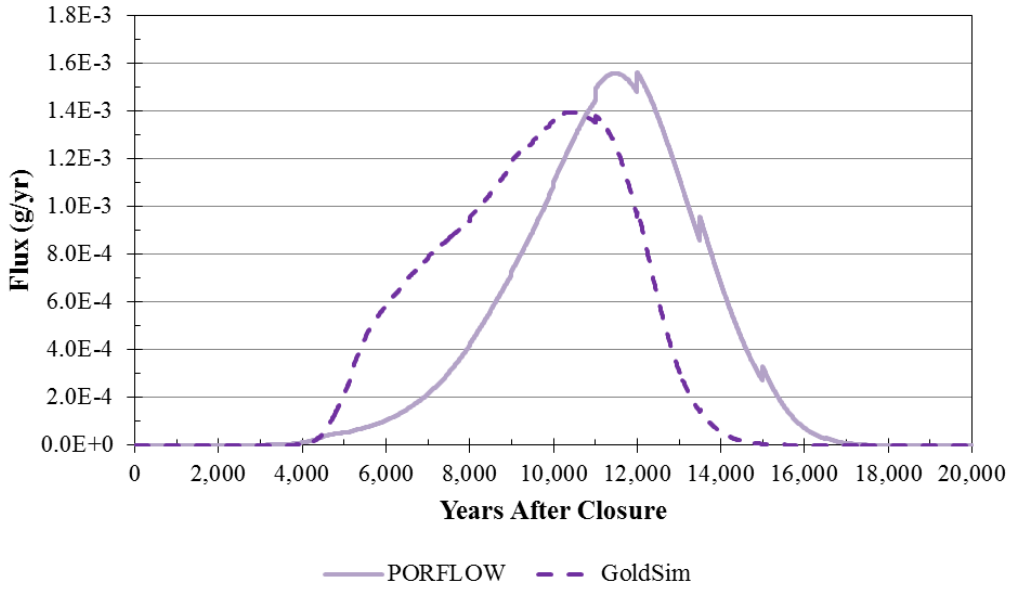

Figure 5.1-30: SDU 3A Cs-135 Release to the Saturated Zone at 11,000 Years

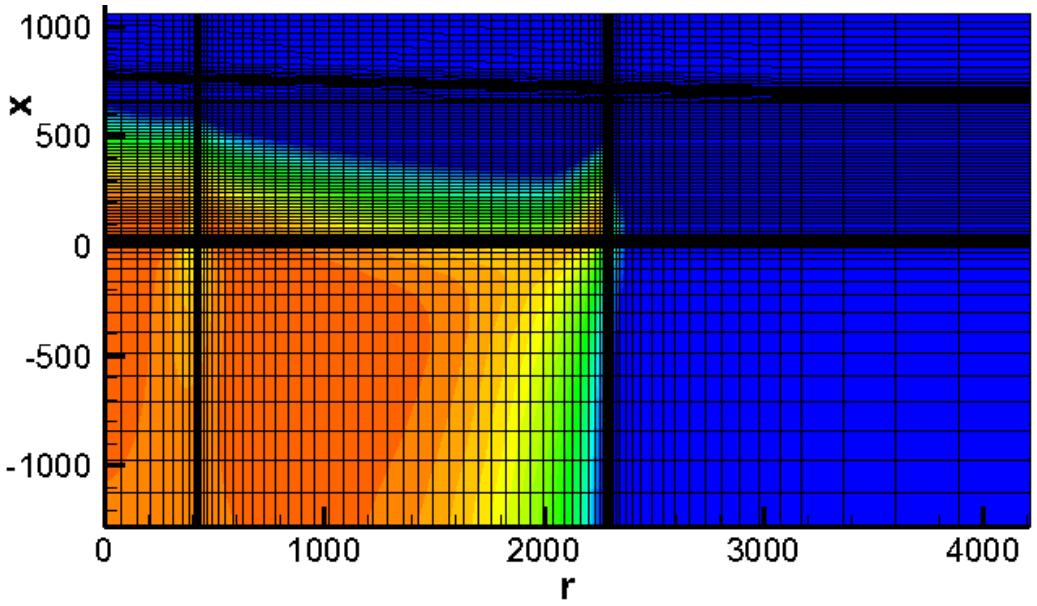

Figure 5.1-31: SDU 3A Flow Field from 10,000 to 11,000 Years

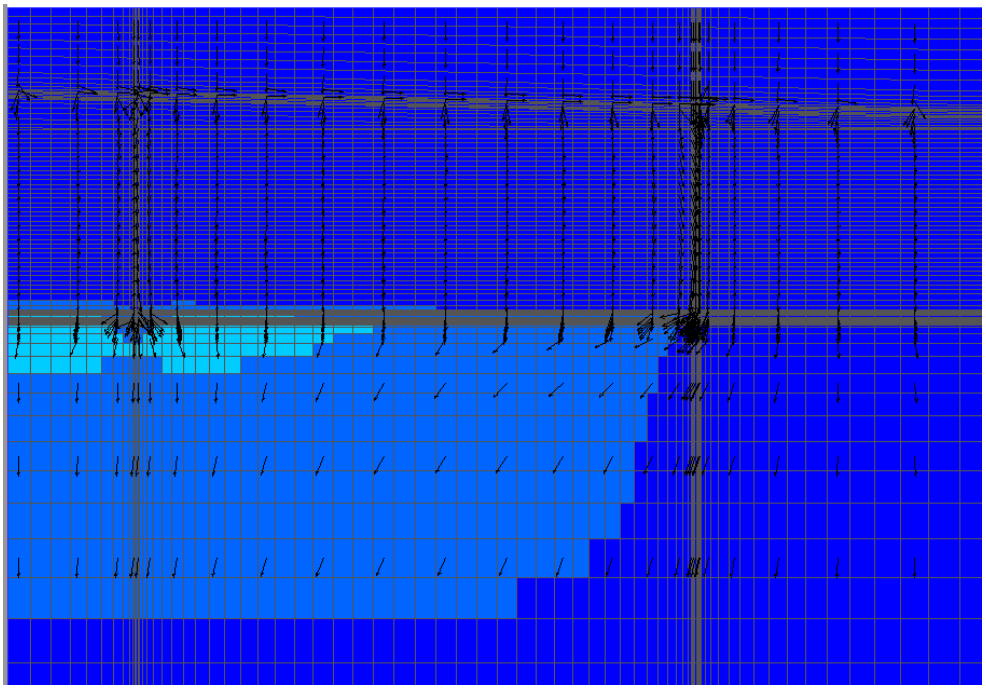

Figure 5.1-32: UZ and Vault Component Cs-135 Releases for SDU 3A (GoldSim)

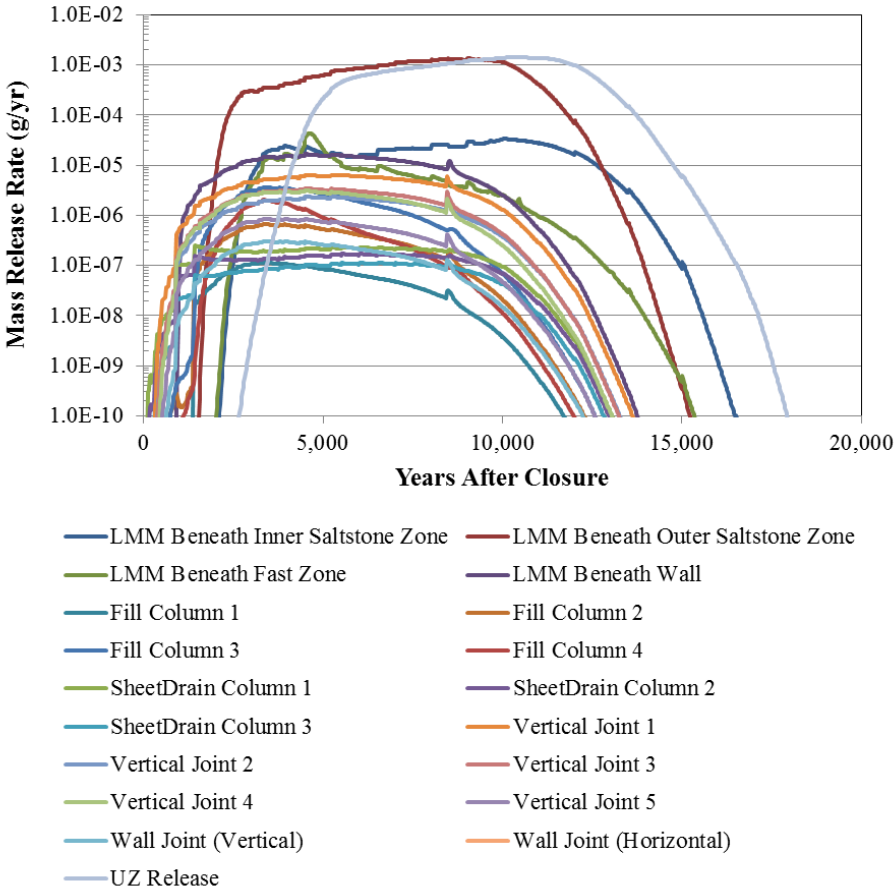

Additionally, the comparison between the PORFLOW model and GoldSim model Ra-226 breakthrough curves presented in Figure 5.1-33 also shows that the GoldSim model is an acceptable abstraction for the PORFLOW model with a 5% difference in peak values and very similar breakthrough times (see Table 5.1-3).

Figure 5.1-33: SDU 3A Ra-226 Release to the Saturated Zone

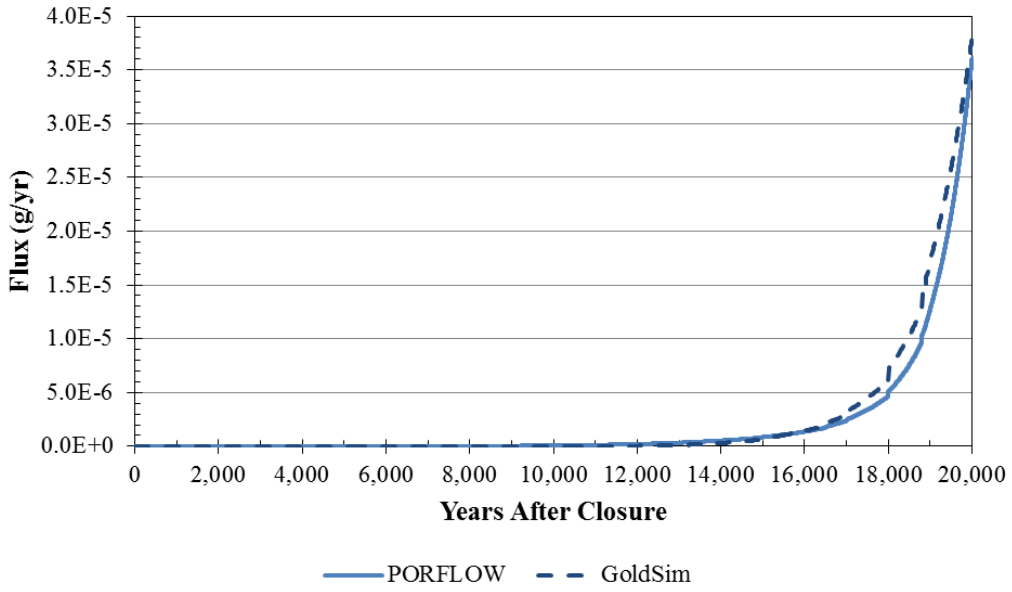

As shown in Figure 5.1-34, the Tc-99 abstraction model has similar trends to the PORFLOW model, but after 35,000 years (see Figure 5.1-35), the GoldSim model release is reflective of high and low spikes, while the PORFLOW model release reflects longer-term pulse type releases. This difference is a function of the cell-based release mechanisms. In the PORFLOW model, the Tc-99 dissolution rate in a cell is reflective of the slag oxidation rate within a cell. In the SDF GoldSim Model, all of the precipitate in a cell dissolves at the time when all of the slag in a cell becomes fully oxidized. Unlike in the SDU 1 and SDU 4 models, in the SDU 3A PORFLOW model the slag is used up before the simulation is finished. This occurs at around 45,000 years and is reflected in the release of the rest of the Tc-99 from the system. In addition, Figure 5.1-35 shows that after 45,000 years (at low releases) the GoldSim Model releases may continue for a while. Figures 5.1-36 and 5.1-37 show that the final release in the PORFLOW model occurs at the bottom of the SDU near the saltstone/wall interface. The consistency between the two models in that area could be enhanced by adding a diffusion boundary approximation to the GoldSim transition-time program logic.

Figure 5.1-34: SDU 3A Tc-99 Release to the Saturated Zone to 20,000 Years

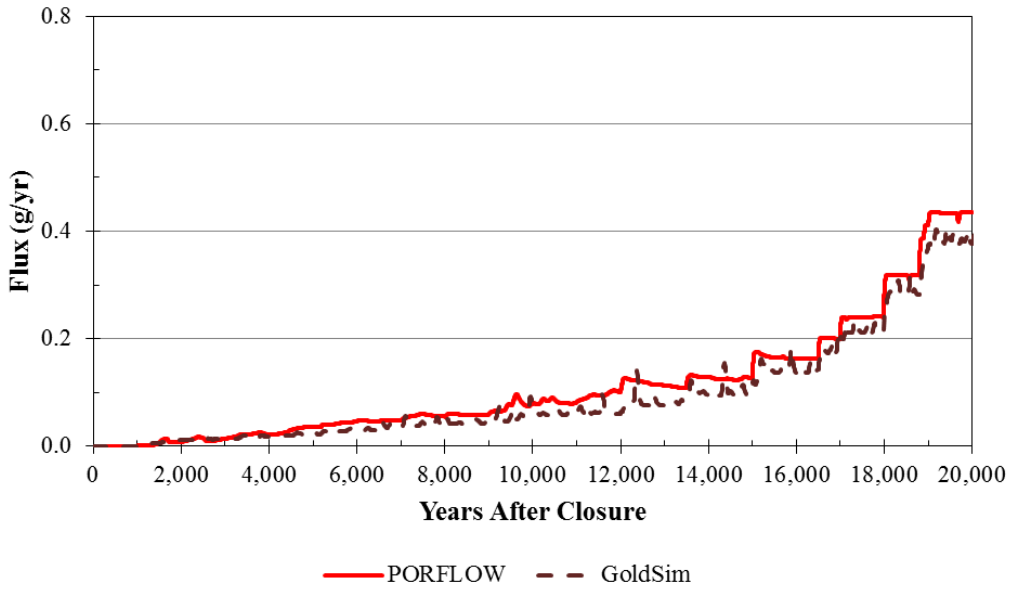

Figure 5.1-35: SDU 3A Tc-99 Release to the Saturated Zone (Log Scale) to 50,000 Years

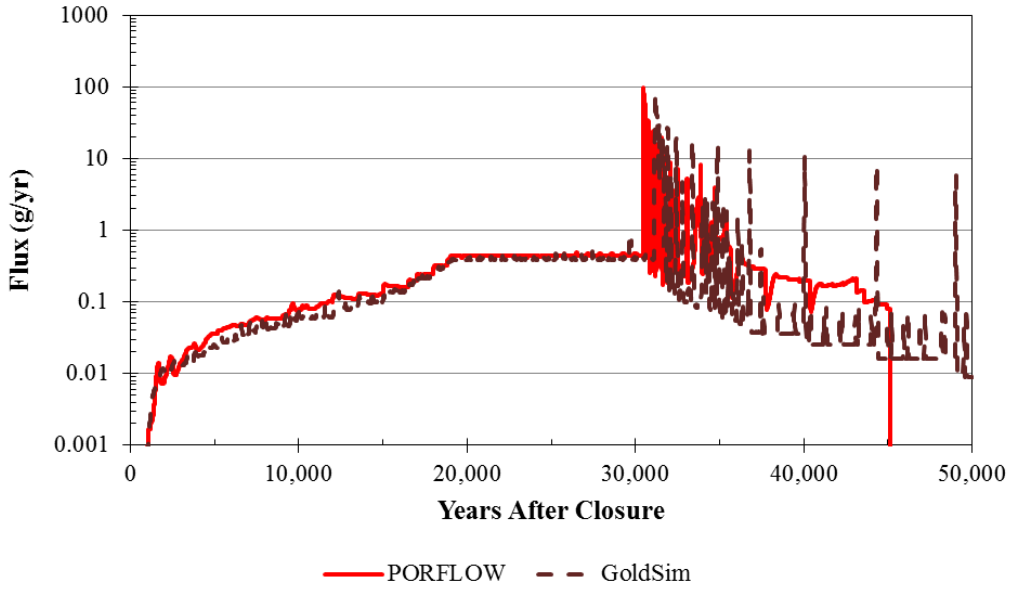

Figure 5.1-36: SDU 3A Tc-99 Concentrations at Saltstone/Wall Contact (40,000 Years)

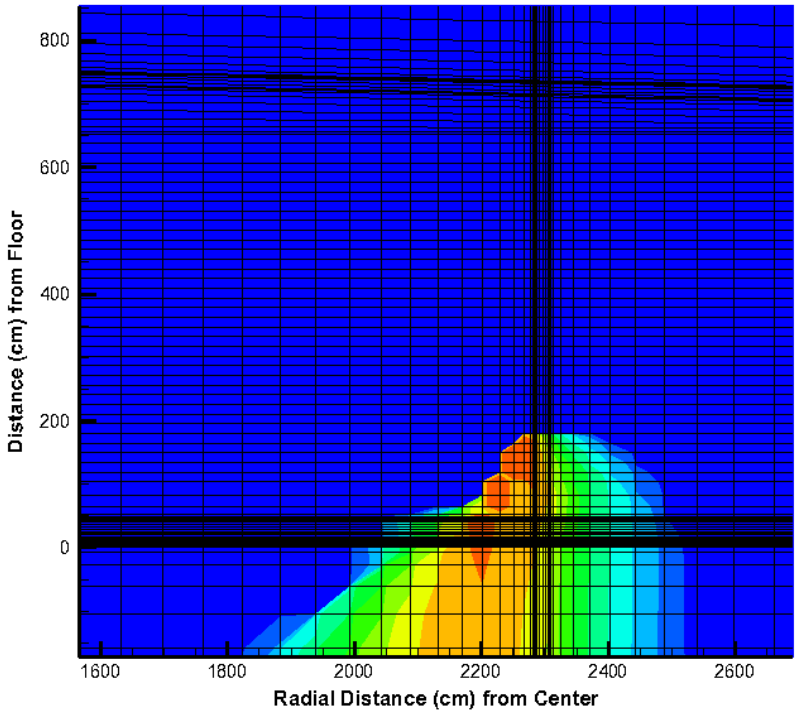

Figure 5.1-37: SDU 3A Slag Concentrations at Saltstone/Wall Contact (40,000 Years)

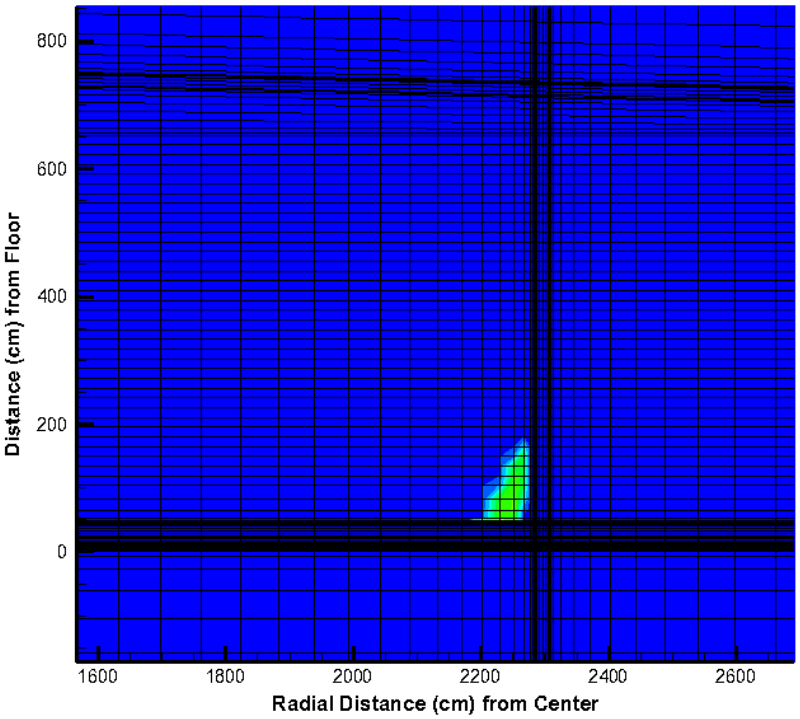

5.1.1.4 375-Foot Diameter SDUs (SDU 6)

The mass releases from the 375-foot diameter SDUs are presented below. Again, these figures indicate that the SDF GoldSim Model produces an acceptable approximation of the releases and trends generated by the PORFLOW model. Table 5.1-4 summarizes the results.

Table 5.1-4: GoldSim and PORFLOW Model Peak Unsaturated Zone Release Comparisons for 375-Foot Diameter SDUs within 20,000 years

Radionuclide	PORFLOW Peak Release (g/yr)	PORFLOW Time of Peak Release (yr)	GoldSim Peak Release (g/yr)	GoldSim Time of Peak Release (yr)	Peak Release Percent Difference GoldSim vs PORFLOW
I-129	4.7E+00	~5,200	4.8E+00	~5,200	3%
Cs-135	3.5E-02	~7,400	3.8E-02	~7,500	8%
Ra-226	8.9E-05	20,000	1.1E-04	20,000	-20%
Tc-99 (0-20,000 years)	2.7E+00	~19,500	2.6E+00	~19,500	-3%
Tc-99 (0-50,000 years)	1.1E+02	~38,500	2.0E+02	~38,000	79%

A comparison between the SDF PORFLOW Model and the SDF GoldSim Model I-129 breakthrough curves for SDU 6, as presented in Figure 5.1-38, shows that the GoldSim model is an acceptable abstraction for the PORFLOW model with only a 3% difference in peak values and quite similar peak breakthrough times. The slightly different shape of the two I-129 breakthrough curves at early time is attributed to the simplification of the flow fields in the abstraction (see Section 5.1.1.1). By comparing the GoldSim model generated I-129 release from the wall (passing through the lower mud mat) and backfill with the UZ release, as presented in Figure 5.1-39, it can be seen that the slightly greater early release (prior to 3,000 years) predicted by the GoldSim model, is mostly associated with the release from the wall and backfill. Slight differences at the tail-end of the PORFLOW generated and GoldSim generated breakthrough curves for I-129 can be attributed to slight differences in the releases from the floor inner cylinder of saltstone (see Figure 5.1-39). Comparing the lower mud mat releases below different zones of the saltstone monolith with the UZ release (see Figure 5.1-39), it can again be seen how quickly the poorly-sorbed I-129 from the saltstone migrates through the unsaturated zone.

Figure 5.1-38: SDU 6 I-129 Release to the Saturated Zone

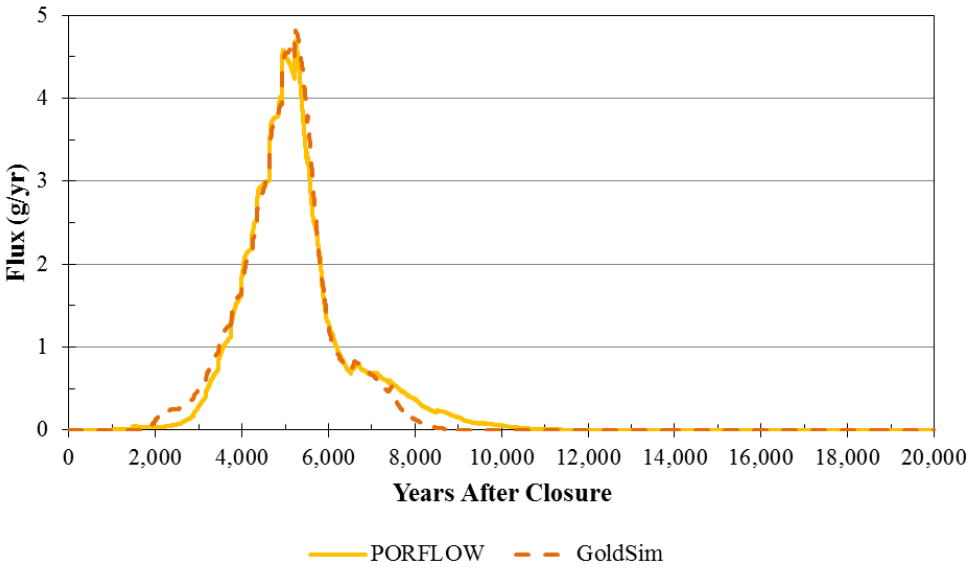

Figure 5.1-39: UZ and Vault Component I-129 Releases for SDU 6 (GoldSim)

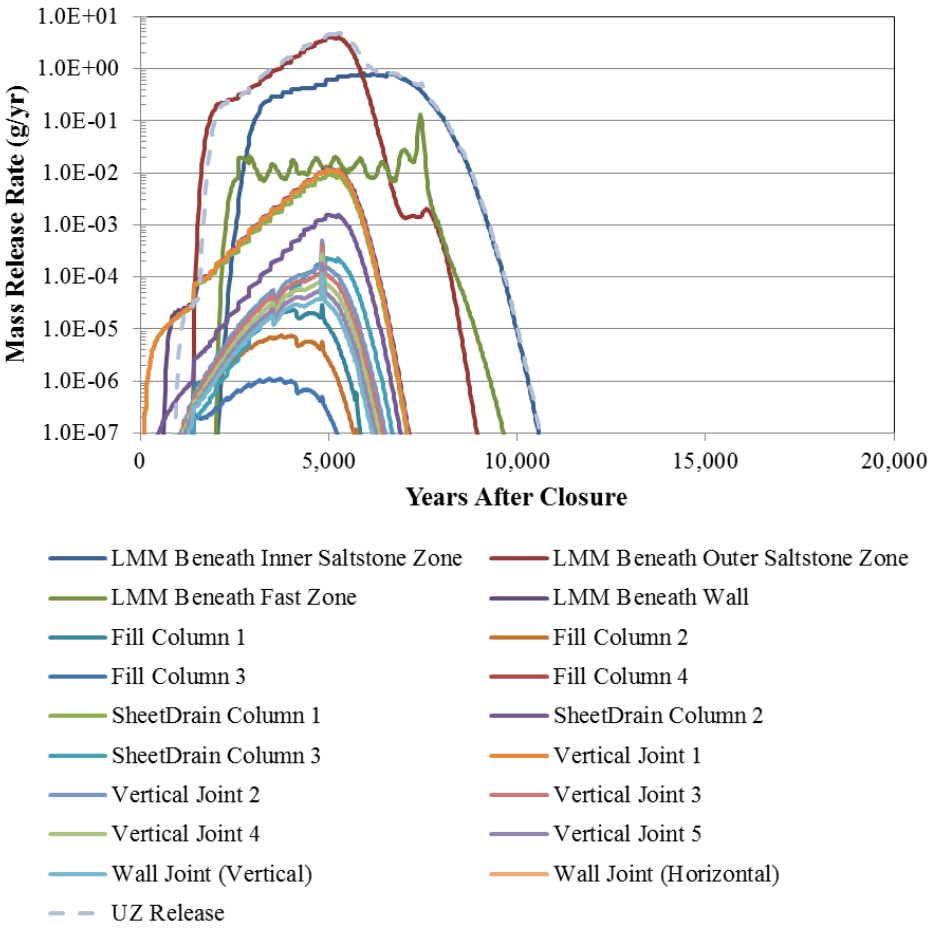

The comparison between the PORFLOW model and GoldSim model Cs-135 breakthrough curves as presented in Figure 5.1-40 shows that the GoldSim model is an acceptable abstraction for the PORFLOW model with an 8% difference in peak values and 100 years difference in peak breakthrough times. Differences at the tail-end of the PORFLOW generated and GoldSim generated breakthrough curves for Cs-135 can also be attributed to slight differences in the releases from the floor inner cylinder of saltstone (see Figure 5.1-41). The extended tails of the PORFLOW breakthrough curves, are a function of the inward trending decrease in vertical Darcy velocity of about 14 cm/yr to 3 cm/yr (exemplified by the 11,000 year to 12,000 year flow field) in the inner cylinder of the saltstone. A similar inwards trending variance of about 16 cm/yr to 5 cm/yr is also exhibited in the UZ, below the inner cylinder of the saltstone. This spatial trend in the velocity field in the PORFLOW model as opposed to the spatially averaged values controlling transport through the saltstone and UZ in the abstraction model, generates longer tails on the PORFLOW breakthrough curves.

Figure 5.1-40: SDU 6 Cs-135 Release to the Saturated Zone

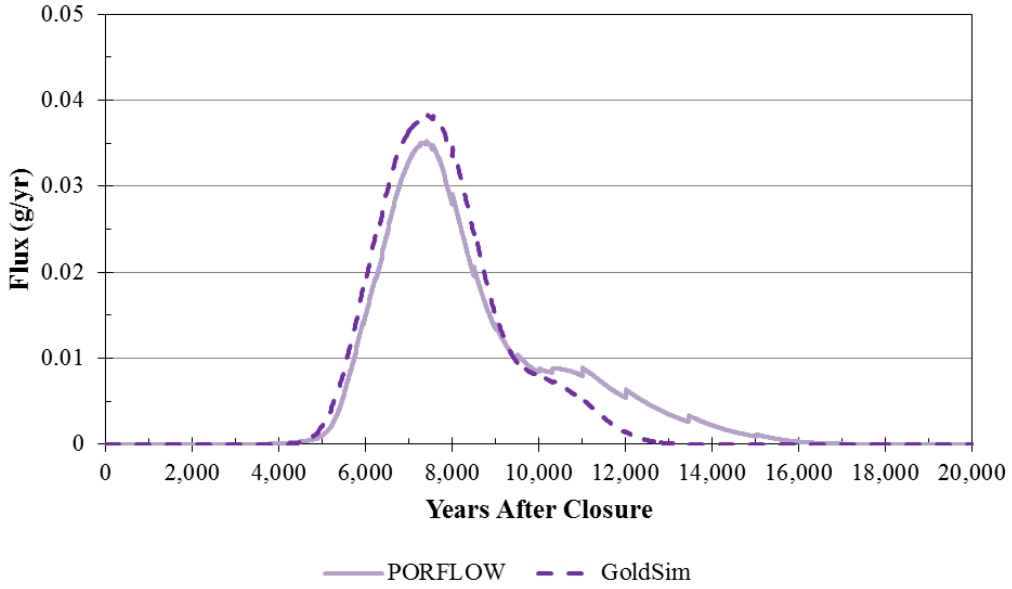

Figure 5.1-41: UZ and Vault Component Cs-135 Releases for SDU 6 (GoldSim)

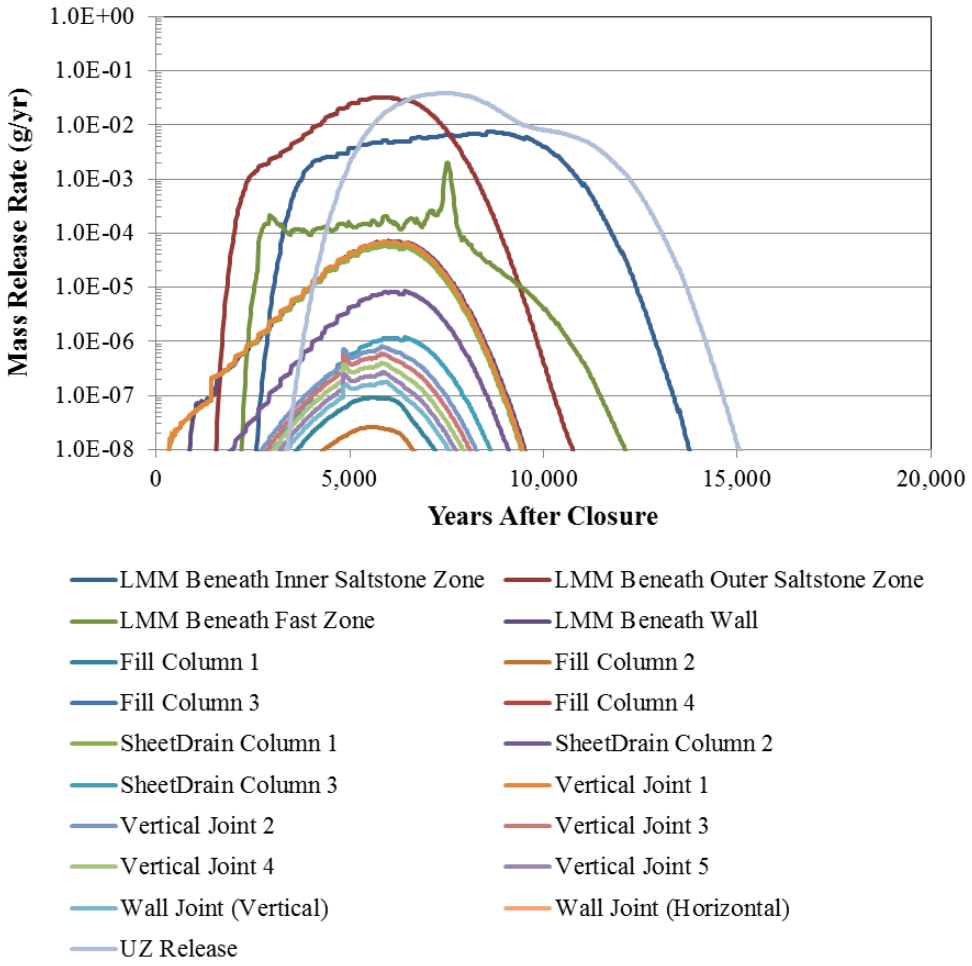

As with the SDU 4 results, the Ra-226 curves do not match quite as well as some of the other comparisons (Figure 5.1-42), but when viewed in a semi-log plot the similarity of the trends of the curves is readily seen (Figure 5.1-43). The 20% difference between the PORFLOW and GoldSim Model results is considered acceptable, especially within the context of being within the increasing gradient leg of the breakthrough curve. The earlier breakthrough of the PORFLOW breakthrough is associated with the influence of the faster (vertical) velocity of the UZ flow field below the outer zone of the saltstone (see Figure 5.1-44). The GoldSim model does not pick up this subtlety because it uses a spatially averaged vertical flow rate throughout the UZ.

Figure 5.1-42: SDU 6 Ra-226 Release to the Saturated Zone

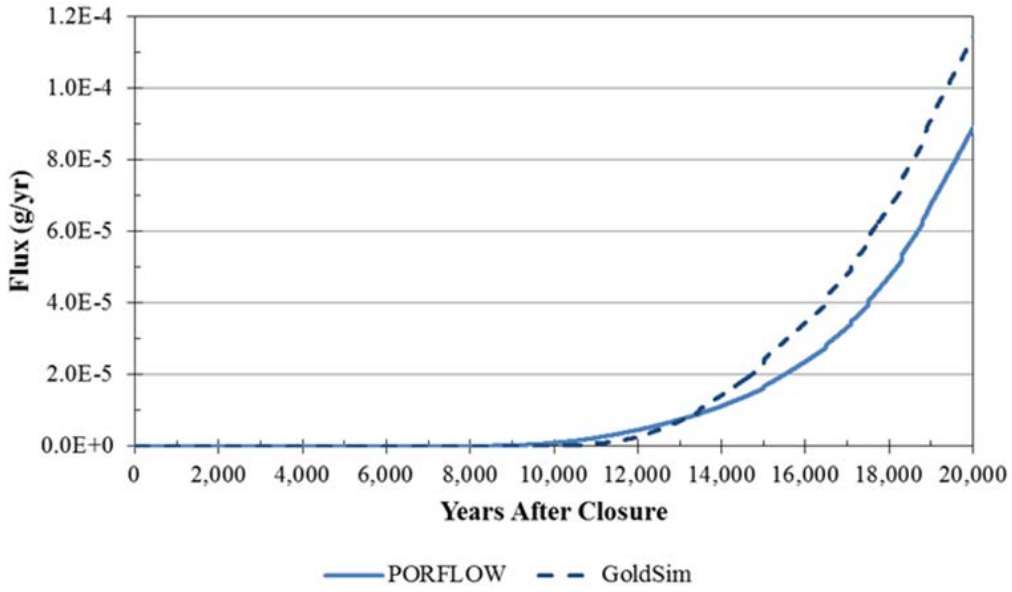

Figure 5.1-43: SDU 6 Ra-226 Release to the Saturated Zone (Log Scale)

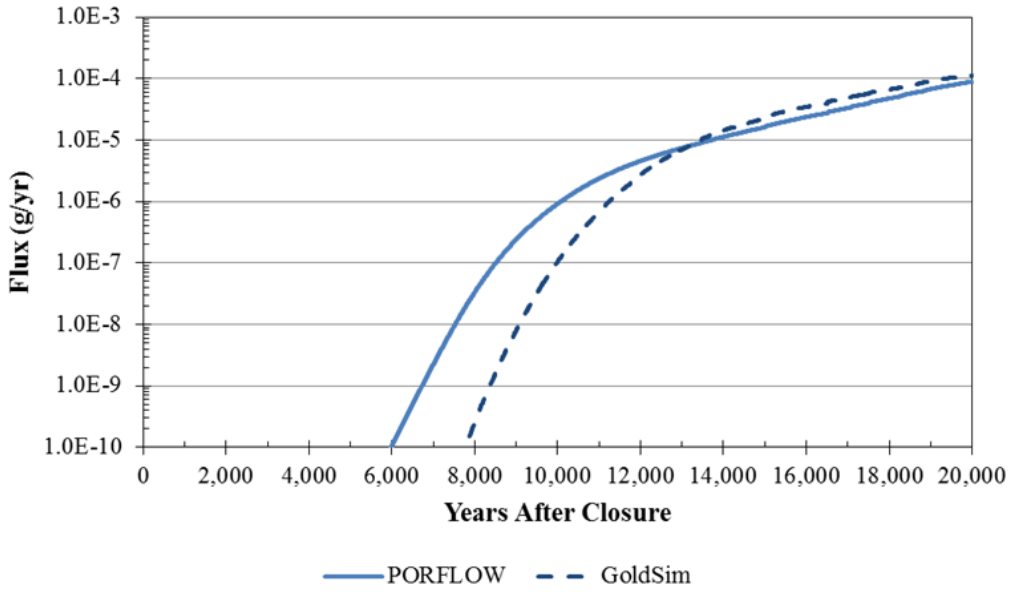

Figure 5.1-44: Contours of SDU 6 Ra-226 Concentrations at 6,750 years

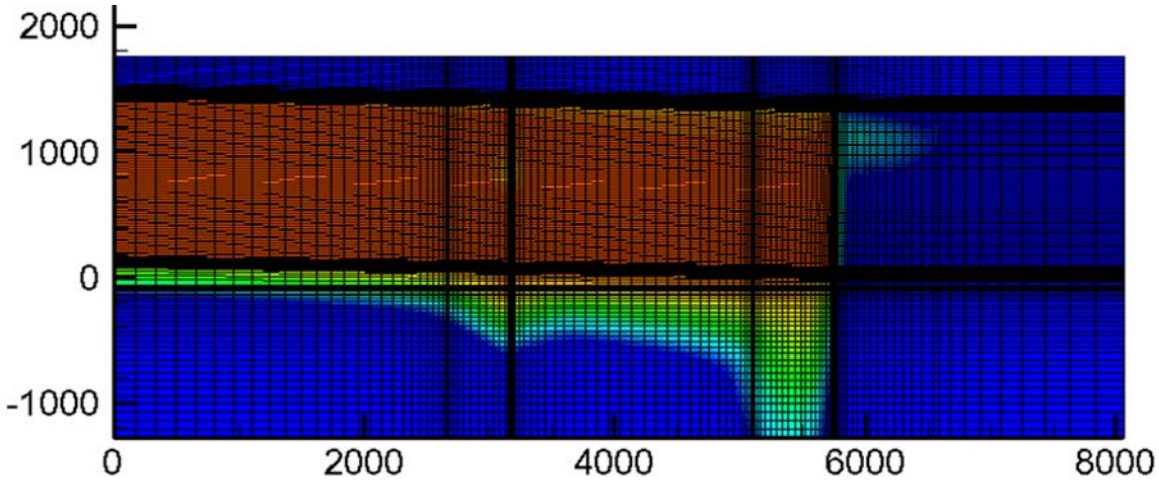

Similar to the SDU 3A results, the Tc-99 results (Figure 5.1-45) reflect the differences in the dissolution models at later times, when the releases are low. For the 375-foot diameter SDUs, the Tc-99 buildup in the oxygen shadow zone, just inside the outer wall will control the final release of Tc-99 from the SDUs (Tecplot© generated Figures 5.1-29 and 5.1-30). Again, the Tc-99 abstraction model captures the major trends of the PORFLOW mass release breakthrough curve, and provides an acceptable representation of the Tc-99 release.

Figure 5.1-45: SDU 6 Tc-99 Release to the Saturated Zone

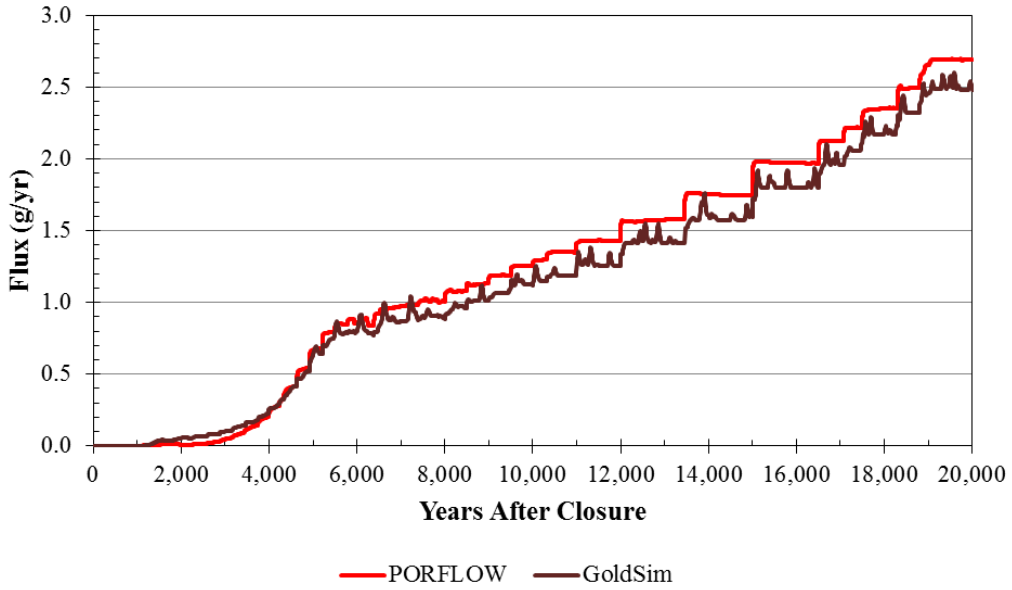

Figure 5.1-46: SDU 6 Tc-99 Release to the Saturated Zone

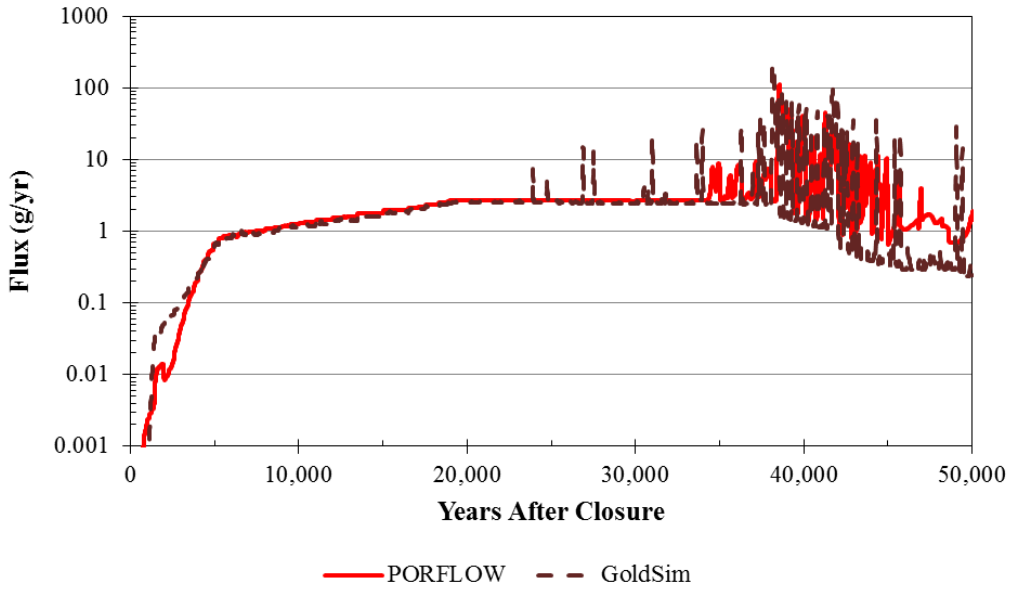

Figure 5.1-47: SDU 6 Tc-99 Concentrations at Saltstone/Wall Contact (40,000 Years)

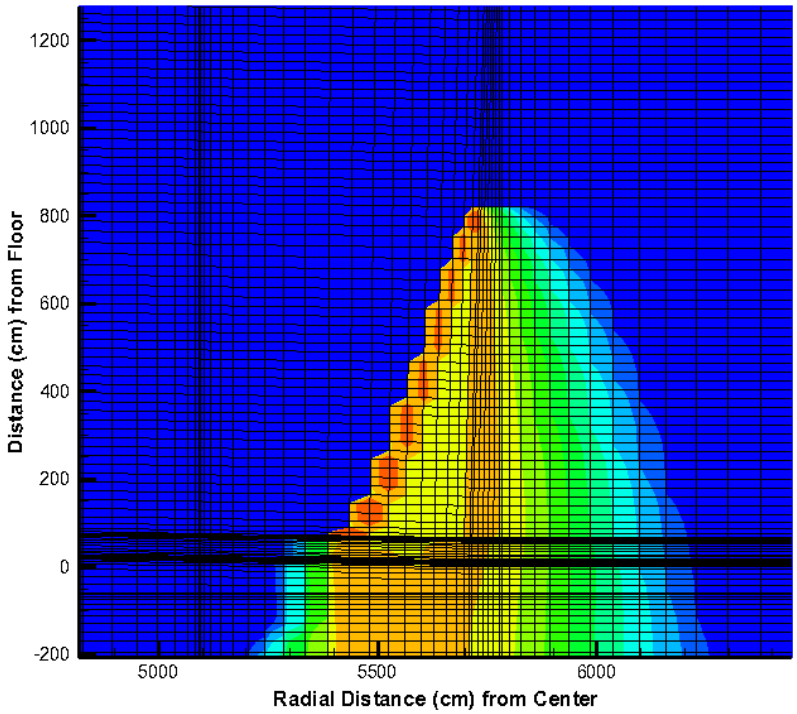

Figure 5.1-48: SDU 6 Slag Concentrations at Saltstone/Wall Contact (40,000 Years)

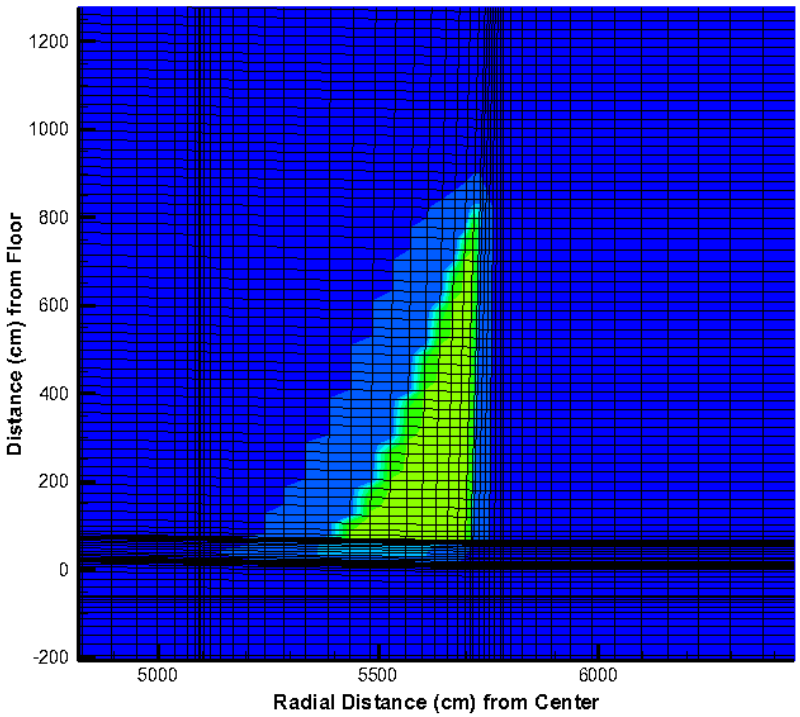

5.1.2 Radionuclide Concentrations at the 100-Meter Boundary

The second phase of the benchmarking process focuses on examining how well the abstracted model approximates the radionuclide transport behavior in the saturated zone. Radionuclide concentrations (in picocuries per liter) in four sectors (Sectors B, I, J, and K) were examined for this task (See Figure 4.1-2). Sector B was selected for this analysis because it contains the highest PORFLOW and SDF GoldSim Model concentrations of the southern sectors. Sector K was chosen because it contains the peak model concentrations for the northern locations (in both GoldSim and PORFLOW results) and Sectors I and J were selected due to their proximity to Sector K. Concentration comparisons between PORFLOW and SDF GoldSim Model results showed less consistency in Sector J, which is located above a groundwater divide, than for the other sectors. For this exercise, PORFLOW and GoldSim model concentration curves for four species (I-129, Cs-135, Ra-226, and Tc-99) were examined.

5.1.2.1 Sector B

An examination of PORFLOW and GoldSim-generated radionuclide concentrations presented in Figure 5.1-49 indicates that the SDF GoldSim Model can provide a computationally efficient approximation of 100-meter boundary radionuclide concentrations in Sector B. There is a consistency in the trends observed in the two sets of model results throughout the 20,000-year simulation. The basic dilution/attenuation processes in the saturated zone are captured by the abstraction. Note that there are also differences but they will have little impact on the utility of the abstraction model to evaluate peak doses.

Figure 5.1-49: Maximum Radionuclide Concentrations at 100-Meter Boundary, Sector B

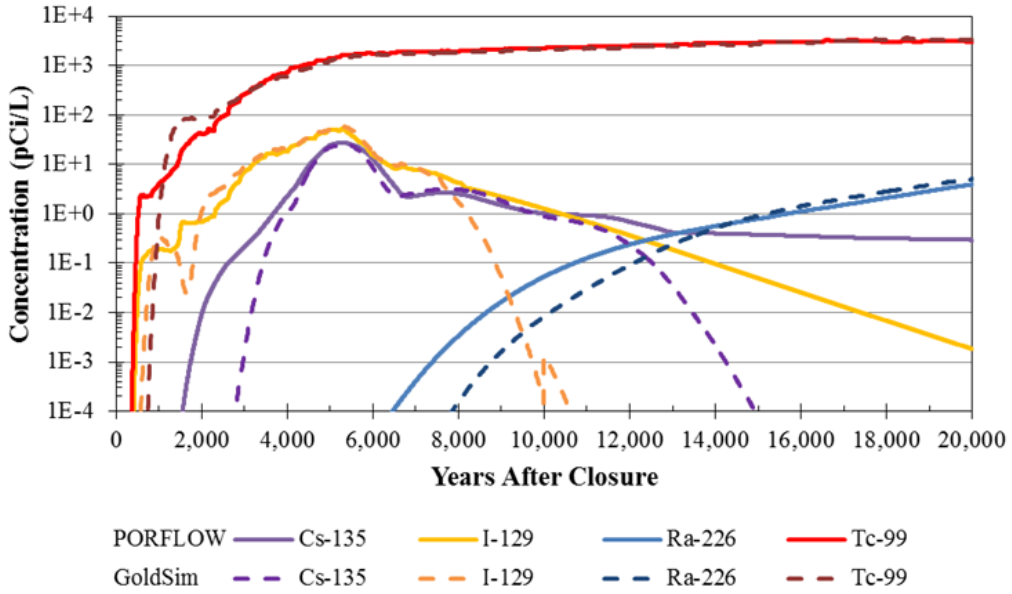

The concentration curves in Figure 5.1-49 show that the general behavior, of the PORFLOW concentration curves, is accurately reproduced by the SDF GoldSim Model. Note that the basic trends reflect flow field and chemistry changes captured by the SDF GoldSim Model.

Figure 5.1-49 also shows that the GoldSim concentrations decrease at a faster rate than the PORFLOW concentrations. This difference in the curves is associated with the occurrence of the "green clay" layer (i.e., the Gordon Confining Unit), which is modeled explicitly in the PORFLOW model, but not in the SDF GoldSim Model. The "green clay" layer provides a storage zone for more sorptive elements such as cesium, from which, radionuclides like Cs-135 are released slowly over time. Since the concentration curves differ at well below peak levels, the simplification in the SDF GoldSim Model is not important in dose calculations.

5.1.2.2 Sector I

Radionuclide concentrations at the 100-meter boundary are presented here for Sector I because Sector I is near Sector K. Figure 5.1-50 presents the concentrations from the SDF PORFLOW Model and the SDF GoldSim Model at the 100-meter boundary for all the examined species.

An examination of PORFLOW and GoldSim-generated radionuclide concentrations presented in Figure 5.1-50 indicates that the SDF GoldSim Model provides a computationally efficient approximation of 100-meter boundary radionuclide concentrations in northern sectors such as Sector I. There is a consistency in the trends observed in the model results throughout the 20,000-year simulation. The basic dilution/attenuation processes in the saturated zone are captured by the abstraction, but again there are also differences that will have little impact on the utility of the abstraction model to evaluate peak doses.

Figure 5.1-50: Maximum Radionuclide Concentrations at 100-Meter Boundary, Sector I

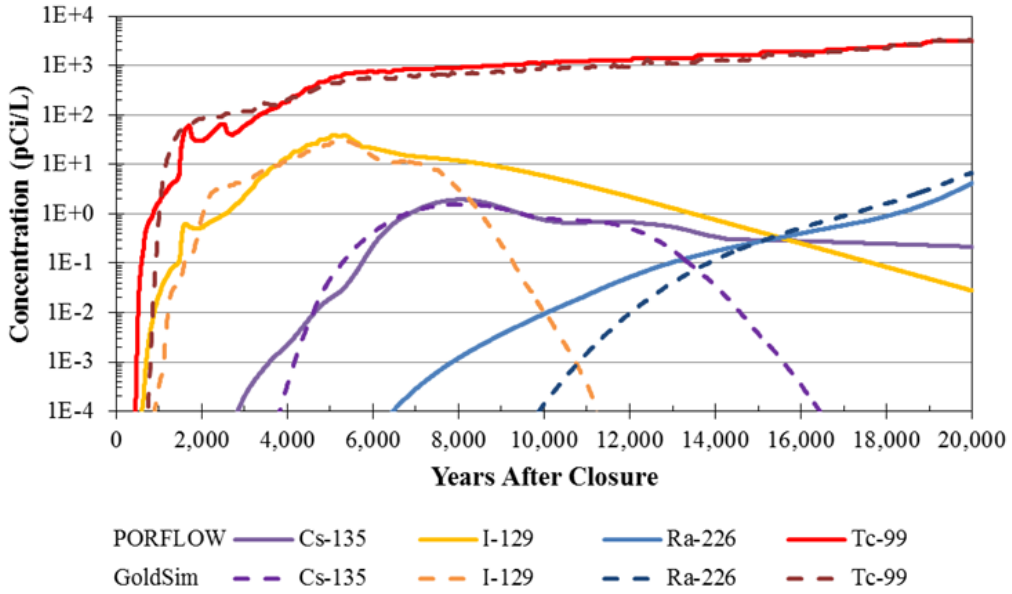

5.1.2.3 Sector J

Radionuclide concentrations at the 100-meter boundary are presented here for Sector J because Sector J is near Sector K. Although a comparison of the Sector J results does not show as close a match to the magnitudes as seen in Sector I, the behavior is still very similar. This difference is due to the simpler analytical solutions used in the SDF GoldSim Model which do not fully capture the three-dimensional influence of the groundwater divide (as reflected in the streamlines presented in Figure 2.0-1) on the 100-meter boundary concentrations in Sector J. Figure 5.1-51 presents the concentrations from the SDF PORFLOW Model and the SDF GoldSim Model at the 100-meter boundary for the examined species. Note that despite underestimating the concentrations, the basic trends indicative of flow field and chemistry changes are captured by the SDF GoldSim Model.

Figure 5.1-51: Maximum Radionuclide Concentrations at 100-Meter Boundary, Sector J

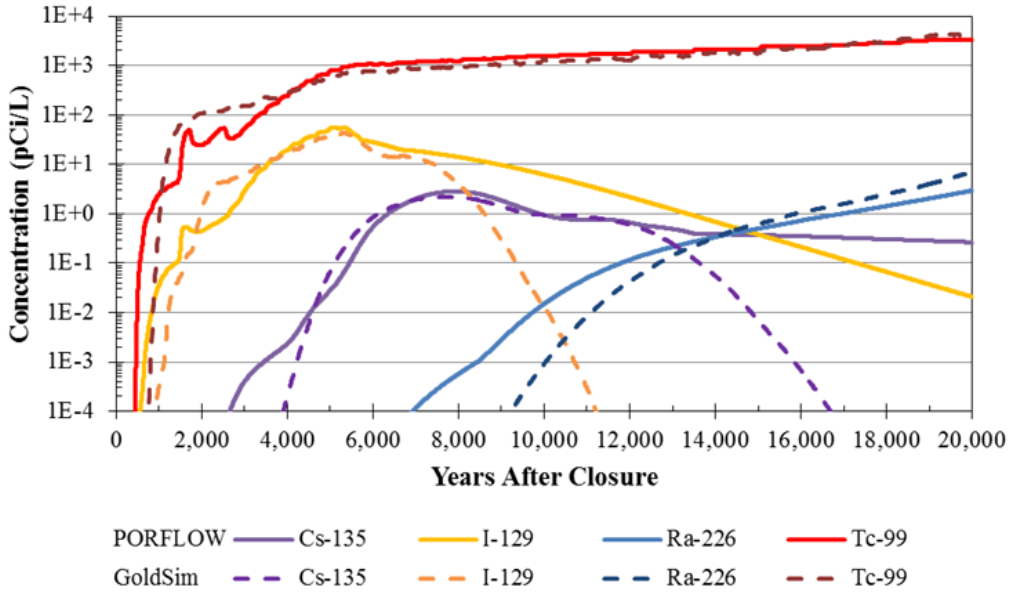

5.1.2.4 Sector K

Sector K was chosen because this sector had the highest peak dose results in the northern sectors (in both GoldSim and PORFLOW). An examination of PORFLOW and GoldSim-generated radionuclide concentrations presented in Figure 5.1-52 indicates that the SDF GoldSim Model can also provide a computationally efficient approximation of 100-meter boundary radionuclide concentrations in northern sectors such as Sector K. There is a consistency in the trends observed in the two sets of model results throughout the 20,000-year simulation. The basic dilution/attenuation processes in the saturated zone are captured by the abstraction, but again there are also differences that will have little impact on the utility of the abstraction model to evaluate peak doses.

Figure 5.1-52: Maximum Radionuclide Concentrations at 100-Meter Boundary, Sector K

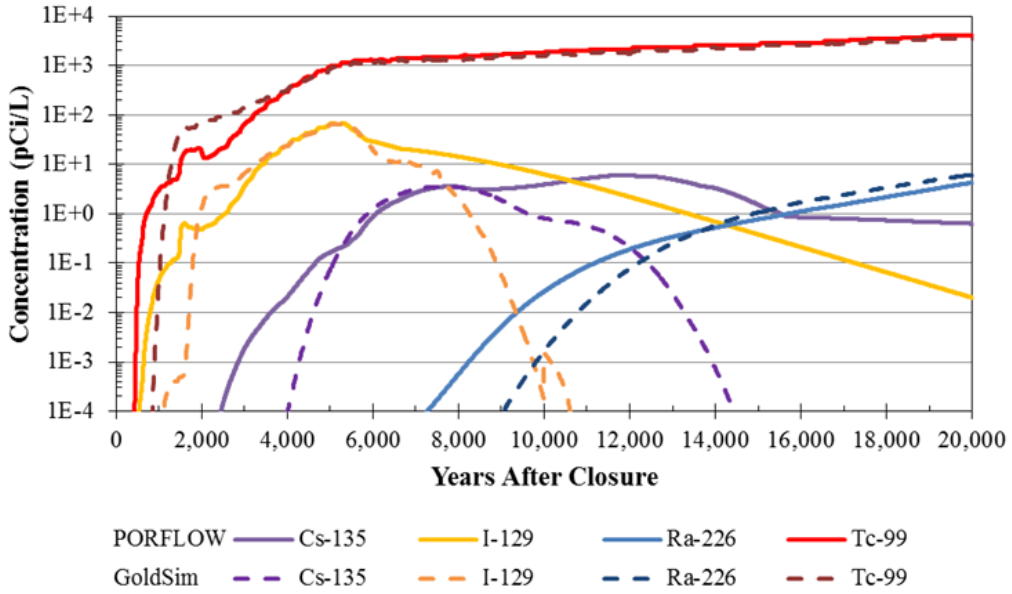

5.1.3 MOP Dose Time Histories

The third phase of the benchmarking process focuses on examining how well the abstracted model approximates the MOP dose results. Comparisons of the maximum total MOP dose levels (in millirem per year) generated by the two models form the basis of the benchmarking effort along with a comparison of dose contributions from the major contributing radionuclides.

5.1.3.1 Total MOP Dose Time Histories

An important check on the appropriateness of the SDF GoldSim Model as a surrogate for the SDF PORFLOW Model is a comparison between the maximum total doses generated by the two models. The Evaluation Case total dose is the highest sector dose over time. The sector specific dose time histories over 20,000 years from the PORFLOW model are presented in Figure 5.1-53. The maximum dose and sector specific dose time histories from the GoldSim model over 20,000 years are depicted in Figure 5.1-54.

Figure 5.1-53: PORFLOW Evaluation Case, Sector MOP Dose Results over 20,000 Years

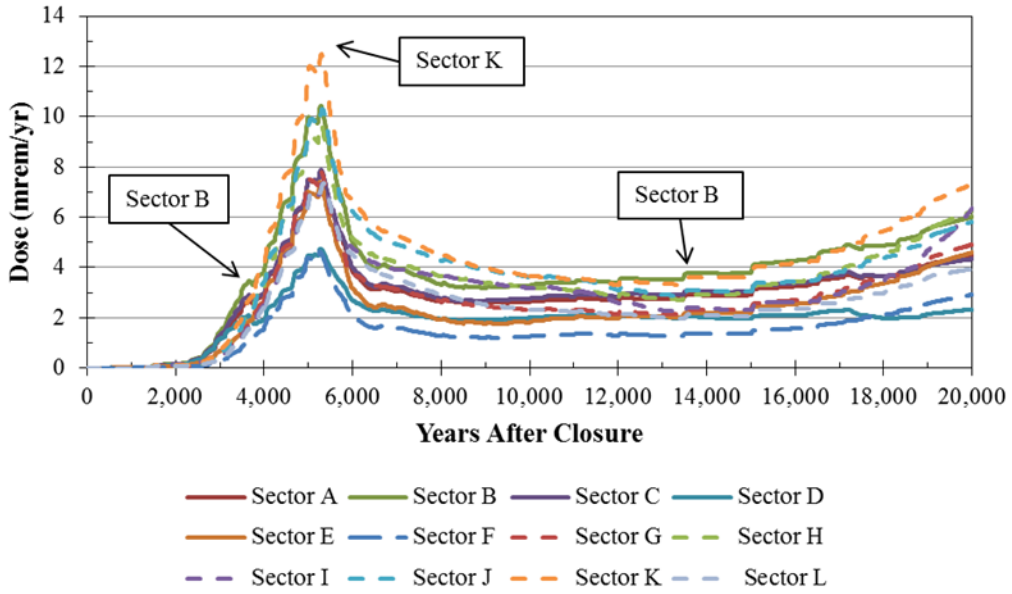

Figure 5.1-54: GoldSim Evaluation Case, Sector MOP Dose Results over 20,000 Years

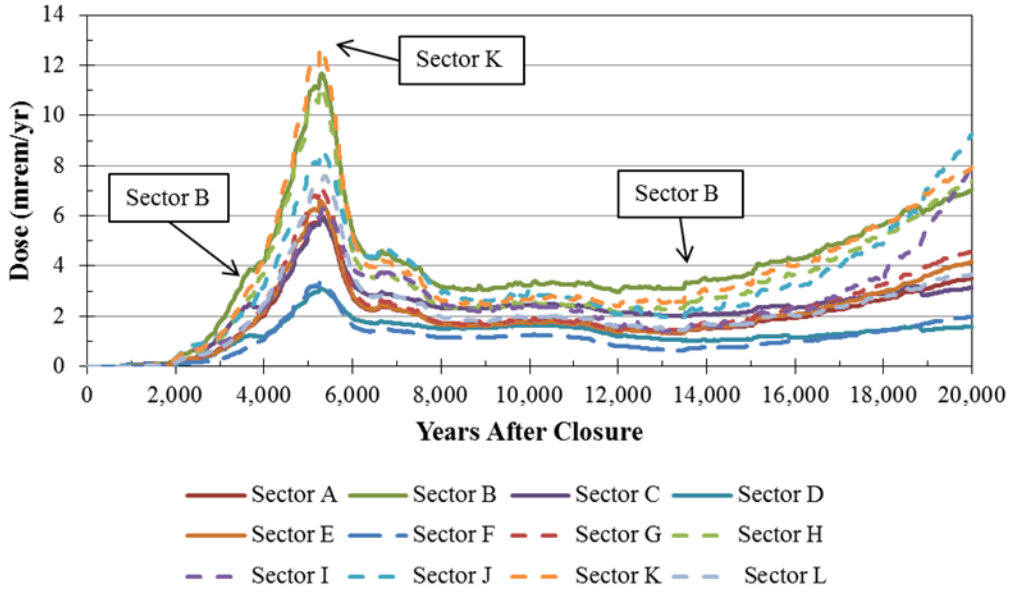

These figures demonstrate a very close comparison for all sectors.

In addition to the influence of the groundwater divide, other simplifications in the SDF GoldSim Model that influence how well individual sector results from both models match include the nature of the spatial and temporal discretization of the models. Because the PORFLOW results are generated at each node in a finely discretized grid, for a given time, sector results are based upon the maximum concentration of any node within the sector, including nodes from the UTRA-UZ, the UTRA-LZ, or the Gordon Aquifer. In contrast, the SDF GoldSim Model results are based on the concentrations generated at an

assumed well location (or two well locations) per sector, typically near the centerline of concentration plumes from the various SDU releases. This center-point analysis may potentially underestimate the GoldSim peak doses relative to the PORFLOW results. The major discrepancy between the two models may be a function of the well locations used in the GoldSim model for each sector and the relative distance between the source or contaminant plume to each well. The PORFLOW model can consider anywhere, including the zone of contact between sectors in its evaluation. Although the GoldSim model results for some sectors may be underestimated, the location of the well used for Sector K would dominate the peak dose results and generate results similar to PORFLOW. Another difference (which would have an opposite effect but should be noted) between the two models is in the manner in which the vertical position of plumes is handled in the two models. Vertically, in the SDF GoldSim Model, superimposed plume concentrations from multiple SDUs are all evaluated at the same depth in the plumes vertical profile (the depth of maximum concentration), tending to overestimate the combined concentrations. The PORFLOW maximum point analysis will also add a degree of numerical dispersion to the PORFLOW breakthrough curves since the point of analysis can shift in time.

Figure 5.1-55 provides a comparison of the maximum dose curves, regardless of sector, for both the PORFLOW and the GoldSim models. This figure shows that the SDF GoldSim Model closely approximates the maximum dose results calculated from the PORFLOW model.

Figure 5.1-55: Comparison of Maximum MOP Dose Evaluation Case Results over 20,000 Years

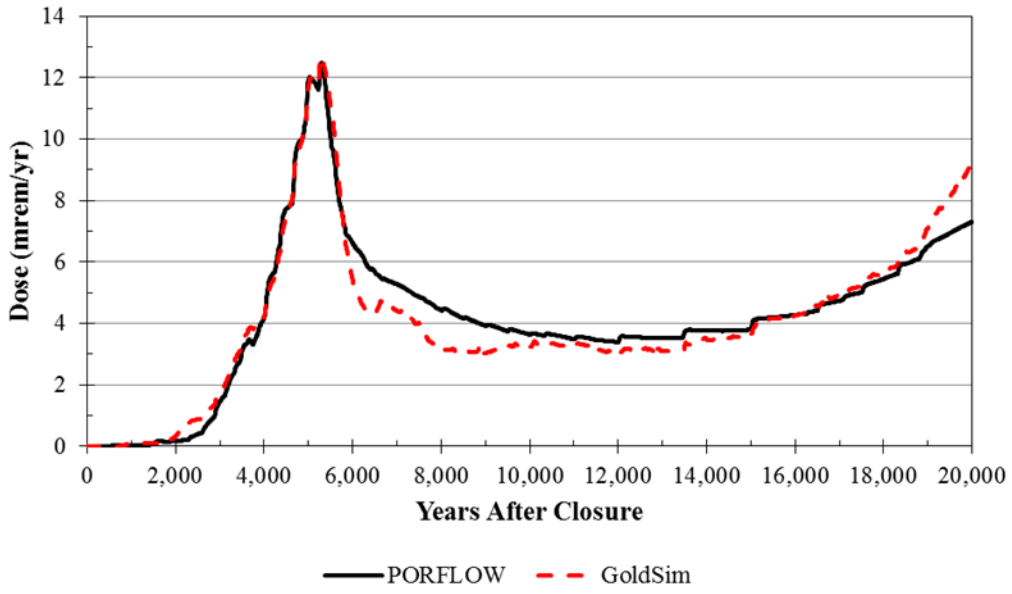

Despite the GoldSim model simplifications, the similarity between GoldSim model results and PORFLOW model results justifies the use of the SDF GoldSim Model for evaluating parameter sensitivity and the influence of parameter uncertainty on the system

to support DOE decision making related to reasonable expectation/assurance that performance objectives will be met for the SDF.

5.1.3.2 Radionuclide Contributions to Total MOP Dose Time Histories

This section presents a comparison of the GoldSim SDF and PORFLOW Model dose breakthrough curves for the major contributing species to MOP dose: I-129, Cs-135, K-40, Ra-226, and Tc-99. The MOP dose breakthrough curves are presented for Sectors B, I, J, and K.

5.1.3.2.1 Sector B

As can be seen by comparing the PORFLOW model generated species dose contributions presented in Figure 5.1-56 to the comparable results from GoldSim presented in Figure 5.1-39, the SDF GoldSim Model closely approximates the PORFLOW generated results for Sector B for all species. Both models peak at approximately 5,300 years in Sector B. The peak dose from the PORFLOW model over the 20,000-year analysis period is 10.4 mrem/yr, while the peak dose from the SDF GoldSim Model over the same period is 11.7 mrem/yr. The GoldSim generated Sector B peak dose is therefore less than 1/4th higher than PORFLOW. As can be readily seen, the release of I-129 dominates the peak dose results over the 20,000-year period.

Figure 5.1-56: Individual Radionuclide Contributions to the PORFLOW Sector B 100-meter Peak Groundwater Pathway Dose Results within 20,000 Years

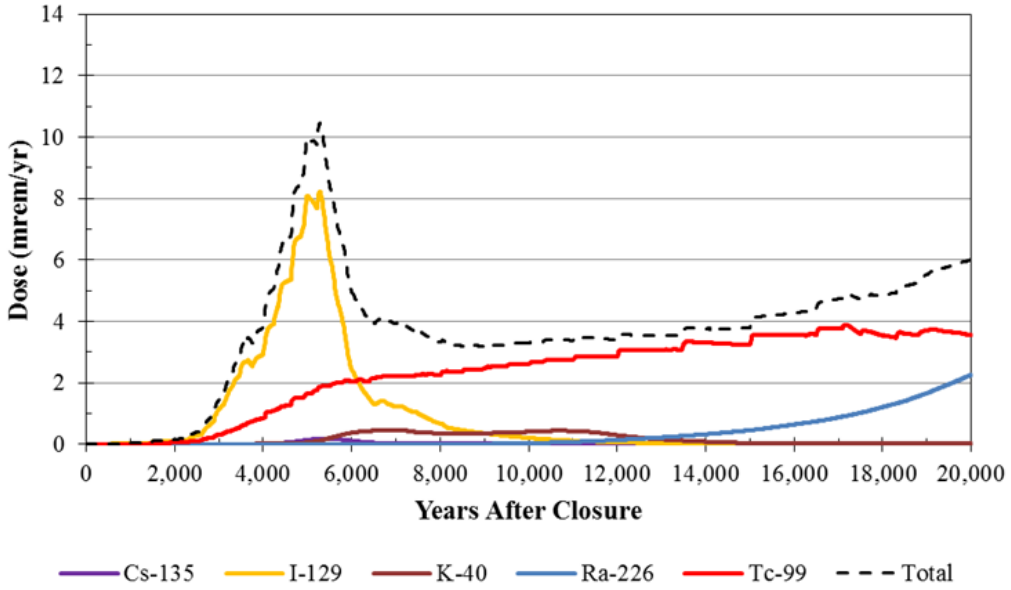

Figure 5.1-57 Individual Radionuclide Contributions to the GoldSim Sector B 100-meter Peak Groundwater Pathway Dose Results within 20,000 Years

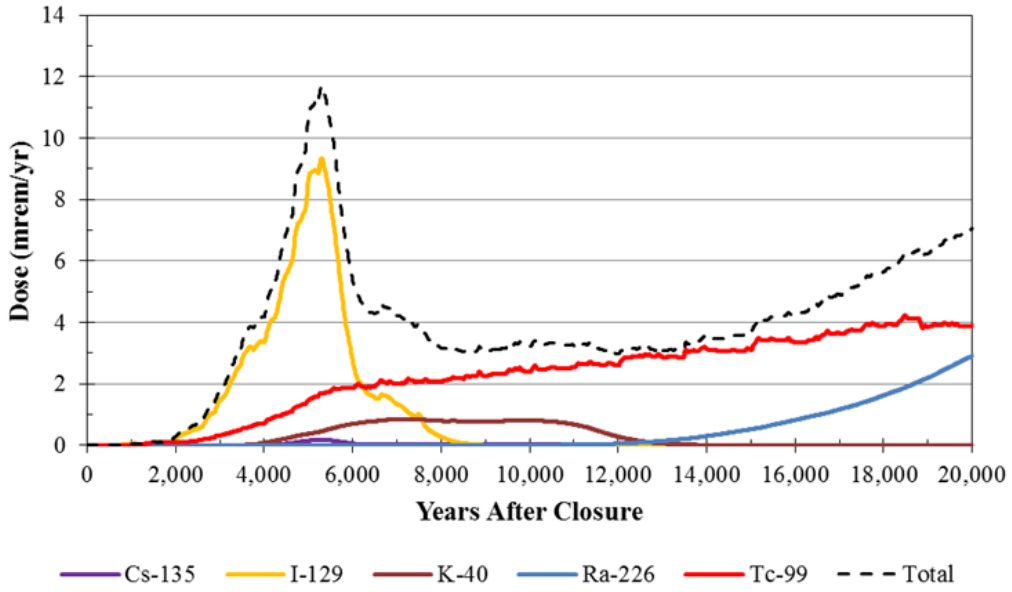

5.1.3.2.1 Sector I

By comparing the PORFLOW model generated species dose contributions presented in Figure 5.1-58 to the comparable results from GoldSim presented in Figure 5.1-59, it can be seen the SDF GoldSim Model closely approximates the PORFLOW generated results in Sector I for all species, although this time PORFLOW shows the higher dose. Both models peak near 5,300 years for Sector I. From the PORFLOW model the peak dose is 7.4 mrem/yr. For the SDF GoldSim Model the peak dose over the same period is 6.3 mrem/yr. As with Sector B, the release of I-129 dominates the peak dose results in Sector I over the 20,000-year period.

Figure 5.1-58: Individual Radionuclide Contributions to the PORFLOW Sector I 100-Meter Peak Groundwater Pathway Dose Results within 20,000 Years

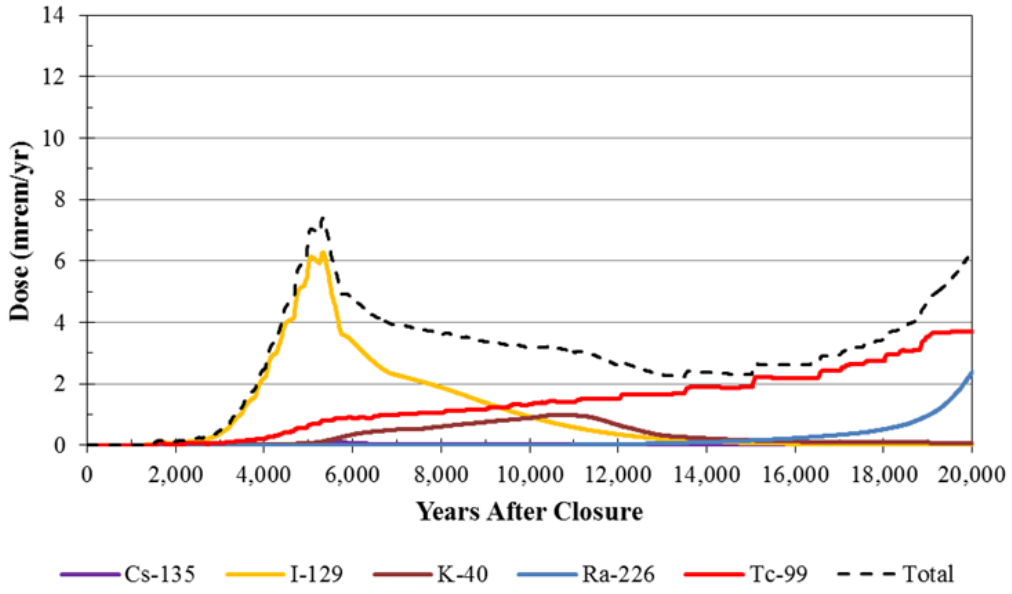

Figure 5.1-59 Individual Radionuclide Contributions to the GoldSim Sector I 100-meter Peak Groundwater Pathway Dose Results within 20,000 Years

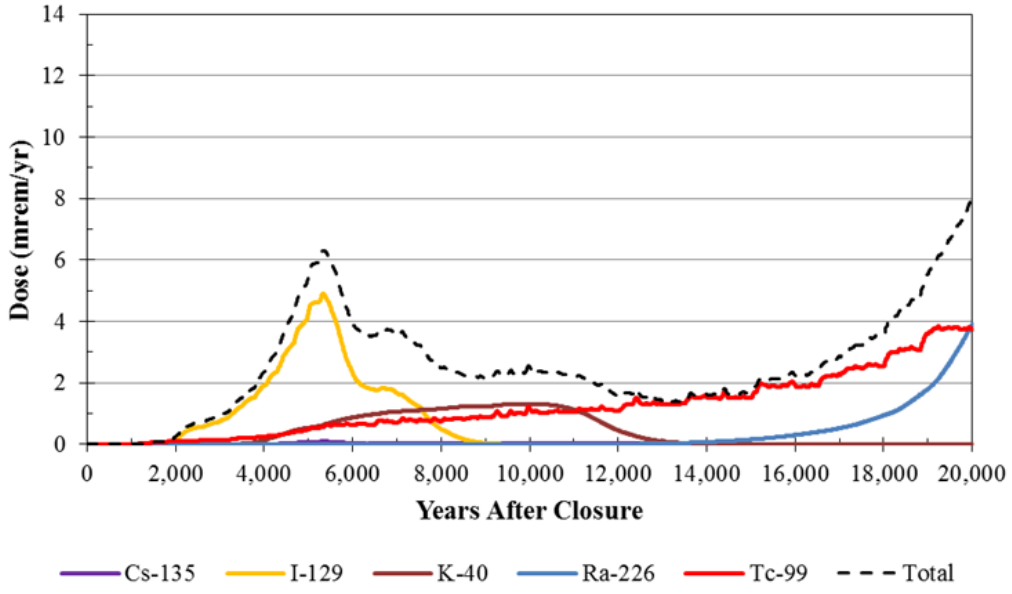

5.1.3.2.3 Sector J

As discussed above (see Section 5.1.3.1), the GoldSim results for Sector J do not match the PORFLOW results as well as within the other Sectors due to modeling simplifications and difficulty in replicating the complexity of the three-dimensional groundwater divide within a one-dimensional numerical plume calculation.

However, as Sector K dominates the dose results for the Northern Sectors, the differences between PORFLOW and GoldSim in Sector J are not expected to adversely affect the applicability of the GoldSim model. Figures 5.1-60 and 5.1-61 provide the Sector J dose results for PORFLOW and GoldSim, respectively. Note that although I-129 and Tc-99 do not match as closely as in other sectors, the other radionuclides show general similarities.

Figure 5.1-60: Individual Radionuclide Contributions to the PORFLOW Sector J 100-meter Peak Groundwater Pathway Dose Results within 20,000 Years

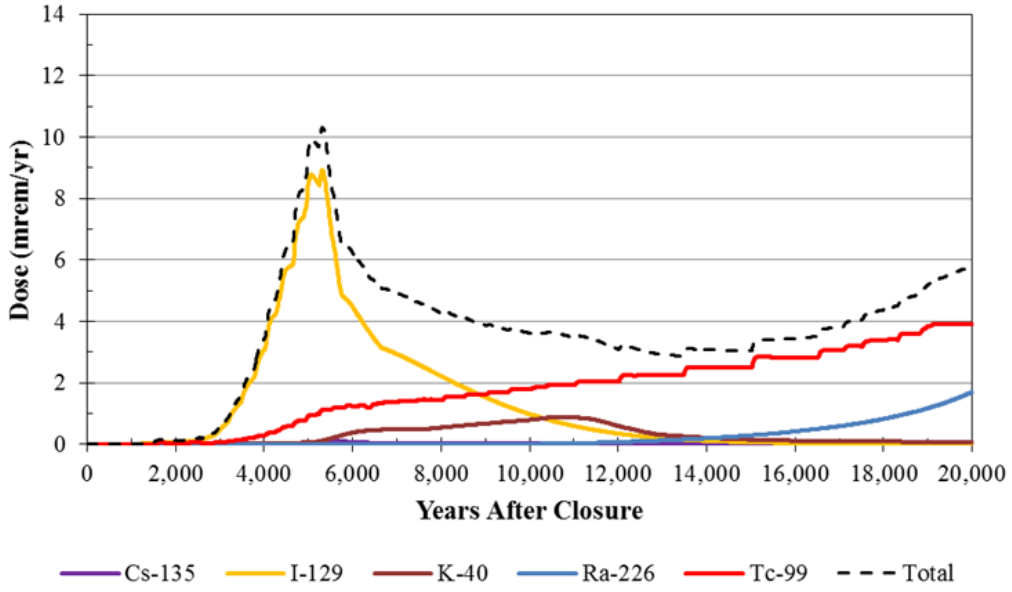

Figure 5.1-61 Individual Radionuclide Contributions to the GoldSim Sector J 100-meter Peak Groundwater Pathway Dose Results within 20,000 Years

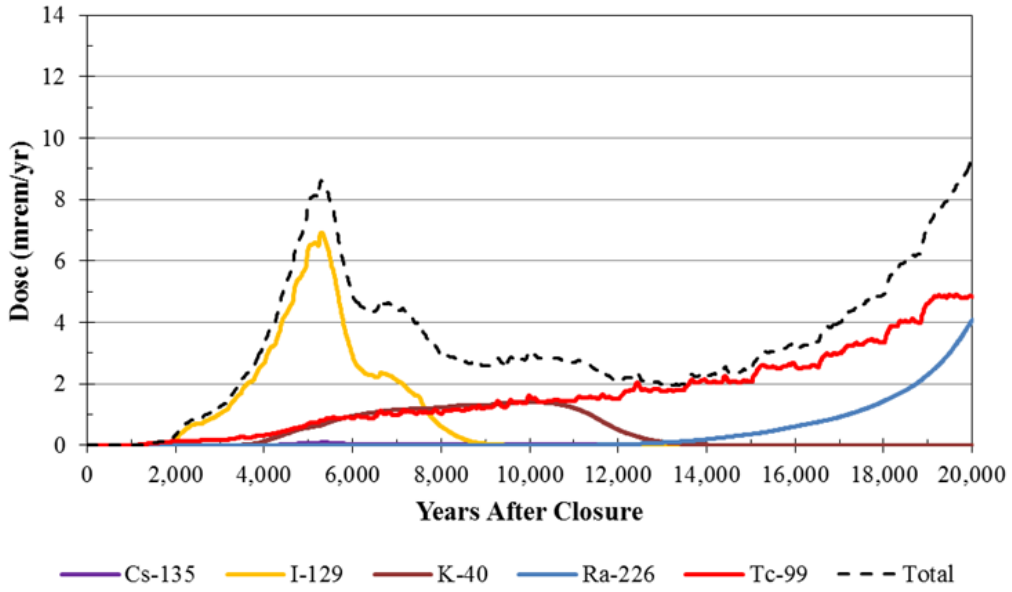

5.1.3.2.4 Sector K

By comparing the PORFLOW model generated species dose contributions presented in Figure 5.1-62 to the comparable results from GoldSim presented in Figure 5.1-63, it can be seen the SDF GoldSim Model very closely approximates the PORFLOW generated results in Sector K for all species. For Sector K, both models peak near 12.5 mrem/yr at approximately 5,300 years. Given that Sector K provides the highest MOP dose results in both PORFLOW and GoldSim for the Evaluation Case in the northern sectors, the similarities between these two result sets justifies the use of the GoldSim model for evaluating parameter sensitivity and parameter uncertainty to support DOE decision making related to reasonable expectation/assurance that performance objectives will be met for the SDF.

Figure 5.1-62: Individual Radionuclide Contributions to the PORFLOW Sector K 100-meter Peak Groundwater Pathway Dose Results within 20,000 Years

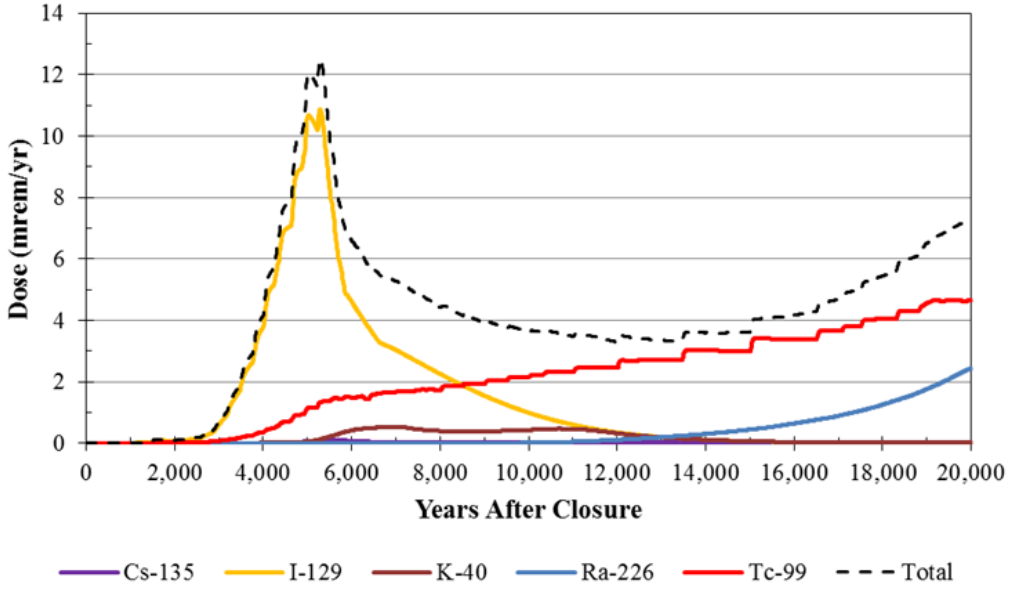

Figure 5.1-63 Individual Radionuclide Contributions to the GoldSim Sector K 100-meter Peak Groundwater Pathway Dose Results within 20,000 Years

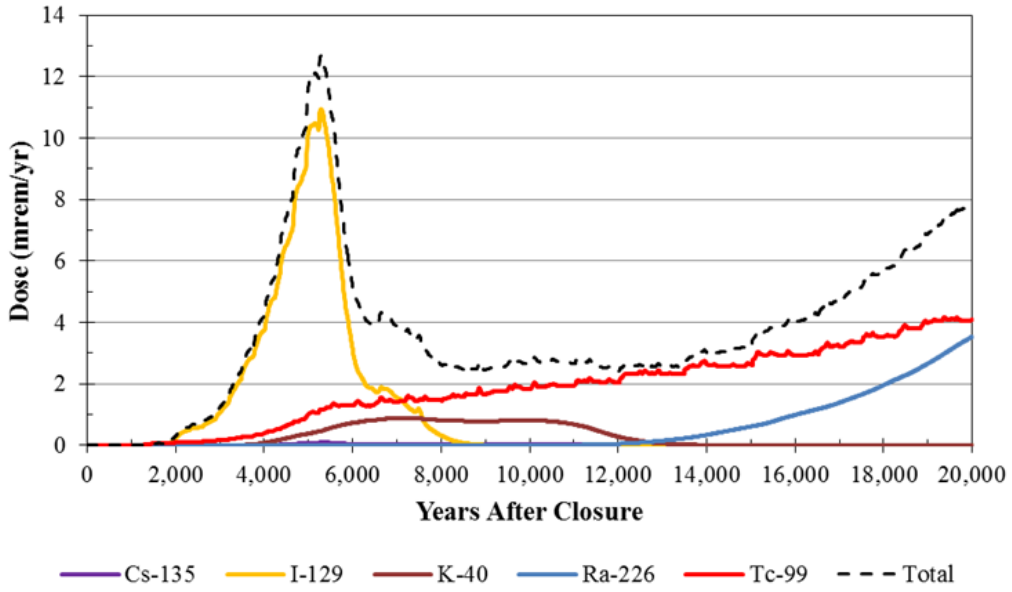

5.1.4 IHI Well Dose Time Histories

The fourth phase of the benchmarking process focuses on examining how well the abstracted model approximates the IHI dose results at the seven wells analyzed in the GoldSim and PORFLOW Models. Comparisons of the maximum total dose results (in millirem per year) and individual well dose levels generated by the two models for the IHI are the basis for the fourth phase.

5.1.4.1 Total IHI Dose Time Histories

In this section, the IHI analysis for the SDF PORFLOW and SDF GoldSim Models are compared to demonstrate how closely the SDF GoldSim Model approximates the PORFLOW IHI dose time histories. The results are presented in the form of dose time histories for the seven wells (IHI Well 1 through IHI Well 7) whose locations are shown in Figure 4.1-2.

The results of the IHI dose history analyses for the two models are presented in Figures 5.1-64 (for the PORFLOW model) and 5.1-65 (for the SDF GoldSim Model). Note that the PORFLOW model also includes a dose for "1-Meter". This dose is determined by finding the highest concentration from all of the modeling nodes along a one-meter boundary surrounding the SDUs, for each radionuclide. For example, if a node near SDU 9 has the highest I-129 concentration and a node near SDU 4 has the highest Tc-99 concentration, then these two concentrations were used together to calculate the one-meter boundary doses. This conservatism is not included in the GoldSim transport model.

As a group, it can be seen that the trends predicted by the SDF GoldSim Model are quite similar to the trends predicted by the PORFLOW model. For the PORFLOW model, the maximum peak value for all IHI wells generated by the PORFLOW model is about 17

mrem/yr and occurs near 5,300 years. For the GoldSim model, the maximum peak value for all wells is 24 mrem/yr and also occurs near 5,300 years. A closer look at the curves shows that though trends are always similar, there are differences with respect to which of the individual wells has the higher peak value and differences in the magnitudes of the peak values.

Figure 5.1-64: PORFLOW Model IHI Well Dose Time Histories

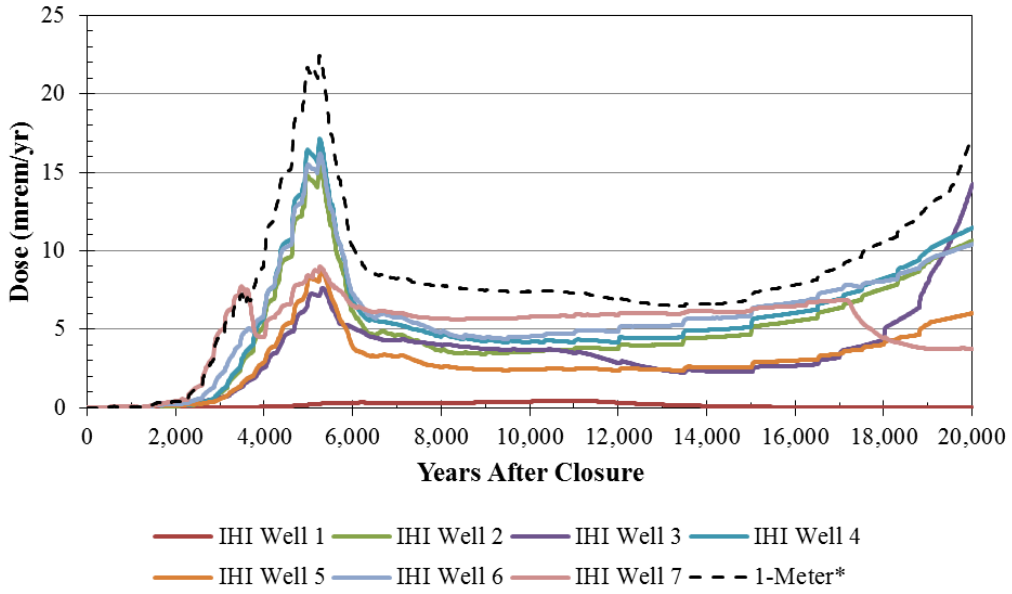

* Note that the one-meter boundary dose is artificially higher than any single location because the one-meter boundary dose assumes the highest concentration for each radionuclide along the one-meter boundary, regardless of where those concentrations occur, as described in the SDF PA, Section 6.1. [SRR-CWDA-2009-00017] For example, the highest Tc-99 concentration could occur in southern sectors while the highest I-129 concentration could occur in the northern sectors; combining these high values together produces a higher total dose than using only the concentrations from a single location.

Figure 5.1-65: GoldSim Model IHI Well Dose Time Histories

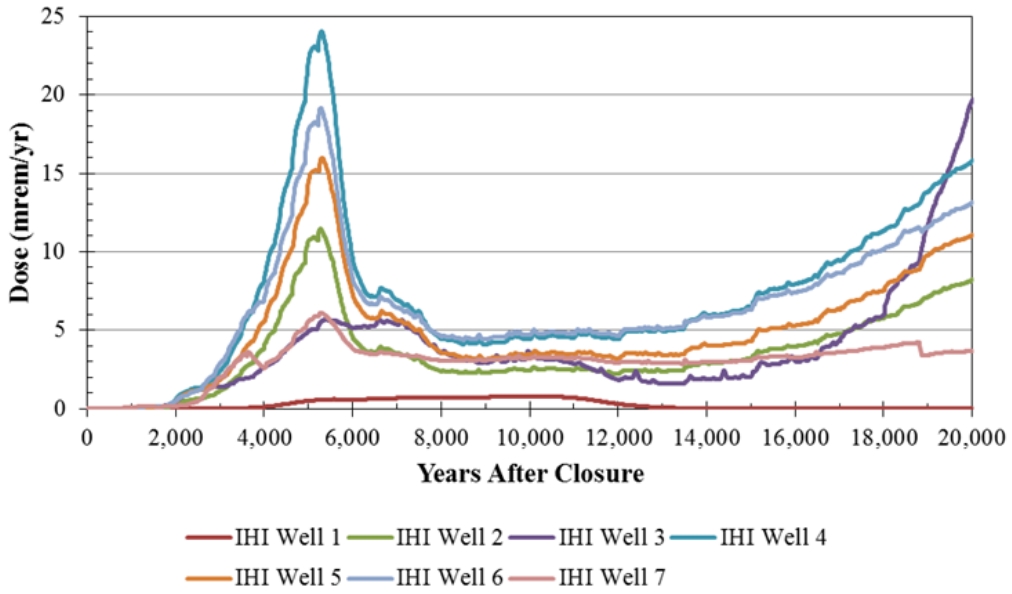

Note: The GoldSim model does not include a maximum one-meter boundary concentration or dose.

Figures 5.1-66 (for the PORFLOW model) and 5.1-67 (for the SDF GoldSim Model) show the dose time histories for the northern wells. The peak IHI doses from the wells in the GoldSim model tend to be higher than the peak IHI doses from the wells in the PORFLOW model (e.g., IHI Well 4 is about 50% higher); however, for Well 2 the GoldSim peak is about 30% lower.

Figures 5.1-68 (for the PORFLOW model) and 5.1-69 (for the SDF GoldSim Model) show the dose time histories for the southern wells. The peak values tend to be around 15% higher for IHI Well 6 in the GoldSim results, although, IHI Well 7 is about 25% lower.

Figure 5.1-66: PORFLOW Model IHI Well Dose Time Histories for the Northern Wells

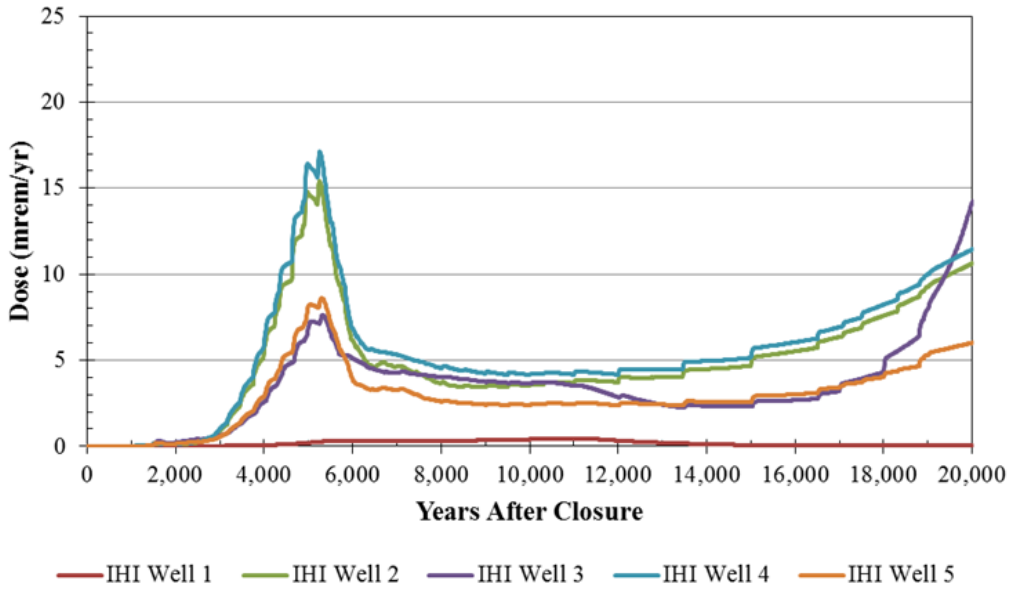

Figure 5.1-67: GoldSim Model IHI Well Dose Time Histories for the Northern Wells

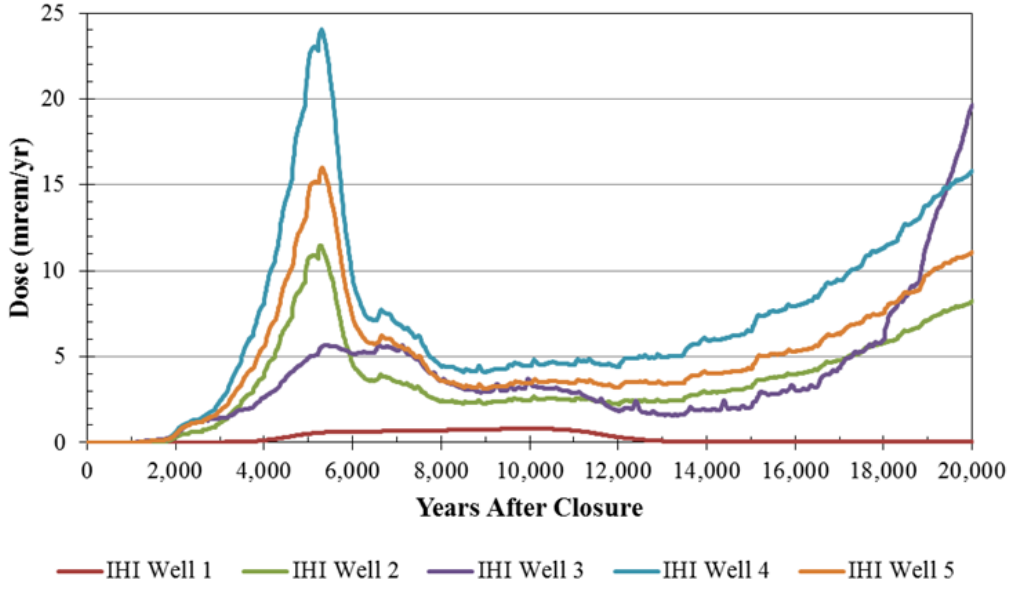

Figure 5.1-68: PORFLOW Model IHI Well Dose Time Histories for the Southern Wells

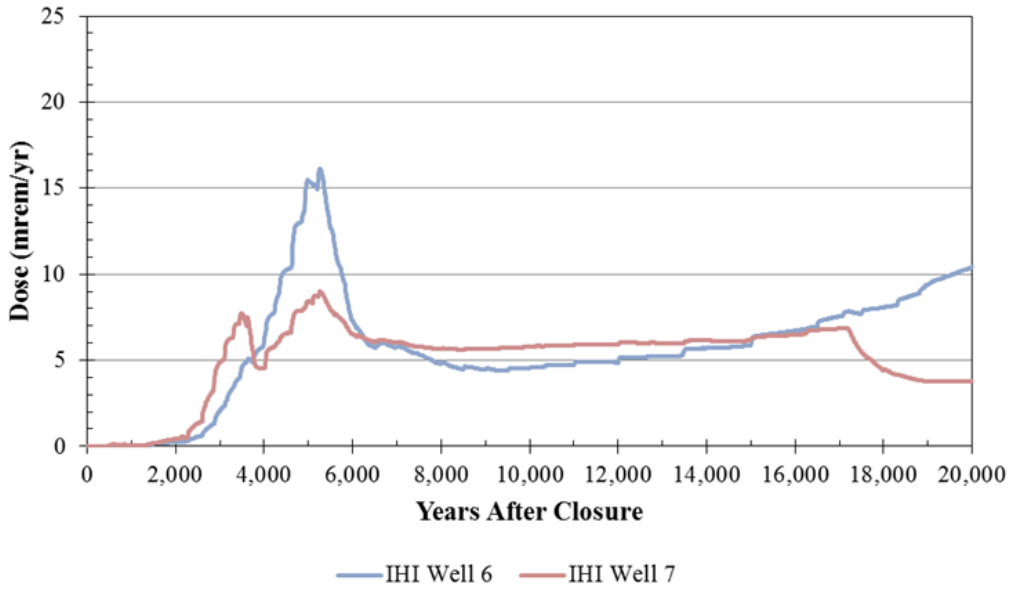

Figure 5.1-69: GoldSim Model IHI Well Dose Time Histories for the Southern Wells

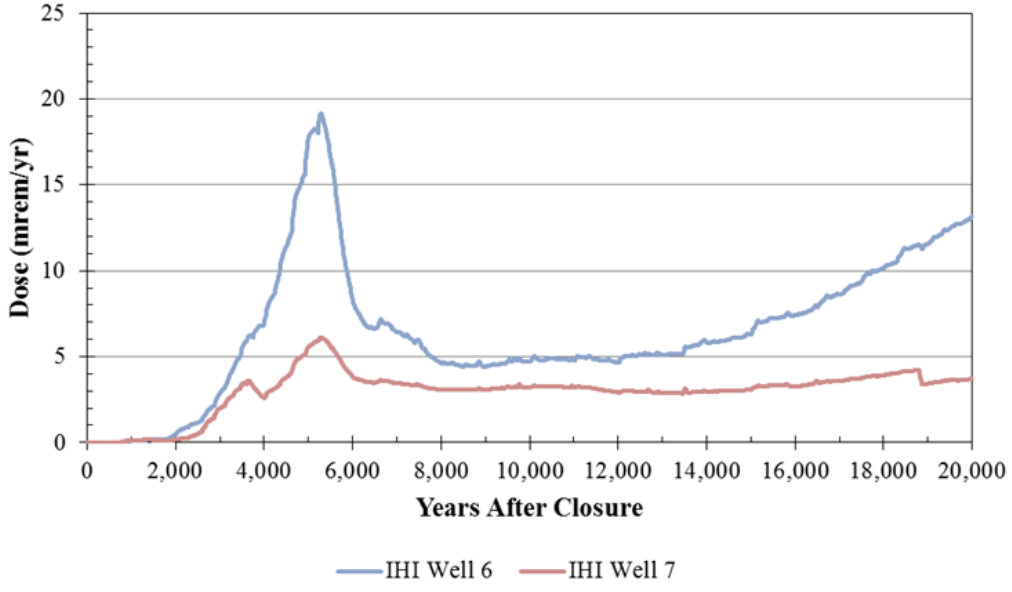

For the IHI well analyses, the differences between GoldSim and PORFLOW generated results tend to be accentuated. There are several competing processes involved, each of which may affect the comparisons differently. For instance, the IHI Well 2 comparison shows that the PORFLOW dose is of greater magnitude than the GoldSim result. This difference may be attributed to the averaging process used to generate Darcy velocities along flow paths. Because the velocities are determined, by evaluating breakthrough curves, the averaging is harmonic, and slower zones, such as beneath SDU 8 (Figure 4.1-2) have a strong influence on the velocity averaging process. For IHI Well 4, the opposite trend (a higher

GoldSim peak) is observed. For IHI Well 4, a more complex mixing process occurs. In addition to any differences associated with velocity averaging, the results here are controlled by the superposition of two plumes, one from SDU 9 and one from SDU 7. In PORFLOW, the vertical component of flow would tend to enhance the vertical dispersion within the combined plume. In the SDF GoldSim Model, the superposition process always combines values at the elevation of maximum concentration.

The differences between the individual well results are not surprising because of the velocity averaging in conjunction with the proximity of the wells to the SDUs. Other possible influences include numerical dispersion due to grid effects in PORFLOW and the more rigorous evaluation of plume geometry in PORFLOW. Note that the velocity averaging and vertical mixing difference would not be as apparent in the 100-meter boundary calculations where, due to generally longer travel pathways, a greater degree of vertical mixing has occurred. Figure 5.1-70 presents a comparison of the composite PORFLOW model and GoldSim model, dose breakthrough curves based on the maximum dose value at any well at a given time. Although it can be seen that the overall peak dose is about 7 mrem/yr higher for the GoldSim model when comparing only the IHI wells, there is a much closer match when the comparison also includes the conservative one-meter boundary dose from PORFLOW. Therefore, as a simplification, use of the GoldSim model for IHI modeling is appropriate.

Figure 5.1-70: GoldSim and PORFLOW Model Maximum IHI Well Dose Time Histories

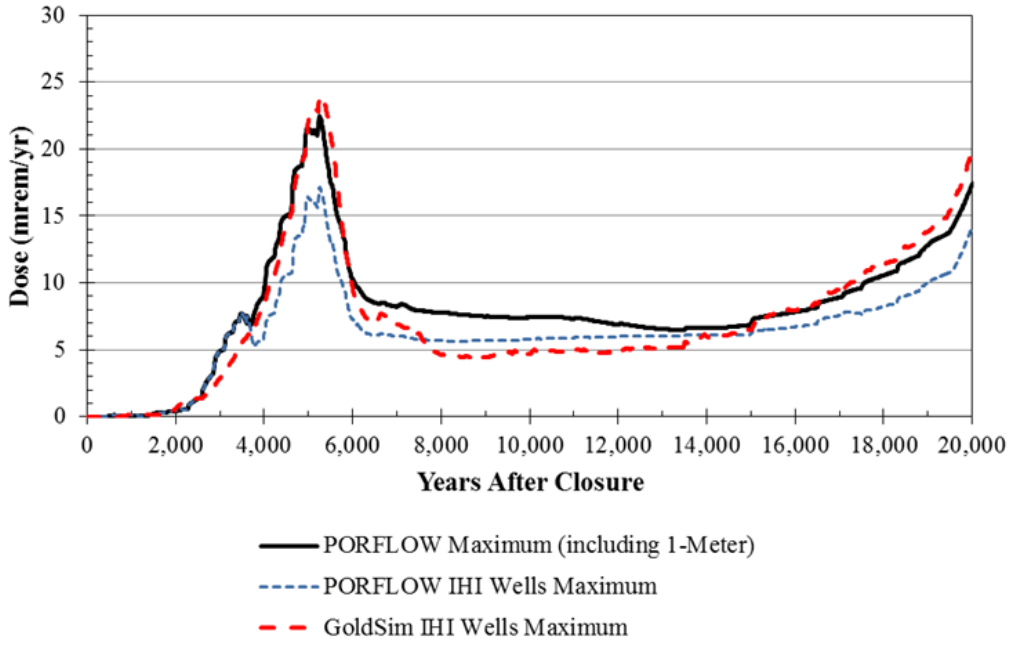

5.1.5 Mass Releases to the Saturated Zone

Before using GoldSim for stochastic simulations, it is important to demonstrate that the SDF GoldSim model provides an acceptable abstraction of the three-dimensional SDF PORFLOW Model with respect to the alternative flow cases being sampled (see Section 3.1.4). Figure 5.1-71 shows a dose comparison between the two modeling approaches for five of the alternative flow cases (F01, F04, F05, F14, and F30) over the 20,000-year PORFLOW

simulation period. In general, the GoldSim dose results are slightly higher, however the behavior of each flow profile is relatively consistent. Therefore, the SDF GoldSim model provides a valid approach for considering the longer-term impacts of each flow case.

Figure 5.1-71: Comparison of PORFLOW and GoldSim MOP Dose Profiles for Selected Flow Cases for 20,000 Years

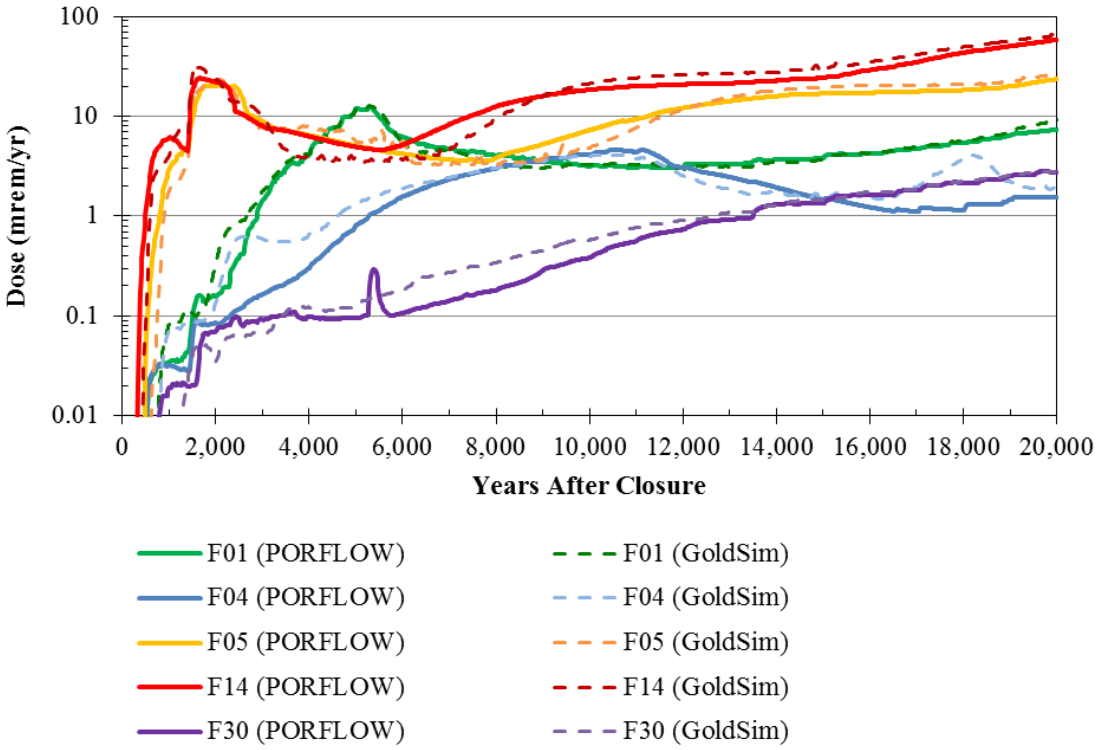

5.2 Benchmarking Conclusion

The benchmarking analysis described in Section 5.1, presents comparisons between SDF PORFLOW Model radionuclide releases to the saturated zone and releases produced by the GoldSim-based abstraction of the PORFLOW model. The SDU release model, is comprised of two components, the All-Species (evaluates all species except for Tc-99 when choosing the "shrinking core model" option) and the Tc-99 "shrinking core" component. The comparisons show similarities in trends that indicate that the GoldSim SDF All-Species Model (Section 4.1) and Tc-99 mixing-cell networks (Section 4.2) that simulate engineered barrier and unsaturated zone transport, can provide a acceptable approximation of the SDU radionuclide releases to the saturated zone. In the SDF GoldSim Model, the releases of radionuclides from the SDU abstraction model are applied as boundary conditions to the saturated zone abstraction model. The saturated zone abstraction model is based on a one-dimensional analytical solution (GoldSim pipe-model element) used in conjunction with a Green's Function based GoldSim plume function that evaluates the influence horizontal and vertical transverse dispersion on plume attenuation. The product of the pipe-element solution and the plume function define the concentrations at the 100-meter boundary (and seven wells for the IHI analysis).

A comparison of the 100-meter boundary concentrations produced by the SDF GoldSim Model with the concentrations generated by the SDF PORFLOW Model, as presented in Section 5.1.2, show that the SDF GoldSim Model reproduces the trends found in the PORFLOW model results. The concentrations generated at the 100-meter boundary, are used by the SDF GoldSim Model dose-calculator to evaluate dose-based exposure to the MOP. The comparisons between GoldSim and PORFLOW model generated total-dose levels and the radionuclide dose contributions from species dominating the results, presented in Section 5.1.3, show an acceptable match in trends. A similar comparison of dose results for the IHI analysis, presented in Section 5.1.4 also shows an acceptable match in trends for the maximum total dose. GoldSim model concentrations (and associated doses) for individual IHI wells tend to be slightly higher than the PORFLOW generated values, but the trends are still similar (see Section 5.1.4). The differences are accentuated by the difference in handling of mixing (dispersive) processes, in the two models. For example, in the PORFLOW model, mixing of superposed plumes mixing at the well location occurs at varied depths while in the SDF GoldSim Model, peak concentrations, with respect to depth, are superimposed. Time histories of maximum doses, for a set of five alternative flow cases, were also generated using the GoldSim model and compared to PORFLOW results as a check on the validity of the GoldSim abstraction as an analogue for the PORFLOW model (see Section 5.1.5). The comparison showed that the GoldSim model was an acceptable abstraction. Based upon these assessments it is concluded that uncertainty and sensitivity analyses conducted using Version 5.006 of the SDF GoldSim Model are expected to be representative of the SDF conceptual model for the SA Evaluation Case and other cases to be presented in the FY2014 SDF SA.

6.0 REFERENCES

Note: References identified as (Copyright) were used in the development of this SDF GoldSim Model Document, but are protected by copyright laws. No part of the publication may be reproduced in any form or by any means, including photocopying or electronic transmittal, without permission in writing from the copyright owner.

B-SQP-C-00002, Hommel, S., *Software Quality Assurance Plan for GoldSim© for the Savannah River Site's Liquid Waste Program*, Savannah River Site, Aiken, SC, Rev. 0, April 23, 2012.

GTG-2010c (Copyright), *GoldSim User's Guide, Volumes 1 & 2*, GoldSim Technology Group LLC, Issaquah, WA, January 2010.

GTG-2010d, (Copyright), *User's Guide, Probabilistic Simulation Environment, Version 10.5, Volumes 1 & 2*, GoldSim Technology Group LLC, Issaquah, WA, December 2010.

GTG-2010e, (Copyright), *GoldSim User's Guide, GoldSim Containment Transport Module*, Version 6.0, GoldSim Technology Group LLC, Issaquah, WA, December 2010.

HLW-SSF-TTR-2013-0021, *Liquid Waste (LW) Technical Task Request - 30 Million Gallon Saltstone Disposal Unit (SDU) PORFLOW Modeling for SDU-6 Special Analysis (SA),* Savannah River Site, Aiken, SC, Rev. 2, October 23, 2013.

SRNL-STI-2009-00115, Flach, G.P., et al., *Numerical Flow and Transport Simulations Supporting the Saltstone Disposal Facility Performance Assessment*, Savannah River Site, Aiken, SC, Rev. 1, June 17, 2009.

SRNL-STI-2013-00118, Flach, G. P. and F. G. Smith III, *Degradation of Cementitious Materials Associated with Saltstone Disposal Units*, Savannah River Site, Aiken, SC, Rev. 1, November 2013.

SRNL-STI-2013-00280, Jordan, J.M. and Flach, G.P., *PORFLOW Modeling Supporting the FY13 Saltstone Special Analysis*, Savannah River Site, Aiken, SC, Rev. 0, September 29, 2010.

SRNL-STI-2014-00083, Flach, G. P. and G. A. Taylor, *PORFLOW Modeling Supporting the FY14 Saltstone Special Analysis*, Savannah River Site, Aiken, SC, Rev. 0, March 2014.

SRR-CWDA-2009-00017, *Performance Assessment for the Saltstone Disposal Facility at the Savannah River Site*, Savannah River Site, Aiken, SC, Rev. 0, October 29, 2009.

SRR-CWDA-2011-00178, *Saltstone Disposal Facility Stochastic Fate and Transport Model*, Savannah River Site, Rev. 1, Aiken, SC, January 10, 2012.

SRR-CWDA-2013-00058, Hommel, S., *Dose Calculation Methodology for Liquid Waste Performance Assessments at the Savannah River Site,* Savannah River Site, Aiken, SC, Rev. 1, July 2014.

SRR-CWDA-2013-00062, *FY2013 Special Analysis for the Saltstone Disposal Facility at the Savannah River Site*, Savannah River Site, Aiken, SC, Rev. 2, October 3, 2013.

SRR-CWDA-2013-00064, Sheppard, R.E. to Rosenberger, K.H., *PORFLOW Input to Support the Development of the SDF FY13 Special Analysis*, Savannah River Site, Aiken, SC, Rev. 1, April 2013.

SRR-CWDA-2013-00073, *Updates to the Saltstone Disposal Facility Fate and Transport Model,* Savannah River Site, Aiken, SC, Rev. 0, June 2013.

SRR-CWDA-2013-00147, *SDF Inventory Estimates for Transport Modeling*, Savannah River Site, Aiken, SC, Rev. 0, December 9, 2013.

SRR-CWDA-2014-00033, Lester, B., *Software Quality Assurance Plan for TransitionTime.dll for the Savannah River Site's Liquid Waste Program*, Savannah River Site, Aiken, SC, Rev. 0, April 2014.